

NETWORK DENSITY ESTIMATORS AND DENSITY-AWARE WIRELESS
NETWORKS

A THESIS SUBMITTED TO
THE GRADUATE SCHOOL OF NATURAL AND APPLIED SCIENCES
OF
MIDDLE EAST TECHNICAL UNIVERSITY

BY

ALPEREN EROĞLU

IN PARTIAL FULFILLMENT OF THE REQUIREMENTS
FOR
THE DEGREE OF DOCTOR OF PHILOSOPHY
IN
COMPUTER ENGINEERING

OCTOBER 2020

Approval of the thesis:

NETWORK DENSITY ESTIMATORS AND DENSITY-AWARE WIRELESS NETWORKS

submitted by **ALPEREN EROĞLU** in partial fulfillment of the requirements for the degree of **Doctor of Philosophy in Computer Engineering Department, Middle East Technical University** by,

Prof. Dr. Halil Kalıpçılar
Dean, Graduate School of **Natural and Applied Sciences**

Prof. Dr. Halit Oğuztüzün
Head of Department, **Computer Engineering**

Prof. Dr. Ertan Onur
Supervisor, **Computer Engineering, METU**

Examining Committee Members:

Prof. Dr. Volkan Atalay
Computer Engineering, METU

Prof. Dr. Ertan Onur
Computer Engineering, METU

Prof. Dr. Ahmet Coşar
Computer Engineering, Ankara Bilim University

Assoc. Prof. Dr. İlker Demirkol
Mining, Industrial and ICT Engineering,
Universitat Politècnica de Catalunya

Assist. Prof. Dr. Hande Alemdar
Computer Engineering, METU

Date:



I hereby declare that all information in this document has been obtained and presented in accordance with academic rules and ethical conduct. I also declare that, as required by these rules and conduct, I have fully cited and referenced all material and results that are not original to this work.

Name, Surname: Alperen Eroğlu

Signature :

ABSTRACT

NETWORK DENSITY ESTIMATORS AND DENSITY-AWARE WIRELESS NETWORKS

Eroğlu, Alperen

Ph.D., Department of Computer Engineering

Supervisor: Prof. Dr. Ertan Onur

October 2020, 176 pages

New network architectures and communication technologies continue to emerge to meet rapidly increasing and changing user demands requiring continuous connectivity and high data rate transmissions. These ubiquitous infrastructures result in a paradigm shift in mobile communications with the advent of mobile robots equipped with sensors, unmanned aerial vehicles, and mobile small-cells, which makes the future networks highly dynamic. This dynamism poses unpredictable variations in the network density causing many run-time problems such as disrupted coverage, undesirable quality of service, and inefficient resource usage. Pre-configurations are no longer suitable because of the network topology variations, which prompts us to develop density-adaptive protocols and self-configured system designs. Therefore, the most crucial objective of this thesis is to make future wireless networks density-aware and -adaptive. We propose novel network density estimators using received signal strength and density-aware networking applications. We introduce a distance matrix-based density estimator, multi-access edge cloud-based density estimator, and interference-based density estimator for wireless networks. We also develop density-aware network outage, transmit power adaptation, and channel utilization approaches

by considering the effective network density as an optimization parameter for clustered ad hoc networks, mobile cellular networks, and flying ad hoc networks. We validate the results by implementing Monte-Carlo simulations on MATLAB. Outputs of this thesis may help network operators enhance service quality, create the best deployment strategies, reduce operational expenditures, and meet increasing user expectations without wasting network resources. Density-aware and -adaptive applications make wireless networks self-organized and run-time adaptable.

Keywords: Wireless networks, Ad hoc networks, Flying Ad hoc networks, Cellular networks, Moving base stations, Base station density estimation, Density-adaptive networking, Network coverage, Network outage, Density-aware transmit power adaptation.

ÖZ

AĞ YOĞUNLUĞU KESTİRİCİLERİ VE YOĞUNLUK-UYARLI TELSİZ AĞLAR

Eroğlu, Alperen

Doktora, Bilgisayar Mühendisliği Bölümü

Tez Yöneticisi: Prof. Dr. Ertan Onur

Ekim 2020 , 176 sayfa

Sürekli bağlantı ve yüksek veri hızı iletimi gerektiren, hızla artan ve değişen kullanıcı taleplerini karşılamak için yeni ağ mimarileri ve iletişim teknolojileri ortaya çıkmaya devam ediyor. Bu yaygın altyapılar, algılayıcılarla donatılmış hareketli robotların, insansız hava araçlarının ve hareketli küçük hücrelerin ortaya çıkmasıyla mobil iletişimde bir paradigma değişikliğine neden olur ve bu da gelecekteki ağları oldukça dinamik hale getirir. Bu dinamizm, kesintili kapsama alanı, istenmeyen hizmet kalitesi ve verimsiz kaynak kullanımı gibi birçok çalışma zamanı sorununa neden olan ağ yoğunluğunda tahmin edilemeyen değişimler ortaya çıkarır. Statik yapılandırmaların ağ topolojisinde değişimler nedeniyle uygun olmaması bizi yoğunluk-uyarlı protokoller ve kendi kendine yapılandırılmış sistem tasarımları geliştirmeye yöneltmiştir. Bu nedenle, bu çalışmanın en önemli amacı, gelecekteki kablosuz ağları yoğunluk farkında ve uyarlı hale getirmektir. Bu tezde, alınan sinyal gücünü kullanan yeni ağ yoğunluğu kestiricileri ve yoğunluk-uyarlı ağ uygulamaları sunuyoruz. Kablosuz ağlar için mesafe matrisi tabanlı yoğunluk kestiricisi, çoklu erişimli uç bulut tabanlı yoğunluk kestiricisi ve girişim tabanlı yoğunluk kestiricisi öneriyoruz. Kümelenmiş

tasarsız ađlar, mobil hücreseľ ađlar ve uçan tasarsız ađlarda, etkili ađ yoğunluđunu optimizasyon parametresi olarak dikkate alan yoğunluk-farkında ađ kesintisi, iletim gücü uyarlaması ve kanal kullanımı yaklaşımları geliştiriyoruz. MATLAB üzerinde Monte-Carlo benzetimlerle beklenen sonuçları doğruluyoruz. Bu tezin çıktıları, ađ operatörlerinin hizmet kalitesini artırmasına, en iyi dağıtım stratejilerini oluşturmaya, operasyonel harcamaları azaltmasına ve ađ kaynaklarını boşa harcamadan artan kullanıcı beklentilerini karşılamasına yardımcı olabilir. Yoğunluk uyarlı ve uyumlu uygulamalar, kablosuz ađları kendi kendine organize eder ve çalışma zamanında uyarlanabilir hale getirir.

Anahtar Kelimeler: Telsiz ađlar, Tasarsız ađlar, Uçan tasarsız ađlar, Hücreseľ ađlar, Hareketli Baz İstasyonları, Baz İstasyonu Yoğunluk Tahmini, Yoğunluk-uyarlıklı ađ oluşturma, Ađ kapsamı, Ađ kesintisi, Yoğunluk farkında iletim gücü uyarlama.



To my family

ACKNOWLEDGMENTS

First of all, I would like to express my sincere gratitude to my supervisor Prof. Dr. Ertan Onur for the continuous support during my Ph.D. thesis and research at the Department of Computer Engineering in Middle East Technical University. I am grateful to him because of his incredible patience, motivation, enthusiasm, friendship, and immense knowledge. His guidance helped me in all the time of my research and writing of this thesis. I could not have imagined having a better advisor and mentor for my Ph.D. thesis.

I would like to thank my thesis monitoring committee members Prof. Dr. Ahmet Coşar, and Assist. Prof. Dr. Hande Alemdar for their continuous interest and encouragement in my thesis.

I would also like to thank other Jury members of my Ph.D. thesis, Prof. Dr. Volkan Atalay, and Assoc. Prof. Dr. İlker Demirkol for their precious discussions and suggestions about my thesis.

Sincere thanks to all my friends, especially Shahram Mollahasani, Hüsni Yıldız, Adnan Kılıç, M. Çağrı Kaya, Farnaz Hassanzadeh, all other WINSLAB and CENG members for their kindness and moral support during my study. Thanks for their friendship and memories.

All my family, my wife, my parents, and my brother deserve special mention for their inseparable support and prayers. My wife, Hatice Ünlü Eroğlu, always helped and encouraged me. Thanks to her endless patience.

I would like to thank everybody important to the successful realization of this thesis and express my apology that I could not mention personally one by one.

Finally, thanks to TÜBİTAK because this work was supported by TÜBİTAK, Project 215E127.

TABLE OF CONTENTS

ABSTRACT	v
ÖZ	vii
ACKNOWLEDGMENTS	x
TABLE OF CONTENTS	xi
LIST OF TABLES	xvi
LIST OF FIGURES	xviii
CHAPTERS	
1 INTRODUCTION	1
1.1 Problem Definition	8
1.2 Motivation	9
1.3 Methodology	10
1.4 Contributions	11
1.5 Structure of the Thesis	14
2 BACKGROUND AND RELATED WORK	17
2.1 Ad Hoc Networks	17
2.2 Cellular Networks	18
2.2.1 Distribution of Base Stations	18
2.2.2 Existing Density Estimation Methods	19

2.2.3	How Density of Base Stations affects Network Coverage and Capacity	20
2.2.4	Relation between Aggregate Interference, Path-loss and BS Density	21
2.3	Flying Ad Hoc Networks (FANET)	22
3	DENSITY-AWARE MOBILE NETWORKS : OPPORTUNITIES AND CHALLENGES	25
3.1	Introduction	26
3.2	Why is Density-awareness Important?	27
3.2.1	Paradigm Changes in Mobile Communications	28
3.2.2	Why Does Infrastructure Become Dynamic?	29
3.2.3	Why Will The Present Architectures Fail?	30
3.2.4	Impact Analysis of Base Station Density	31
3.2.5	How Can the BS Density be Estimated?	35
3.3	Challenges and Opportunities	37
3.3.1	Densification	37
3.3.2	Quality of Service and Experience	39
3.3.3	Modulation Techniques	41
3.3.4	Ubiquitous Coverage and Connectivity	42
3.3.5	Mobility Management of Cells	44
3.3.6	Reliable Communication	45
3.3.7	Scalability	46
3.3.8	Antenna Type Selection	47
3.3.9	Dynamic (in-band) Backhauling	48

3.3.10	Low Latency	49
3.3.11	Energy Efficiency and Green Operations	50
3.3.12	Management of Dynamic Architecture	50
3.3.13	Transmit Power Adaptation	51
3.3.14	Interference Management	53
3.4	Conclusion	58
4	NETWORK DENSITY ESTIMATORS	61
4.1	Density Estimation in Ad Hoc Networks	61
4.1.1	Distance Matrix-based Density Estimator	61
4.1.2	Other Estimators	65
4.1.2.1	RSS-based Collective Distance Estimator	65
4.1.2.2	Kendall's Distance Estimator	65
4.2	Density Estimation in Cellular Networks	66
4.2.1	System Model	66
4.2.2	Network Density Estimators	68
4.2.2.1	Interference-based Network Density Estimator (IDE)	69
4.2.2.2	Multi-access Edge Cloud Based Network Density Estimator (CDE)	70
4.3	Density Estimation in FANETs	71
5	DENSITY-AWARE NETWORKING APPLICATIONS	73
5.1	Density-aware Network Outage	73
5.1.1	Network Outage in Two-Dimensional Wireless Networks	73
5.1.2	Network Outage in Three-Dimensional Wireless Networks	74

5.2	Density-aware Transmit Power Adaptation (DTPA)	75
5.2.1	Transmit Power Adaptation in Two-Dimensional Wireless Networks	75
5.2.2	Transmit Power Adaptation in Three-Dimensional Wireless Networks	75
5.3	Density-aware Channel Utilization in FANETs	76
5.3.1	System Model	77
5.3.2	Further Assumptions	79
5.3.3	Updating The Channel Access Probability	80
5.3.4	Other Proposals	81
5.3.4.1	Slotted ALOHA Protocol (SAP)	81
5.3.4.2	Stabilized Slotted ALOHA Protocol (STSAP)	81
6	VALIDATION AND EXPERIMENTAL RESULTS	83
6.1	Validation of Density Estimators	83
6.1.1	Validation of Density Estimator for Ad Hoc Networks	83
6.1.2	Validation of Density Estimator for Cellular Networks	85
6.1.2.1	Simulator Design	85
6.1.2.2	Validation of the Interference-based Network Density Estimator (IDE)	87
6.1.2.3	Validation of the Multi-access Edge Cloud-based Network Density Estimator (CDE)	89
6.1.2.4	Discussions About Density Estimators	91
6.1.2.5	Impact of Neighbor Proximity Indices	92
6.1.2.6	Impact of Log-normal Shadowing	94
6.1.2.7	Impact of Path-loss Model	95

6.1.2.8	Impact of Non-uniform Distributions	97
6.1.3	Validation of 3-D Density Estimator for FANETs	102
6.2	Validation of Density-adaptive and -aware Applications	104
6.2.1	Validation of 2-D Density-aware Network Outage and Density-aware Transmit Power Adaptation (DTPA) for Wireless Networks	104
6.2.2	Validation of 3-D Density-aware Network Outage and Density-aware Transmit Power Adaptation (DTPA) for Wireless Networks	107
6.2.2.1	Density-aware Outage Analysis	108
6.2.2.2	Validation of Density-aware Outage Probability	114
6.2.2.3	Validation of the Density-aware Transmit Power Adaptation	117
6.2.2.4	Validation of Density-aware Power Adaption Technique with Edge Computing	117
6.2.2.5	Validation of Density Estimator and Power Adaption Technique without Edge Computing	119
6.2.3	Validation of Density-aware Slotted ALOHA Potocol (DASAP) for FANET	121
7	CONCLUSION AND FUTURE WORK	141
	REFERENCES	145
	CURRICULUM VITAE	171

LIST OF TABLES

TABLES

Table 3.1	The qualitative discussion of the impact of the density regime on network performance.	32
Table 3.2	Approaches for estimating density of nodes in a network.	36
Table 3.3	The challenges-I of dynamic mobile networks and some of the existing enabling technologies that can be employed to address these challenges.	38
Table 3.4	The challenges-II of dynamic mobile networks and some of the existing enabling technologies that can be employed to address these challenges.	39
Table 3.5	The nomenclature for symbols, notations, values and units of the simulations' parameters.	54
Table 6.1	The symbols, notations, values and units of the 3-D simulation parameters for cellular networks.	86
Table 6.2	The AAPD and 99% confidence limits in the estimators for various deployments (λ) (nodes/m³) where $\gamma = 1.5$ and $N = 6$	88
Table 6.3	The AAPD in the CDE for various actual deployment densities λ (nodes/m³) where $\gamma = 3$, and $\hat{\lambda}_{CDE_1}$ (nodes/m³).	89
Table 6.4	The impact of the path-loss exponent (γ) on the CDE and the AAPD in the estimators where the actual deployment density is $\lambda = 5 \times 10^{-3}$ (nodes/m³), and $\hat{\lambda}_{CDE_1}$ (nodes/m³)	90

Table 6.5	The accuracy of different estimation AAPD results of $\hat{\lambda}_{IDE}$ (nodes/m ³), and $\hat{\lambda}_{CDE}$ (nodes/m ³), respectively when $\gamma = 1.5$	91
Table 6.6	The actual densities (λ) (nodes/m ³) versus the estimated densities ($\hat{\lambda}$) (nodes/m ³) for $\hat{\lambda}_{CDE_1}$ and $\hat{\lambda}_{CDE_6}$. The AAPD (%) results are also presented.	93
Table 6.7	When λ equals to $1(\times 10^{-4})$ (λ) (nodes/m ³), ($\hat{\lambda}$) (nodes/m ³) of $\hat{\lambda}_{IDE}$ and $\hat{\lambda}_{CDE}$ for different distributions are presented. AAPD (%) results are presented with their 99% confidence interval ($CI_{99\%}$).	99
Table 6.8	The AAPD and 99% confidence limits in the estimators for various utilization rates (%) with estimated density ($\hat{\lambda}$) and actual density (λ). Actual density (λ) is between the range in 2×10^{-9} and 7.5×10^{-9}	104
Table 6.9	The validation of the transmit power adaptation technique in (5.3) for various outage probability requirements P_O^* where $\lambda = 0.05$ nodes/m ²	105
Table 6.10	Required outage probability (P_O^*) vs calculated outage probability (P_O) by using the $\hat{\lambda}_{IDE}$, $\hat{\lambda}_{CDE}$, which are the global density of base stations, and AAPD (%) results.	119
Table 6.11	Required outage probability (P_O^*) vs calculated outage probability (P_O) by using the $\hat{\lambda}_{IDE}$ (nodes/m ³), $\hat{\lambda}_{CDE}$ (nodes/m ³), which are the local density results belong to each of BSs, and AAPD (%) results.	121
Table 6.12	The symbols, notations, values and units of the 3-D simulation parameters for DASAP.	122
Table 6.13	When the actual density value equals to $1(\times 10^{-4})$ (λ) (nodes/m ³), utility results (λ) (nodes/m ³) and $\hat{\lambda}$ (nodes/m ³) for different uniform and non-uniform distributions are presented. All AAPD (%) results are also presented with their 99% confidence interval ($CI_{99\%}$).	137

LIST OF FIGURES

FIGURES

Figure 1.1	An illustration of a FANET scenario where UAVs can communicate by using a single channel, and the density of UAVs is always changing which constructs a typical ad hoc network.	5
Figure 1.2	How network performance measures change while the network density is getting increasing when the slotted ALOHA protocol is employed, where the number of slots is equal to 1000, and $p = 1/63$, which is ideal for $\lambda = 4.5 \times 10^{-9}$	6
Figure 3.1	A scenario where the household is able to change the location of a femto-cell deployed inside the house.	40
Figure 3.2	Mobile or stationary BSs may form an ad hoc infrastructure to backhaul traffic to the core network; for example, when a stationary BS fails as we exemplify here.	43
Figure 3.3	Different interference sources [foreseen] in dynamic networks.	47
Figure 3.4	Impact of BSs density (λ) (nodes/m ³) on the probability of network outage (P_O) when the transmit power of base stations (P_t) is changing.	53
Figure 3.5	A cellular network scenario including a set of base stations, user equipment and a macro-cell for backhauling.	55
Figure 3.6	Impact of path loss exponent γ and density λ on aggregate interference from all nodes.	56

Figure 4.1 The illustration of the proposed density estimator. Three nodes in a randomly deployed ad hoc network, namely, the leader node L , the most distant node to the leader B and B 's most distant node C are shown. We use the distances to compute the effective area and assume that the leader knows the total number of nodes in the cluster. 62

Figure 5.1 The first mini-time slot called **estimation mini-slot** to perform the estimation of the UAV density (nodes/m³). Some of the UAVs are selected based on a selection probability as estimating UAVs, and others will be assigned as transmitting UAVs. The estimating UAVs can determine the effective UAV density by total signal strength on the estimation mini-slot from the transmitter UAVs in its communication range. Then, estimating UAVs use the estimated density by the selection probability to obtain the whole network density. The second mini-time slot named as **communication mini-slot** where UAVs can transmit their packets based on the dynamic channel access. 78

Figure 5.2 A MAC frame example with three UAVs and n time slots. Each of the UAVs send several packet replicas. Slots t , and $t + 2$ are successful transmissions. Slots $t + 3$, and $t + n$ are collided on the other hand slots $t + 1$ is a wasted slot. 78

Figure 5.3 Two sample scenarios in two estimation mini-slots. For the sake of simplicity, we present estimating and transmitting UAVs as different view-design. In the fact that, UAVs designates themselves independently and randomly with probability p_s as transmitting or estimating nodes locally. Communication between UAVs is performed with in the boundaries of corresponding UAV communication range. 79

Figure 6.1 The relative standard deviation (%) of the estimator for various cluster densities where $\sigma = 0$; i.e., no error in the measurements. 84

Figure 6.2 The comparison of the estimators based on average absolute percentage deviation (AAPD) where $\lambda = 0.05$ nodes/m². 85

Figure 6.3	Mean aggregate interference power (mW) for various deployment densities when $\gamma = 1, 1.5$ and 2 , respectively, and $P_t = 100 \text{ mW}$	88
Figure 6.4	The accuracy of different estimation, average absolute percentage deviation (AAPD) results of $\hat{\lambda}_{IDE}$ and $\hat{\lambda}_{CDE}$, respectively (nodes/m ³) when $\gamma = 1.5$	92
Figure 6.5	Collecting RSS measurements from the k^{th} nearest BS.	93
Figure 6.6	The estimator $\hat{\lambda}_{IDE}$ results along with different proximity indexes k where $\gamma = 3$, and $\lambda = 0.005$ (nodes/m ³).	94
Figure 6.7	The comparison of isotropic and anisotropic path-loss model for different estimations, and average absolute percentage deviation (AAPD) results of $\hat{\lambda}_{IDE}$ when isotropic $\gamma = 2$	96
Figure 6.8	The comparison of isotropic and anisotropic path-loss model for different estimations, and average absolute percentage deviation (AAPD) results of $\hat{\lambda}_{CDE}$, respectively when isotropic $\gamma = 2$	96
Figure 6.9	The Probability Density Function (PDF) of B Distribution vs. x parameter when different a and b parameters are used.	98
Figure 6.10	Averages of channel access probability results with using estimated density ($\hat{\lambda}$) and actual density (Λ) when the network density is increasing. Actual density (Λ) is between the range in 2×10^{-9} and 7.5×10^{-9}	102
Figure 6.11	Different deployment density values vs. channel utilization rates (%) with estimated density ($\hat{\lambda}$) and actual density (λ). Actual density (λ) is between the range in 2×10^{-9} and 7.5×10^{-9}	103
Figure 6.12	The impact of density on outage probability.	106
Figure 6.13	Transmit power adaptation based on estimated density ($\hat{\lambda}$).	107
Figure 6.14	Impact of density on outage probability for different transmit powers.	109

Figure 6.15	Impact of density on outage probability for various thresholds.	109
Figure 6.16	Impact of density on outage probability for different network conditions.	110
Figure 6.17	Impact of transmit power on outage probability for particular thresholds.	111
Figure 6.18	Impact of transmit power on outage probability for various deployments.	111
Figure 6.19	Impact of transmit power on outage probability different network conditions.	112
Figure 6.20	Impact of path-loss exponent (γ) and threshold (T) on outage probability for various deployments.	113
Figure 6.21	Impact of path-loss exponent (γ) and threshold (T) on outage probability for particular transmit powers.	113
Figure 6.22	Impact of path-loss exponent (γ) and threshold (T) on outage probability for different channel conditions.	114
Figure 6.23	Analytic outage values based on the estimated network density $\hat{\lambda}_{IDE}$ and $\hat{\lambda}_{CDE}$ for different transmit powers (P_t) when the network density is changing.	116
Figure 6.24	Collecting $\hat{\lambda}$ measurements (nodes/m ³) from the first k nearest UEs.	120
Figure 6.25	Time for different deployment densities vs. averages of channel utilization, waste and collision rates when $\lambda_{t+2} > \lambda_t > \lambda_{t+1}$, where $\lambda_{t+2} = 7 \times 10^{-9}$, $\lambda_t = 4.5 \times 10^{-9}$, and $\lambda_{t+1} = 2 \times 10^{-9}$, and channel access probability (p) is fixed and optimal for λ_t , $p = 1/63$, and the number of slots are equal to 1000.	125

Figure 6.26	Averages of channel utilization rates from the comparison results of DASAP with other opponents which are slotted ALOHA protocol and stabilized slotted ALOHA protocol while the network density is soaring, when the number of time slot is selected as 10000, and $\alpha = 0.9$.	126
Figure 6.27	Averages of channel access probability rates from the comparison results of DASAP with slotted ALOHA protocol and stabilized slotted ALOHA protocol while the network density is soaring, when the number of time slot is selected as 10000, and $\alpha = 0.9$.	128
Figure 6.28	Averages of channel utilization, waste and collision measurements when different number of time slots are selected.	129
Figure 6.29	Instant channel utilization measurements' averages of different subsequent time slots are utilized when different number of initial probabilities are considered, and α is selected as 0.5. The time is divided into 1000 time-slots.	130
Figure 6.30	Averages of instant channel utilization rates of different subsequent time slots are utilized when different number of UAVs (N) are considered, and $\alpha = 0.5$. The time is divided into 1000 time-slots.	130
Figure 6.31	How channel access probabilities change in different number of time slots. The averages of measurements are presented when different network scenarios, namely, different number of UAVs are considered.	131
Figure 6.32	Averages of channel utilization rates for different number of time slots when different network scenarios are considered.	132
Figure 6.33	Averages of channel utilization rates by considering different actual deployment densities when different number of time slots are utilized.	132
Figure 6.34	Initial channel access probabilities versus channel utilization error rates when p is increasing by 0.1 from 0.1 to 0.9, also a different p is changed depending on $(1/N)$ with different values of α . The number of time slots is 1000.	133

Figure 6.35	Averages fo channel utilization rates for different values of moving average smoothing factor when $\lambda = 7.5 \times 10^{-9}$ and number of time slot is selected as 1000.	134
Figure 6.36	Averages fo channel utilization rates for different values of moving average smoothing factor when $\lambda = 7.5 \times 10^{-9}$ and number of time slot is selected as 1000.	135
Figure 6.37	Different speeds of UAVs vs. channel access probabilities when different deployments are considered, and number of time slot is selected as 1000.	138
Figure 6.38	Different speeds of UAVs vs. channel utilization rates when different deployments are considered, and number of time slot is selected as 1000.	139
Figure 6.39	Different network optimization time intervals vs. channel access probabilities when different deployments are considered, and number of time slot is selected as 1000.	140
Figure 6.40	Different network optimization time intervals vs. channel utilization rates when different deployments are considered, and number of time slot is selected as 1000.	140



CHAPTER 1

INTRODUCTION

As wireless technologies continue to enter users' lives rapidly, it is also clear that there will be an increasing demand for wireless data services when this trend is combined with the massive growth of the Internet. Next-generation wireless networks are expected to be a mixture of data traffic such as messaging, web browsing, and file operations, as well as traffic that requires real-time and high data rates such as voice, multimedia content, and games [1]. All of these applications will require increased quality of service (QoS) and better coverage. Various wireless network architectures have been designed to support data traffic over wireless media. A wireless network is able to connect two or more nodes via radio waves. There are various types of wireless network architectures, such as ad hoc networks, mobile cellular networks, and flying ad hoc networks that we address in this thesis. The characteristics and definition of a network node change depending on the network type. For instance, the nodes can be called sensors for ad hoc networks, small base stations and user equipment for mobile cellular networks, drones, or unmanned aerial vehicles for flying ad hoc networks. The distribution and deployment of these nodes, depending on the requirements, present a critical parameter, the density of nodes. Density implicitly incorporates the number of nodes. Density correlates the number of nodes in a spatial manner and adds the location information and distance implicitly in the model. In self-organizing networks, it should be known how the distribution of the nodes change, in which part of the topology the nodes come together, or which part of the topology is sparse. The effective area of the topology is crucial to understand the resolution of the distribution of the nodes so that changing the network functions based on run-time variations. To do so, we need to know both the number of nodes and the location information at the same time. In this thesis, we concentrate on the

network density that is defined as the number of nodes per unit area or volume.

In ad hoc networks many challenging aspects such as mobility management, localization, sleep scheduling, energy-aware applications for efficient consumption, clustering, interference management, capacity and coverage require dynamic, self-configurable and reliable distributed solutions to make network performance better [2, 3, 4]. Mobile ad hoc networks (MANETs) draw considerable attention with respect to their intrinsic characteristics such as dynamically changing network topology, limited resources, and multi-hop communication. Therefore, MANETs necessitate self-configurable, self-organizing, energy-aware and density-adaptive solutions [5, 6, 7]. Clustering is a promising solution for ad hoc networks in terms of network performance, resource and topology management [7]. In addition, since MANETs have a dynamic topology because of nomadic nodes or node failures, the density of nodes in such dynamic networks always changes. The network density should be considered while performing clustering since it significantly impacts the network performance and network operations [8].

A new trend for future networks is emerging along with the recent applications, innovations, and technologies in cellular networking. In order to meet the requirements of emerging applications for a larger capacity, cellular networks morph away from inflexible and centrally-managed infrastructures to large-scale collectives of small and mobile cells. Cellular networks equipped with mobile and nomadic base stations present a change in the characteristics of networks toward densified deployments of mobile base stations (BSs), incessantly changing topologies and dynamic infrastructures [9, 10]. The dynamism in the infrastructure reflects itself as unpredictably base station density introducing some new challenges that have to be managed at run-time [11]. Most of the changes in the topology are not predictable in advance [12]. Hence, applications such as capacity planning, coverage control, interference management, energy conservation and quality of service provisioning have to be critically modified for efficient and proper operation by taking into consideration of future trends [9, 10, 13].

Density of base stations in future cellular networks, e.g., 5G networks, will vary in time and space because of mobile base stations (e.g., cell on wheels and unmanned

aerial vehicles (UAVs) [9, 14], user-controlled base stations [15] (e.g., femtocells bought and controlled by end users), green operation (e.g., sleep scheduling of base stations), and gradual deployment of base stations [16, 17]. Resources in radio access, transport, and core networks will be wasted if related parameters are not adapted to the network density [18]. For instance, in Section 6.2.2.1, it is illustrated that any changes in the base station density affect the network parameters such as transmit power and network outage [19, 20]. A decrease in the network density increases the outage probability. If the network is dense, the outage probability will then decrease with the same transmit power. For adapting the network to the changes in the density of base stations, robust network density estimators in a three-dimensional field are required [20, 21]. We assert the third dimension considering drone base stations (cells on wings).

The need for energy-efficient dynamic networks presents the concept of cell zooming [22]. Cell zooming concept may include different schemes such as controlling the physical layer parameters like changing transmit power of the base stations, relying on relaying, sleep scheduling of base stations, or employing multiple base stations [23, 22]. Algorithms for cell zooming can be classified into: static and dynamic algorithms. Considering the network density together with the transmit power is presented as a solution in the scope of cell zooming [20]. Adapting and optimizing the transmit power with the help of user equipment, reducing energy consumption without switching off base stations, determining the optimal height of the antenna of base stations, considering received signal strength (RSS) with a propagation model are presented as self-healing approaches under the concept of cell zooming [24, 25]. In this thesis, we control the cell size dynamically with the help of an density-adaptive transmit power mechanism considering outage probability and effective density of moving base stations.

Unmanned aerial vehicles (UAVs) have been increasingly used in many aspects of life, especially in civilian and military applications under the favor of advances in communication, avionic, and sensor technologies in the last decades [26]. Thanks to their flexible and capable structures, UAVs can easily be deployed by controlling remotely or autonomously [27]. They can be utilized in different applications such as disaster management, search and rescue operations, smart agriculture oper-

ations, traffic monitoring, relaying for ad hoc networks [28, 29, 30]. All of these applications require low-cost, scalable, survivable, faster, and reliable protocols to provide an efficient data delivery and channel utilization [31]. Instead of a single UAV, multiple UAVs can come together and communicate with each other to meet these requirements. Many of the unmanned aerial vehicles construct a typical ad hoc network, which is called flying ad hoc networks (FANETs) [32, 33]. A FANET is a special kind of vehicular ad hoc networks (VANET) and mobile ad hoc networks, but there are some critical differences such as higher mobility degree, more frequent topology changes, larger distances between nodes (UAVs), and the dimension of the network [34, 35].

In this thesis, we propose a dynamic slotted-ALOHA-based medium-access control approach for FANETs. Our dynamic random access approach is composed of two substantial steps: one of them is the estimating the UAV density, and the second step is the adaptation of the channel access probabilities of UAVs based on the estimated UAV density. We claim that by considering the density of UAV whether sparse or dense we can find an optimum channel access probability of each UAV in addition to maximize the channel utilization. Our approach guarantees that the density of UAVs can be known by each UAV or infrastructure. In that sense, we need to answer the following questions.

What does UAV density mean? In FANETs, the number of UAVs per unit volume is defined as the density of UAVs measured in nodes/m³ [36, 37]. Why is the UAV density ever-changing parameter in FANETs? In a FANET, UAV density may continuously experience temporal and spatial changes due to high degree of mobility in addition to other factors such as failures of UAVs and instant deployments [38, 39]. Bearing this fact in mind, if the network functions and parameters are adapted to UAV density, then valuable resources such as communication channel will be utilized efficiently, otherwise the wasting resources will be inevitable. Towards this aim, FANETs require accurate, fast and simple estimators. Since FANETs have an agile and highly mobile technology which provides a flexible and fast deployment, in addition they are battery-powered devices and requires efficient energy consumption instead of complex computational power. It is important to propose fast, simple and accurate solutions for FANETs. Since receive signal strength is prone to network

conditions the accuracy is also significantly important [40]. How can we estimate UAV density of a FANET requiring three dimensional solutions? Flying nodes have also a key difference which is the dimension of the network [41]. FANETs require three dimensional solutions since we need to consider the height of a UAV which is a special characteristic element of a FANET. We also fill this gap in this thesis. We propose a three dimensional interference-based density estimator (IDE) for cellular communication in [42]. We also utilize and improve IDE to perform in FANETs to enhance channel utilization.

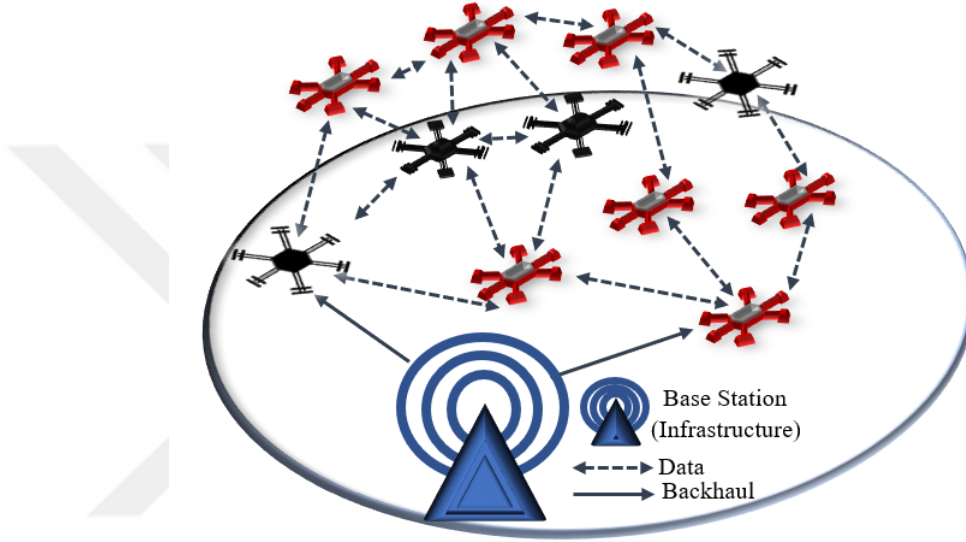


Figure 1.1: An illustration of a FANET scenario where UAVs can communicate by using a single channel, and the density of UAVs is always changing which constructs a typical ad hoc network.

Why is the random channel access scheme such as slotted ALOHA protocol (SAP) important for UAVs' communication in FANETs? A FANET requires an efficient collaboration and coordination among UAVs [43]. UAV-to-UAV links can be used in FANETs instead of UAV-to-infrastructure links as shown in Figure 1.1 [44]. Multiple UAVs may share the same medium to communicate with each other. We need efficient protocols to manage the shared medium by preventing the collisions and providing a fair transmission channel [44, 32]. However, the coordination of all UAVs before the transmission is inapplicable. Simple random access techniques promise effective and applicable solution to this problem. However, the random access protocols require

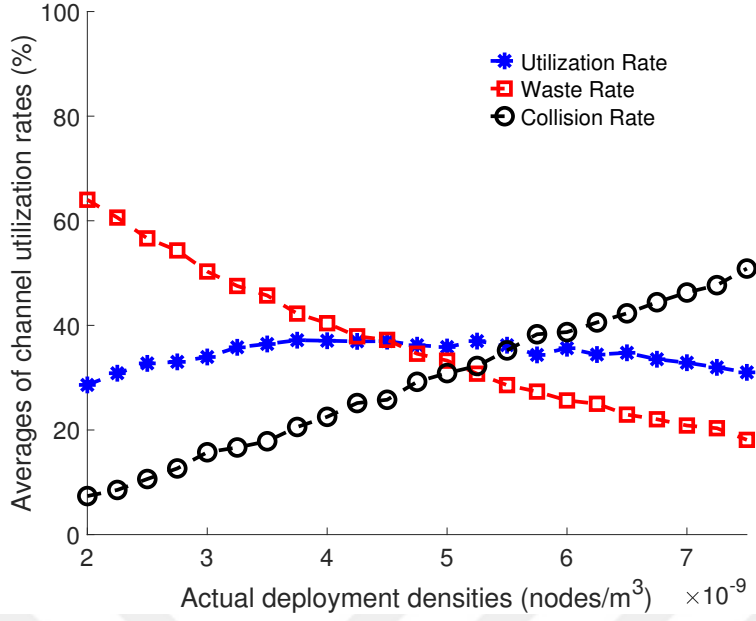


Figure 1.2: How network performance measures change while the network density is getting increasing when the slotted ALOHA protocol is employed, where the number of slots is equal to 1000, and $p = 1/63$, which is ideal for $\lambda = 4.5 \times 10^{-9}$.

an adaptive scheme to manage resources and control protocol against ever-changing UAV density in FANETs [45]. The random access approaches can be roughly categorized into two parts: the methods are based on the dynamic frame length, and the second one is on the basis of the dynamic random access probability [46]. Random access schemes such as slotted ALOHA is utilized in many technologies including Radio Frequency Identification (RFID), Random Access Channel (RACH) of Long Term Evolution (LTE), Narrow Band Internet of Things (NB-IoT), Weightless, and satellite communication systems [45, 47, 48]. In RFID technologies a slotted ALOHA based contention-free channel access mechanism is used. In cellular networks, user equipments (UEs) utilize contention free or contention-based procedure leveraging slotted ALOHA protocol to carry out initial network association, make a request for transmission resources, and perform a connection re-establishment to the base station (eNodeB) in LTE technology. NB-IoT and Weightless systems utilize also a slotted ALOHA scheme [47]. In this thesis, we chose a slotted ALOHA scheme by considering the following reasons: First of all the slotted ALOHA protocol based models have an analytic simplicity [39]. Moreover, it is implemented and performed eas-

ily as MAC protocol. SAP also is still utilized for the initial access in both satellite communication and cellular terrestrial networks as stated in [48].

How can we enhance the slotted ALOHA protocol using with UAV density? In our thesis, the proposed scheme leverages the estimation of UAV density based on received signal strength, which uses the aggregate interference power on a channel. Since FANET topologies always change, estimating the density of UAVs provides the effective number of active UAVs information in a frame. By using the density information which should be as accurate as possible, we can update the access probability of active UAVs in a slotted ALOHA scheme [49]. In that sense, we can divide the channel into time slots [50]. The slotted ALOHA protocol has the same behaviour [51, 52]. However, the slotted ALOHA protocol has some deficiencies such as its utilization is not always close to 37% and the nodes do not know how they should update channel access probability since the number of nodes is always changing at run-time [33]. Moreover, SAP gives fluctuated utilization results instead of maximum stabilized results as demonstrated in Figure 1.2 when UAV density is getting denser or sparse. Why and how can UAV density be used as an optimization parameter for network communication? We claim that each node can independently set its own channel access probability by estimating the effective number of active nodes per unit volume. The fact that centralized configuration or real-time centralized monitoring are not applicable due to the difficulties in acquiring global information about the network and computational complexity of the management and optimization tasks require solving NP-hard problems [53]. In this thesis, considering the dynamic topology of the network, with the possibility of UAV-to-UAV communication, a dynamic and distributed channel access scheme based on density-awareness is proposed.

All in all, dynamic networks require self-organized solutions to make the network performance better and provide efficient resource usage. It is clearly seen that there is a great expectation for the adaptive solutions to control the dynamic topology. We fill this gap in this thesis by proposing density-aware and -adaptive network protocols and applications.

1.1 Problem Definition

Next-generation networks, including mobile ad hoc networks, flying ad hoc networks, and cellular networks, are dynamic networks since node density, which is defined as the number of nodes per unit area or volume, always changes due to the human-made and environmental factors. In order to provide increasing user demands, the network performance should consider this dynamism at run-time. However, static configurations before and after deployment are not practicable since some problems such as unsteady coverage, higher interference, and more energy consumption may arise. To make a network self-organized requires flexible run-time configurations such that nodes in a network can adapt their parameters such as their transmit power to the density variations. We need to know the effective density of a network to tackle these problems caused by dynamic topology. We have to develop robust network density estimators. By using the density estimators, for instance, network coverage can be adapted to the network density changes. Since future networks resemble ad hoc networks, the topology always changes. Therefore, this thesis addresses adaptation to these variations by proposing novel network density estimators that can easily be implemented in any wireless communication stack, and new density-aware and -adaptive protocols leveraging the density as a network optimization parameter.

One of the most important contributions of this thesis is the interference-based density estimator (IDE), which benefits from received signal strength measurements within each node's communication range. Assume that we have a meeting. Participants can communicate with each other. While the number of participants is increasing, if we want further participants to hear us, we should raise our voice or vice versa. This case is similar to a cellular network scenario. Assume that there are mobile base stations called small-cells in a specified volume. If the number of small cells increases in this environment, the aggregate interference in the environment increases. One of the outcomes of this thesis reveals this relationship between the network density and the aggregate interference power, which results in a novel density estimator design for mobile networks. Let us consider a wireless network for a three-dimensional Euclidean space where there is uniform randomly deployed nodes with a density ($nodes/m^3$). Assume that a node is selected as a reference node in this network and receives power

signals from its k^{th} nearest neighbor. Each node can measure received signal strength (RSS), which is a function of the distance between two nodes. The simple path-loss model that we choose as the channel model provides received signal strength calculation between two nodes by considering the estimated distances. We assume that each node has the ability to measure the aggregate interference power with the summation of received signal strengths from the closest k neighbors and calculate the density. Obtaining effective density measurement facilitates optimizing the network performance parameters and adapting the communication protocols.

In this thesis, we present novel techniques for estimating nodes' density in a multi-dimensional Euclidean space. The estimators are based on received signal strength. The proposed analytic models follow a Poisson distribution, and the simple path-loss model is used as the propagation model. Then, we present the density-aware outage model. On top of the network outage and node density, we propose a density-aware transmit power adaptation technique for coverage control and a density-adaptive channel utilization protocol in wireless networks where the number of nodes varies in time and space.

1.2 Motivation

Growing communication technologies and heterogeneous networking architectures such as multi-access edge computing, cloud computing, cells on wings and wheels, mobile ad hoc networks add a new dimension to the existing network characteristics. With the arrival of the last developments, the next-generation networks have to be self-configurable instead of steady configurations in order to meet rapidly rising users' expectations, and provide the required services for many applications requiring fast deployments and real-time data such as smart city applications, smart agriculture, military services, rescue operations, and disaster management. There is a great expectation for self-organization and adaptation to run-time variations in the upcoming network management solutions. Research on new network management approaches is widespread in recent years. This trend motivates us to study on this research.

Future wireless networks have a dynamic topology since the number of nodes always changes because of high mobility, instant deployments, sleep scheduling, green oper-

ations, and node failures due to natural disasters or human-made factors. To increase the network capacity and quality of service, the network's density and the protocols have to be adaptive to these changes. Otherwise, the resources may not be used efficiently, and problems such as high interference, network congestion, patchy coverage will increase. If the network performance parameters and protocols in the communication stack are designed dynamically, network coverage and capacity problems will lessen. Moreover, we can gain energy efficiency by providing density-adaptive protocols such as using the adaptive transmit powers. Therefore, making the networks self-organized and -healed motivates us to research on this topic.

1.3 Methodology

In this thesis, the most important expected result is to make the future wireless network density-adaptive and -aware. In that sense, our methodology is progressed by answering and analyzing the following open research questions:

- Why do the next-generation networks vary the existing architectures?
- Why are the static and human-made configurations not suitable for the new network paradigms?
- Why we need self-organized and run-time adaptable network functions?
- Which developments make wireless networks dynamic?
- What is a density-aware dynamic mobile network?
- How does network density change?
- Why is the density of nodes critically important?
- Why must network operators consider the network density as an optimization parameter?
- Why may the proposed solutions without considering network density fail?
- How can we accurately estimate the effective network density?

- Which spatial distribution can be used for modeling the network density?
- How can we utilize the network density in networking applications and network communication stack?

In this regard, our solution method includes the following steps: firstly, we present a comprehensive analysis to exhibit the opportunities and challenges in density-aware mobile networks. Secondly, we propose novel RSS-based density estimator models following Poisson distribution and validate them using Monte Carlo simulations. The distance matrix-based density estimator is proposed by considering the clustered ad hoc networks. We also introduce interference-based density estimator, and multi-access edge-cloud based density estimator for mobile cellular networks. We then improve interference-based density estimator for flying ad hoc networks. As the second part of our solution, we present the relationship between the network density and network performance parameters. Herein, we also suggest density-adaptive networking protocols regarding network outage, transmit power adaptation, and channel utilization. The density-aware and -adaptive models are also validated by leveraging the Monte Carlo simulations. Finally, we observe and present the simulation outcomes. We manifest the relationship between the nodes' density and network performance parameters by conducting different analysis results examining the impact of parameters on network density and the impact of the network density on other network performance parameters.

1.4 Contributions

In this section, we summarize the contributions as follows:

- The first contribution is that we present a new paradigm, which is density-aware dynamic mobile networks, into the forefront by exhibiting dynamic infrastructure with moving base stations in addition to stating the inadequacy of present architectures in Chapter 3.
- As the second contribution, a qualitative and novel analysis of network density is presented. Section 3.2.4 claims that the network density is a crucial param-

eter since it substantially influences the dynamic network performance. We classified and explained the density estimators in dynamic networks in Section 3.2.5.

- Challenges and enablers in density-aware mobile networks are extensively exposed by considering the dynamic topology in a mobile network as the third contribution. In Section 3.3, the opportunities that can be achieved by adapting the BS density in the current mobile and wireless networks are investigated in a comprehensive manner. We present an extensive list of research challenges in Section 3.3 by discussing them in detail.
- We reveal how the density of base stations can be leveraged, and we illustrate the idea behind this thesis, which is the density-adaptive solutions in Section 3.3. For example a novel aggregate-interference technique is presented to control the interference based on the density changes. Finally, the most prominent ideas are summarized and concluded in Section 3.4.
- We propose a simple, fast and accurate density estimator based on distance matrix in clustered ad hoc networks exhibited in Chapter 4.
- We also present a density-aware and -adaptive transmit power adaptation technique that considers outage probability in two-dimensional fields. In contrast to the related work, we focus on proposing a simple, fast and distributed technique.

In this thesis, we also have contributions for future cellular networks including novel density estimators and network outage in order to adapt the transmit power of base stations for cell zooming in three-dimensional networks.

- The most prominent contribution of this thesis is the interference-based density estimator presented in Section 4.2. Using an aggregate interference model, we propose a system design for density estimation of moving base stations in mobile networks in Section 4.2.2.1. Moreover, we propose multi-access edge cloud-based network density estimator in a three-dimension field in Section 4.2.2.2 following the same approach employed in [54, 55] which was developed for two-dimensional ad hoc networks. Most of the existing density estimators are operational only in two-dimensional Euclidean space. Satisfying

the requirements for having a three-dimensional estimator in mobile networks is the gap this thesis fills in. The interference-based density estimator (IDE) is modeled considering uniform randomly deployed a network of base stations. We validate the proposed estimator by Monte-Carlo simulations. The simulation results validate the model and show the accuracy of the proposed estimator is at an acceptable level.

- A novel outage model based on the density is introduced in Section 5.1.2. We analyze the impact of network density on outage probability in cellular networks by employing a simple analytic model validated by simulation results in Section 6.2.2.1. A concise and simple analysis is the main difference of this contribution from other studies. We propose an analytic model for computing the outage probability based on base station density and validate it using Monte-Carlo simulations. Outage probability analysis in three dimensions is the novelty of the work. The results of this thesis assert that density-awareness in cellular networks is required to increase capacity and provide an efficient network.
- We propose a density-aware transmit power adaptation technique which makes a relation between the density of base stations, network outage, and transmit power presented in Chapter 5. By using the proposed density estimator, moving or stationary base stations will be capable of adapting their transmit power in a distributed fashion. The results of this thesis assert that density awareness in cellular networks is required to increase the capacity and provide an efficient network.
- As a contribution for FANETs, a new density estimator design is the enhanced aggregate interference based density estimator with a dynamic access probability mechanism presented in Section 5.3.
- We also propose a novel probabilistic density-aware channel utilization protocol which is called Density-adaptive Slotted ALOHA Protocol (DASAP) explained in Section 5.3.1. Since a FANET has a three dimensional architecture, our model provides a three dimensional approach which is also different from the existing solutions by considering the slotted ALOHA solutions in the liter-

ature. Compared to the existing alternatives in the literature which are slotted ALOHA protocol, and stabilized slotted ALOHA protocol (STAP), the proposed design is more stabilized, and can be easily implemented in any wireless communication stack.

1.5 Structure of the Thesis

In this section, we present the structure of this thesis.

- Chapter 2 summarizes the related work in comparison to our proposals, and provides important background information regarding the existing solutions. This chapter reviews the existing studies that show the importance of base station density, network outage and transmit power as run-time adaptable and self-optimized parameters for self-organized future networks.
- In Chapter 3, we present the density-aware mobile networks in addition to opportunities and challenges by considering the recent networks' key paradigms. This chapter manifests the importance of the network density and how it is utilized as a network optimization parameter.
- In Chapter 4, we explain our proposed density estimation models for different types of network such as ad hoc networks, cellular networks, and flying ad hoc networks. Our proposed models are easily can be implemented for any wireless network communication stack. We present the density estimators with the detailed analysis of each of these three network architecture.
- Chapter 5 presents proposed density-adaptive and -aware applications. Density-aware network outage model for two-dimensional and three-dimensional wireless networks, the density-aware transmit power adaptation (DTPA), and density-aware channel utilization techniques are explained in this chapter.
- In Chapter 6, validation of the analytic models of density estimators and approaches for density-adaptive and -aware protocols and network parameters in the communication stack are demonstrated. We use Monte Carlo simulations and MATLAB environment for this thesis.

- Chapter 7 concludes this thesis by bringing important results and discussions into the forefront in addition to making a summarize of the thesis.





CHAPTER 2

BACKGROUND AND RELATED WORK

This chapter presents the state of the art about the network density estimators and approaches using network density as an optimization parameter by discussing the literature regarding ad hoc networks, cellular networks, and flying ad hoc networks, respectively.

2.1 Ad Hoc Networks

In ad hoc networks the variations in density impact performance, and introduce many challenges. Take slotted Aloha, the simplest random access protocol, as an example. In dense networks, collisions will considerably degrade the performance of the network. Whereas, slots will not be utilized if the channel access probability is not adapted to the density in sparse networks. Density-awareness is required in communications stacks for resource-efficient operation. Therefore, we need fast and robust density estimators. We fill this gap in this thesis for clustered ad hoc networks. We also demonstrate how to apply the proposed estimator by developing a density-aware transmit power adaptation technique.

Density estimation is easy if nodes are equipped with auxiliary positioning systems such as GPS. An example application of such location-based proposal is node census (NC) [54]. Auxiliary systems consume extra energy that may not be adequate for ad hoc networks where devices are battery-driven. Furthermore, auxiliary systems may not be reliable because of their intolerance to jamming. For density estimation, some parameters that are correlated with density have to be measured. For instance, the amount of traffic flowing over a node may be indicative of density of other nodes

in vicinity. NEST [54] is an example of such neighbor discovery based approaches. Their accuracy may be low and very much dependent on the measured parameter. When density estimation is based on the forwarded number of packets as an example, the accuracy of the estimator is prone to variations of traffic generation rate of neighbors.

Another way to estimate density is to employ some parameter that is closely correlated with distances among nodes such as the received signal strength (RSS). Received signal strengths of packets from neighbors of a node indicate the proximity among nodes. However, wireless signals are prone to many uncontrollable factors such as fading or shadowing. These types of estimators that are based on signal strength may be fast but their accuracy depends on the environmental factors. Whether or not line-of-sight exists impacts the quality of the estimators. An example of signal strength based estimator is presented in [54] for ad hoc networks. To compute that estimator in a cooperative fashion may take a long period of time making it inapplicable in highly-mobile ad hoc networks.

2.2 Cellular Networks

In this section, we present the state of the art by asking the critical questions regarding the distribution of base stations, the impact of the base station density on network performance parameters such as network coverage and capacity, existing density estimation approaches, the relation between the channel conditions, aggregate interference, and base station density.

2.2.1 Distribution of Base Stations

In cellular networks, the spatial distribution of base stations in order to obtain optimal deployments has been coming into prominence. The stochastic models including optimum base station density have paramount importance to analyze the network performance in terms of coverage, energy efficiency and quality of service [56, 57]. With the improvement of the network, to provide higher capacity and coverage to users, increasing the number of base stations is considered as a handy solution which is called

densification. Moreover, with the proliferation of base stations on wheels and wings, small cells, and the user-controlled base stations always result in topology changes in the network. In that sense, analyzing the spatial distribution of base stations by using the theoretical models is always a principal topic in wireless networks and still an open research question for next-generation networks [58]. Although there are different statistical distributions models such as Poisson, lognormal, Weibull, generalized Pareto and alpha-stable in order to model the base station spatial density, most of the studies leverage Poisson due to tractability as stated in [58]. In addition to the base station density, the recent studies reveal that the stochastic models including PPP provide tractable models to control the cell size by considering the coverage probability and adaption of transmit power [56, 59, 60]. To provide an enhanced quality of service, mobile base stations and drone base stations can be used as fast deployments, however, these networks require to transmit power adaption in terms of energy efficiency, trajectory plans, and user connectivity [61, 62, 63]. Transmit power can be minimized by increasing the number of base stations until the network density reaches a threshold value. The optimal network density provides an optimum power consumption and enhanced coverage as stated in [64].

2.2.2 Existing Density Estimation Methods

Since future cellular networks has a dynamic topology, the need for the existence of robust density estimators is an open issue. Existing density estimators can be classified as (1) location-based; (2) neighbor discovery based, and (3) received signal strength (RSS) based methods. Location-based methods rely on GPS; e.g., node census (NC) [65]. Auxiliary systems consume extra energy, and the density estimate is subject to localization errors. Neighborhood discovery based methods estimate density based on inferences drawn from in-network communication; e.g., NEST [66]. The accuracy depends on the traffic amount. The RSS-based density estimators are proposed in [54, 55] for two-dimensional ad-hoc networks. This type combines the merits of location-based and neighbor discovery based estimation and overcomes their drawbacks. However, the time required to compute the estimator may be long.

2.2.3 How Density of Base Stations affects Network Coverage and Capacity

Ultra-dense networks (UDN) are expected to provide high capacity. The potential of higher frequency bands is analyzed in [67]. In that work, UE and BS density, UE distribution and energy efficiency in a network are used to calculate transmit power by considering signal-to-interference-plus-noise ratio (SINR) for providing better coverage. In a mobile network consisting of a large number of uniform randomly deployed BSs, the outage probability decreases with an increasing ratio of mobile-to-BS density [68]. An interference model for wireless networks consisting of uniform randomly distributed nodes is combined with different types of popular fading models in [69]. This model considers the interference power by using a partial cancellation method and outage probability calculated by using the nearest interferer instead of the total interference power since the nearest interferer dominates the total interference. A stationary receiver is considered as a base station for a given user and the same transmit power is considered for mobile units.

In the case of 5G networks, connectivity and coverage are two important optimization parameters related to each other, and designers should consider them jointly as in ad hoc networks [70, 71]. It is underlined that the connectivity problem may not be handled without adapting the transmit power to the network via presenting the results with two-dimensional simulations and models applying the connectivity of nodes, transmit power and density for an ad hoc network. As the dynamic and distributed nature of the future networks' architecture, mobile ad hoc networks have a distributed and self-organized structure [72]. One of the sample applications of MANETs is the vehicular ad hoc networks. [73] states that such networks have a dynamic structure that necessitates adapting the transmit power to some parameters network such as distance between mobile nodes, density, the antenna type and type of broadcasting for enhancing network performance. Density and distance are the selected parameters for adapting transmit power in [73]. Density refers to the number of nodes in a network per unit area. In dense networks, the distance among nodes will be shorter. On the other hand, the distances among nodes will be larger when the network is sparse. Hence, if the network is sparse, the transmit power should be increased based on the distance between the nodes, but if the network is dense then we need less transmit

power since the distance between nodes will be smaller. However, we should consider the outage and the interference in the network [13, 74]. When the network is sparse, the probability of outage will be higher and when the network is dense then the interference between nodes will be higher if the transmit power is not adapted to these changes.

2.2.4 Relation between Aggregate Interference, Path-loss and BS Density

Understanding the characterization of aggregate interference power in terms of the base station deployment and interference management can provide better performance for homogeneous and heterogeneous networks [75]. Joint power control and user scheduling are proposed for ultra-dense networks by considering dynamic channel conditions and unknown traffic demands in [76]. The aim of this model is to ensure energy efficiency while supplying the quality of service and reducing the number of UEs in outage depending on queue capacities of BSs. The network outage is considered the fraction of undesired UEs whose handovers cannot be admitted because of the queue capacity limitations, and the density is determined as the average inter-site distance (ISD) for a large homogeneous UDN deployment. In addition to homogeneous cellular networks, a heterogeneous network is considered, and a model consisting of optimal BS density by conceiving the QoS limitations is analyzed in [77]. The proposed model aims at making the network energy efficient and analyzes the effect of network density on cost. A threshold value obtained by using path-loss and transmit power of the relevant BS is used to define outage probability.

With the proliferation of small cells, the fractal characteristic of the coverage for cellular networks is more prone to the path-loss effects [78, 79, 80]. In small cells, the characterization of wireless propagation environment is volatile and complicated as stated in [78] on the occasion of not only regular but also non-uniform obstructions arising from buildings, infrastructures, trees, and erratic weather conditions. Both the line-of-sight and non-line-of-sight signals affect the path-loss exponent value or path-loss coefficient. Two different path-loss models are introduced, which are isotropic and anisotropic by considering propagation directions. Isotropic models are commonly used in the literature to make models simple as much as possible. However,

due to the fractal characteristics of cellular networks, the anisotropic models can be leveraged to make network models more realistic [79]. In this thesis, we exploit a simple path-loss model which is simplified from Winner II channel models to propose simple and easily tractable models [81]. This model has already been analyzed in [54], and it is illustrated that the RSS-based approaches including simple path-loss model may be used for real-life experiments with 10 percent error rate.

In this thesis, unlike the existing works firstly we propose novel base station density estimators, the interference-based density estimation and multi-access edge cloud-based estimation based on received signal strength, which are operational in a three-dimensional environment. Secondly, two proposed models to control the network outage and cell size are simple and compact solutions. Finally, we present a qualitative and elaborated analysis of different network parameters at the same time depends on the network density. The proposed approaches leverage a three-dimensional Poisson Point Process distribution which provides easily understandable and tractable models.

2.3 Flying Ad Hoc Networks (FANET)

Although the use of unmanned aerial vehicles has been increasing due to their flexible and easily deployable structures, the nature of the flying ad hoc networks where each of UAVs have a data to send and all communication is performed in one wireless shared medium brings up a question [51]: How we can prevent collisions due to the same transmission attempts at the same time and each node can access the channel to make communication with other nodes or a sink point such as a base station in a fair way? The random access schemes are a handy solution to these questions. At this point, the authors in [82] point out the importance of the random access approaches and develop an efficient random access graph-based protocol by utilizing the successive interference cancellation method in which the collision slots are transformed into a transmission recovery slots.

The pure ALOHA approach allows the UAVs to make a transmission whenever they have a packet to send. However, in slotted ALOHA, each UAV's transmission is based on a random access scheme where time slots are created for each UAV can send their

packets depending on an access probability at the beginning of the time slots [46]. The random access approaches such as slotted ALOHA as a medium access control provide an independent but an access probability-based transmission medium without the coordination between the nodes [83]. With such protocols, while some nodes make a transmission, the others become listeners by considering the probability of access. They reveal how the importance of the accurate estimation of the number of active nodes/users is, and their dynamic access probability scheme can provide an efficient approach.

In FANETs, the number of UAVs may not be known certainly. Hence, random access protocols can be developed for these scenarios. In this case, the protocols need an accurate estimation of the number of active users to better network performance [84]. If the number of active users is obtained, then there are different types of random access schemes that consider the estimation result [85]. Estimating the number of active transmitters during the current frame, then tuning the access probability in the next frame approaches is proposed in [46]. To optimize the channel access probability and make it dynamic, the density of nodes is leveraged as presented in [86].

In random access techniques, each node's transmission probability can be different, and these probabilities can be determined based on the number of nodes. In that sense, [49] proves a strong relationship between a dynamic transmission probability, channel utilization, and the number of nodes. In a slotted ALOHA-based ad hoc network with a multi-hop architecture, each node can transmit their packets based on a different transmission probability, and these probabilities can be updated by using the number of each node's neighbors. A flying ad hoc network is a special kind of vehicular ad hoc network. Hence, the solutions for such an ad hoc network can be considered candidate approaches for FANETs, although there is room for improvement if we consider the differences between these two network architecture and features. In VANETs, the mobility factor affects the network's capacity and connectivity due to the ever-changing density of vehicular. To optimize a vehicular ad hoc network channel throughput and transmission probability of vehicular, the density of vehicles and slotted ALOHA protocol, which is analytically simple, is proposed and the dynamic access probability for a vehicular ad hoc network [39].

All in all, since slotted ALOHA is easily implemented in the network stack, and the impact on the UAVs' or nodes' density is presented, a dynamic access scheme implementing the slotted ALOHA as the communication protocol based on the effective density is proposed in three-dimensional for FANETs in comparison to other researches.



CHAPTER 3

DENSITY-AWARE MOBILE NETWORKS : OPPORTUNITIES AND CHALLENGES

We experience a major paradigm shift in mobile networks. The infrastructure of cellular networks is becoming mobile since it is being densified also by using mobile and nomadic small cells to increase coverage and capacity. Furthermore, the innovative approaches such as green operation through sleep scheduling, user-controlled small cells, and dynamic end-to-end slicing will make the network topology and available resources highly dynamic. Therefore, the density of dynamic networks may vary in time and space from sparse to dense or vice versa. This thesis advocates that density-awareness is critical for dynamic mobile networks. Mobile cells, while bringing many benefits, introduce many unconventional challenges that we present in this thesis. Novel techniques are needed for adapting network functions, communication protocols, and their parameters to the network density. Especially when cells on wheels or wings are considered, static and man-made configurations will waste valuable resources such as spectrum or energy if the density is not considered as an optimization parameter. In this thesis, we evaluate the dynamicity of nomadic cells in density-aware mobile networks in a comprehensive and articulable way. The main challenges we may face by employing dynamic networks and how we can tackle these problems by using a density-oriented approach are discussed in detail. As a key concern in dynamic mobile networks, we treat the density of base stations, which is an indispensable performance parameter. For the applicability of such a parameter we present several potential density estimators. We epochally discuss the impact of density on coverage, interference, mobility management, scalability, capacity, caching, routing protocols, and energy consumption. Our findings illustrate that mobile cells bring more opportunities in addition to some challenges which can be solved, such as

adapting mobile networks to base station density in this chapter.

3.1 Introduction

The latest technology in a mobile cellular network has been the stationary, relatively inflexible, and centrally-managed architecture which is not scalable. The recent networks have already encountered the spectrum restrictions. To cope with coverage and capacity problems, we have to make cellular networks dense by employing mobile or nomadic cells. However, deploying more mobile base stations (BSs) may result in huge interference and redundant coverage causing wasted energy [87]. In such cases centralized solutions are not operable because of computational complexity of the jobs and the challenges in globally obtaining dynamic network information. For instance, optimization of network coordination and management require overcoming NP-hard problems in general.

The evolution and proliferation of the technologies bring along rapidly increasing users demands such as more bandwidth, a higher speed of the services with lower latency, and the Internet anywhere [88]. To meet these requirements and to enhance the quality of service (QoS), 5G networks are introduced with a new network architecture and novel technologies to ensure low latency, higher bandwidth, and to support higher mobility rates. In order to increase the network capacity, the cell densification is presented as a promising solution. Densification, which is increasing the number of base stations, brings up the small cell paradigm. Moreover, future network architecture introduces novelties compared to the present network architecture such as cloud-based core network, virtualization, slicing, user-controlled or user-dependent base stations (such as Wi-Fi routers in homes or offices), moving base stations (drones, base stations on wings or wheels), and self-organization. Accomplishing all these enablers also poses many challenges in the dynamicity of the network [88, 89]. Specifically, due to the high flexibility of 5G networks' topology, the number of base stations may change the topology by either reducing or sometimes by increasing in a specific area of the network. All these aspects lead to a dynamic infrastructure that is not predictable in advance [90, 91]. Herein, it should not be overlooked that the density of base stations is ever-changing. If this erratic parameter is not handled as an optimiza-

tion parameter, it will negatively affect the network performance. For instance, in dynamic networks due to higher interference, insufficient coverage, massive power consumption, and higher mobility ratio, the limited network resources may not be used very efficiently [89]. Therefore, new solutions should consider the effective density of base stations to adapt the network performance to the highly dynamic structure.

As the network enlarges and becomes dynamic, its management and control become a symptomatic issue. Operator intervention requirements have to be drastically reduced by employing self-organization. There is a research gap between the state of the art and the ambition of achieving a self-organized, adaptive, and flexible networking architecture [92].

In this thesis, we claim and illustrate that we need to answer the following open research questions arising from the dynamism of the future networks: How do the existing architectures differ from the future networks? What does a density-aware dynamic mobile network express? Why is the network density an erratic parameter? Why is the density of BSs crucially important? Why will the solutions fail if the BS density is not considered as an optimization parameter? How can the density of BSs be measured at run-time? How can the BS density be utilized in network applications and communication stack? Answering all of these questions is the aim of this thesis.

3.2 Why is Density-awareness Important?

In this section, we bring to the light future paradigm changes in mobile networks. We clearly explain what the definition of a density-aware mobile network is, and what its differences from the present networks are. We claim that the present architectures are inadequate. In these discussions, we encounter that the network infrastructure changes, which cause variations in the number of base stations in a specified area. Therefore, in density-aware dynamic networks, network density will change incessantly. This section qualitatively analyzes the impact of BSs density on the performance of dynamic networks, and discusses density estimator algorithms and categorize them based on their features.

3.2.1 Paradigm Changes in Mobile Communications

The control domain of operators has notable paradigm shifts. Formerly, network operators used to manage and install BSs. Before and after the deployments of the BSs, optimization was applicable. Failure mitigation, performance monitoring, and corrections were performed by the network operator throughout the lifetime of a BS. However, this paradigm will diverge greatly in future mobile networks, and network operators' control over cell deployment will be partially lost. We will clarify in this chapter.

The infrastructure of mobile networks has also paradigm change. In the past, stochastic positions of the user equipment (UE), and stationary network infrastructure were assumed. In the future, mobile base stations may cause a dynamic infrastructure. For example, drones may be leveraged for providing service to handle the coverage problems [93, 94, 95]. Assume some sample scenarios where the density of BSs and UEs may dynamically change. In these scenarios, mobile cells may change the topology of mobile networks. Due to the mobility in addition to many other factors explained in this chapter, the infrastructure of ad hoc networks and mobile networks have similar dynamism. As a result, the density of base stations vary unpredictably. Assume a scenario where some emergency situation such as a sports event or a car accident, the density of UEs may increase unexpectedly. The event area is initially sparse. However, right after the traffic accident, the UE density increases significantly. Therefore, to provide the quality of service for capacity and coverage, mobile BSs are located in the environment. In emergency cases, pre-deployment solutions may not be feasible [95]. Communication services have giant importance for disaster management. Natural or man-made disasters such as earthquakes may damage communication services with stationary infrastructures. Leveraging drone BSs may provide a handy solution for establishing a communication infrastructure in these areas and for overcoming coverage problems in blind spots. Drone BSs can also be utilized for acquiring data from rural areas which does not have a communication infrastructure. For example, drone cells may be considered as mobile sinks in massive machine type communication and in applications of the Internet of Things scenarios [96].

Variations in the number of user equipment and base stations in a specified area result

in dynamic topology. This variation is not foreseeable in advance since it changes at run-time. If the user demands increase, the number of associated base stations should be increased to meet the requirements caused by raising user demands. However, in such cases, the density of base stations which is dynamically increased, some problems may occur such as unnecessary energy consumption and high interference[97]. Therefore, network density should be taken into consideration as a network optimization parameter to promote dynamic network solutions. If the critical level of base stations density are considered, the shared resources will be used more effectively, and the quality of service can be improved.

Assume a different scenario which is a derby football match. During this derby, flying base stations are utilized for providing coverage and improving the quality of service. Before and after the derby match, in the stadium the number of user will be low. However, during the football match it will be considerable higher. Instead of deploying stationary cells, flying base stations may be located on the stadium to provide the QoS needs of users via getting closer to them. More BSs can be additionally deployed in a dynamic fashion Depending on the density of users, which in turn varies the density of base stations.

3.2.2 Why Does Infrastructure Become Dynamic?

In the next generation networks mobile cells have a enormous potential to be utilized. In addition to cells' mobility [98] [99], other dynamism factors are as follows:

- User-controlled BSs such as controlled femtocells by users: When base stations are leveraged in customer places like homes, users may make base stations active or passive based on their requirements [100].
- Green operation such as sleep scheduling of BSs: Base stations may perform duty-cycling to provide energy conservation. In such schemes, the density of base stations will change over this period [101].
- Incremental deployment: When base stations are gradually deployed, then the network density will change during the deployment process [102].

- Failures in the topology and Loss of control: Since the distribution of base stations is stochastic, Deterministic deployments are not suitable anymore [15].

If we consider scenarios above, we can make a list for the major advantages of utilizing nomadic or mobile cells as follows:

- Mobile cells may be instantly deployed to remove coverage holes [103].
- In rural areas drone cells may provide ubiquitous coverage [104].
- Mobility of drones cells can facilitate the group mobility by in-lining with the mobility of users, decreasing the costs of mobility management operations [105].
- Mobile cells amplified with fog/edge computing, may promote a closer processing power for the end-users with less power consumption and higher data rates[106].
- Data rates for broadcasting can be enhanced especially for the UEs positioned at cell edges [107].

3.2.3 Why Will The Present Architectures Fail?

It is not applicable today for current mobile communication networks to handle these paradigm variations due to their restrictions [108, 109, 110]:

- Manual and static configurations, inflexible architecture, : In case of a dynamic infrastructure, it is obvious that the static or manual configurations will waste resources. Manual configurations are more prone to human errors result in inflexible network if the network topology is dynamic. Softwarized networks can be handy solutions to these problems.
- Deprivation of common interfaces and control functions: Real-time management is not possible due to vendor-dedicated and vendor lock-in software and hardware components requiring expert system managers. Network virtualization and softwarization may facilitate to handle this problem.

- **Restricted backhauling capacity:** In the network architecture when we consider the capacity of existing fronthaul, backhaul, and backbone, it can be said that among network entities, a small amount of data can be transferred. To meet the requirements of the mentioned paradigm variations by coping with the above restrictions, mobile, nomadic, or stationary small cells which are heterogeneous networks can be a suitable approach. Integrated access backhaul may let us overcome this problem via using relays that allow to deploy nodes flexibly for coverage and capacity enhancement.
- **Not context-aware network, but connection-centric:** Since traffic requirements have a significant change in time and space, content-delivery services are required for the future mobile networks. However, the existing connection-based networks are not suitable to overcome such a high traffic load. To control the context information for obtaining more knowledge about network conditions, including the density of nodes, mobility of network items, and traffic is not accessible within existing networks.
- **High latency:** In the existing network architecture, user applications such as websites and video streaming, can generally tackle the latency by using caching techniques in the network model. However, since remotely-controlled robots, autonomous cars, health monitoring tools, automation systems, and drone cells require real-time data, high latency is undesirable problem in such systems throughout their communications.

3.2.4 Impact Analysis of Base Station Density

A qualitative analysis of the impact of BS density on various mobile network parameters and performance measures is shown in Table 3.1. The analysis is based on the following simple scenario. Assume a set of homogeneous BSs are incrementally and randomly deployed in a field-of-interest. Suppose BSs are initially deployed sparsely, and service can only be given in a cluster of isolated coverage areas. As the density of BSs (λ) gradually increases (e.g., more and more BSs are deployed), isolated clusters merge and produce a huge cluster at a critical density (λ_c). At this stage, the global topology (macroscopic properties) of the network changes, and this phenomenon is

Table 3.1: The qualitative discussion of the impact of the density regime on network performance.

	Sparse ($\lambda < \lambda_c$)	Phase Transition	Dense ($\lambda > \lambda_c$)	References
Network capacity	low	maximum	below maximum	[111, 112, 113, 114]
Inter-cell Interference	low	to be managed	high	[115, 116]
End-to-end throughput	low	maximum	below maximum	[117, 118, 119]
Coverage	patchy	resource-efficient	redundant	[118, 120, 121]
Mobility management	disruptive	optimal	high cost	[118, 120, 121]
Number of relay base stations	few	minimal	large	[122, 123, 124]
Possibility of multi-path routing	none	very low	high	[122, 123, 124]
Redundancy assisted topology control	N/A	possible	possible	[125, 126]
Resilience to failures	N/A	low	high	[127, 128]
Energy consumption	low	optimum	high	[129, 130]
Spectral efficiency	low	maximum	below maximum	[131, 132]
CAPEX and OPEX	low	optimal	high	[133, 134]

called phase transition.

The macro-behavior of the system below and above the critical density λ_c is considerably different. The coverage area as an important component in the network consists

of active BSs in the dense networking regime where $\lambda > \lambda_c$. Whereas, the network is partitioned, and there exist coverage holes in the sparse networking regime where $\lambda < \lambda_c$. The macroscopic behavior of the network changes from disrupted networking (i.e., isolated coverage areas having large capacity) to degraded performance (full coverage with high interference) as the density increases. In this transition, at some density slightly larger than λ_c , resource-efficient operation of the network is possible. Therefore, the performance of the network is largely dependent on its topology that can be represented as a graph.

In graphs, a phase transition is a concept where the probability of the presence of a feature in a graph jumps from zero to one rapidly at a threshold value of the controllable parameter. The left- and right-hand sides of the threshold can be considered as static and chaotic regions. The region around the threshold is referred to as the phase transition region where innovations occur in a resource-efficient fashion.

Take transmit power adaptation as an example. At a critical threshold of the transmit power, the connectivity of the network jumps from disconnected to highly-connected state [135]. A level of transmit power less than the threshold causes a disconnected network, and the network is dysfunctional. Whereas, increasing the transmit power beyond the threshold causes a fully-connected network while increasing the interference and wasting resources. Operating at the critical threshold facilitates resource-efficient networking.

Similar phase transitions can be observed in many network design problems that are NP-hard such as drone cell placement [136]. The complexity of such problems in the phase transition region surges. The centralized solutions of such problems do not scale in large networks. The network has to configure itself locally for using resources efficiently through cell selection [137], service time maximization [138], or bandwidth allocation [139].

The macro-behavior of the system at different density levels (below and above the critical density λ_c) is described in Table 3.1. As the density of small cells increases, the coverage and capacity will grow due to a high level of spatial multiplexing. On the other hand, as the density of a network increases, the capacity will eventually converge due to interference in dense networks [111, 112, 113, 114]. Although, the

total network capacity will be low in sparse networks due to the coverage holes and partitioning, the received inter-cell interference will be reduced due to the low amount of interference. On the other hand, in dense networks where the cells are located very close to each other, the amount of inter-cell interference is high. This can be managed by optimizing the density of active BSs [115, 116]. The densification of networks in fact can provide more available channels and increase throughput [117, 118, 119]. Moreover, the cost of mobility management escalates in dense networks due to the very high number of handovers. Whereas, in sparse networks, the mobility support would be disruptive due to patchy coverage [118, 120, 121]. Concurrent multi-path transfer, multi-homing and utilization of relay BSs also become infeasible in sparse networks due to possible coverage holes in the network [122, 123, 124]. Topology control by exploiting redundancy in dense networks is possible, which can be useful in flexible networks [125, 126]. For instance, sleep scheduling of BSs can be employed considering the load in the network. The same fact also increases the resilience of the network to failures in dense networks [127, 128]. The amount of energy consumption will increase by deploying more BSs. Therefore, the optimal density of BSs (λ_c) is vital for enhancing energy efficiency in networks [129, 130]. Spectral efficiency (SE) will improve until the density of BSs reaches to its critical level (λ_c) and will dramatically degrade by over-deployment of BSs, due to the growth of the overall received interference in the network [131, 132]. Moreover, although when density of BSs is below λ_c , the capital expenditure (CAPEX) and operational expenditure (OPEX) can be low due to the sparsity of BSs, it can not satisfy the minimum QoS requirement in the network. However, when the number of BSs per unit area is around λ_c , although the cost of implementation and maintenance may increase, we can satisfy all UEs QoS requirements with the minimum cost [133, 134].

In dynamic dense networks, collisions over random access channels, high congestion levels, and inconstant capacities may be the significant challenges [140]; whereas in sparse networks, partitioning is the key challenge [141]. Dynamic networks have to collaborate locally for coverage preservation, mobility management, interference control, and efficient resource allocation. However, the state-of-the-art architectures do not rely on localized cooperation. For carrying out those tasks in a density-adaptive fashion, BSs have to discover their neighborhood or estimate the density in an incen-

santly changing topology. Edge computing can be a valuable technology towards this aim by providing a higher-level perspective and having more processing power with respect to BSs; it can collect and evaluate the required data for density measurements from BSs (such as received signal strength (RSS), channel quality indicator (CQI), SINR, etc.) and provide more accurate results [42, 142].

As the cells become sporadic and their size changes, the mobility management will be more cumbersome. When large cells are employed, paging costs are lower since the destination terminal is searched in fewer cells. When the cell sizes become small, paging consumes valuable in-band resources since a large number of cells are paged, considering a constant location area mapping. Therefore, real-time decentralized management of cell sizes and coverage may have an adverse impact on mobility management [143].

3.2.5 How Can the BS Density be Estimated?

As explained in the previous sections, the control of the BS density is important for an efficient network operation. An important question is then how to estimate the BS density. The network density is highly correlated with the location of BSs, the neighborhood structure, the quality of received signals from other BSs or user equipment, and population data [144]. We can roughly categorize the network density estimation approaches as shown in Table 3.2. Location-based estimators employ auxiliary positioning systems such as global positioning system (GPS) that consume extra energy [65, 145, 146, 147]. Neighborhood-based estimators, which are not scalable and suffer from inaccurate results, infer density from a census on packet traffic [91, 148, 149, 150, 151, 152]. Power-based estimators combine the merits of location- and neighborhood-based estimators [42, 55, 153, 154], although RSS is not a robust distance estimator. While some of these approaches are designed for ad hoc networks, they can generally be employed in any wireless network with minor modifications.

In cellular networks, the spatial distribution of BSs is vital for the analysis of connectivity, coverage, and performance [152]. The proper adjustment of spatial distribution and configuration of cells in simulators produce credible models which are important

Table 3.2: Approaches for estimating density of nodes in a network.

Category	Requirement	Advantages	Disadvantages	References
Location-based	The coordinates of devices, location pre-awareness (e.g., GPS)	Ease of integration	Extra energy consumption, errors in GPS measurement	[65, 145, 146, 147]
Neighborhood-based	Monitoring and analyzing traffic, beaconing and neighbor discovery	Existing functions in a stack can be employed	Not scalable, limited to transmission range, accuracy depends on traffic	[91, 148, 149, 150, 151, 152]
Power-based	Received signal strength or SINR measurements	Ease of integration, no other auxiliary function, or monitoring traffic of network	Sensitive to channel characteristics that may not be uniform in a field	[42, 55, 153, 154]

for capacity planning. In [152], the information of BS location obtained from different operators in Germany is used to find out the utility and restrictions of population data as a base for similar cellular deployments, and it is shown that the density of the network is highly correlated to population data. They also figure out that relatively populated areas can be considered as a reasonable co-variate to model large-scale deployments. This study validates that predicting the number of BSs per unit area based on the population density is sensible only for the small areas with partially populated areas. Proposing accurate density estimators is an open research challenge with huge potential in stochastic geometry, especially for non-uniform deployments [58].

To summarize, current mobile networks, due to their limited backhauling capacity,

static and manual configurations, have a limited flexibility to cope with the dynamicity in future networks. However, the density-awareness in future network architecture is essential because BSs may also be mobile, such as the drone cells, yielding a random infrastructure. Therefore, dynamic network solutions should consider the network density as a performance optimization parameter for enhancing the utilization in the resources, and for improving the network QoS. To do so, we need an appropriate density estimator for adapting network parameters such as the modulation techniques, antenna types, and transmit power to the estimated BS density in a dynamic fashion. In the following, we evaluate the potential difficulties we may encounter in dynamic mobile networks in addition to potential solutions to mitigate these difficulties.

3.3 Challenges and Opportunities

Various opportunities and challenges are accompanied by the future 5G networks [155, 156]. Table 3.3 and Table 3.4 categorize and summarize these challenges by featuring the enabler technologies or solutions. Since a feature of dynamic mobile networks may provide an opportunity together with some research challenges, we analyze research challenges and its possible solutions by discussing benefits and enablers specifically. In this section, by considering the density-awareness perspective, we introduce possible solutions for specified challenges, which we will face in the next generations of networks.

3.3.1 Densification

In order to satisfy 5G networks requirements, including higher data rate for a massive number of network entities, densification is introduced as a key feature to enhance the system capacity requirements as stated in [157, 158, 159, 160]. By densifying the mobile networks through employing small cells, higher SINR can be achieved, which can provide a higher data rate for individual UEs and reduce the latency in the network [203]. One of the major drawbacks of small cells is limited coverage area they provide due to their low power functionalities. Moreover, small cells can also provide service for a low number of UEs due to their limited resources [89, 160]. Therefore, we

Table 3.3: The challenges-I of dynamic mobile networks and some of the existing enabling technologies that can be employed to address these challenges.

Challenges	Solutions	References
Densification	Small cells, density-adaptive algorithms, coverage preservation techniques	[88, 89, 157, 158, 159, 160]
Quality of service and experience	Small cells, multi-homing in user plane, MEC, mu-MIMO,	[58, 161, 162]
Modulation techniques	Density aware small cells, cyclic-prefix insertion, adaptive MCS	[163, 164, 165, 166]
Ubiquitous coverage and connectivity	Cells on wings or wheels, network densification, D2D, relaying, ad hoc networks of BSs (MANET, FANET), NTN	[167, 168, 169]
Mobility management	Multi-homing, group mobility support, MEC, lightweight-EPC, motion and deployment planning, DTN, virtual cell	[133, 170, 171, 172, 173]
Reliable communication	Multi-homed protocols, dual-connectivity, fault tolerance techniques, MEC	[174, 175, 176, 177, 178, 179]
Scalability	Distributing management and resource allocation, inter-numerology interference management NFV, SDN, C-RAN, NTN	[180, 181]
Antenna Type Selection	Directional, Omnidirectional, MIMO	[182, 183]
Dynamic (in-band) backhauling	Mobile or nomadic cells, mu-MIMO, IAB	[184, 185]
Low latency	Distributed and collaborative caching, D2D, mobile cells	[186, 36, 187, 188, 189, 190]
Energy efficiency and green operations	Small cells, MEC, sleep scheduling, cell zooming	[142, 160]

Table 3.4: The challenges-II of dynamic mobile networks and some of the existing enabling technologies that can be employed to address these challenges.

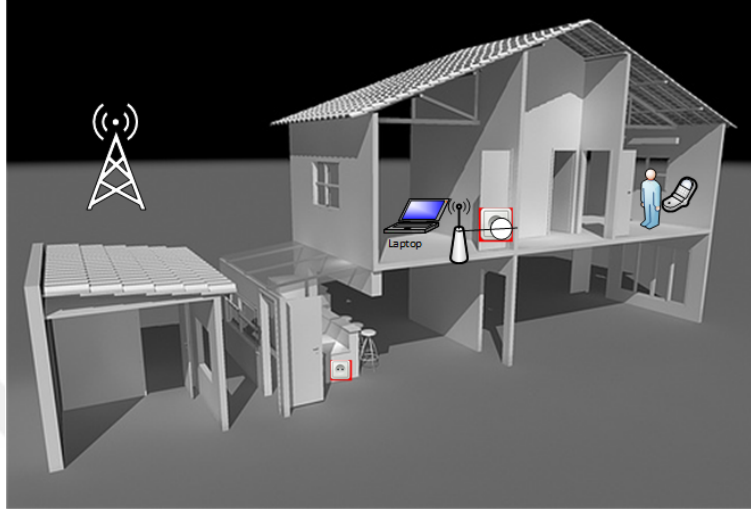
Challenges	Solutions	References
Management of dynamic architecture	SDN and NFV, slicing, orchestration, self-organizing and self-healing functions, density- and dynamics-aware protocols, antenna directivity, tilt or antenna count, MEC	[130, 131, 191, 192, 193, 194, 195]
Transmit power adaptation	MEC, cell-zooming techniques	[130, 196]
Interference management	MEC, density- and interference-aware protocols, e-ICIC	[148, 197, 198, 199, 200, 201, 202]

need to tackle these problems by employing density-adaptive algorithms, which can optimize the density of BSs in order to prevent coverage holes in the network while UEs can achieve higher throughput by connecting to BSs with higher capacity and lower load. Many research studies consider and manifest that small cells resemble random ad hoc networks, which is a well-known observation [88]. In such dense networks the area spectral efficiency is directly susceptible to base station density, as stated in [88].

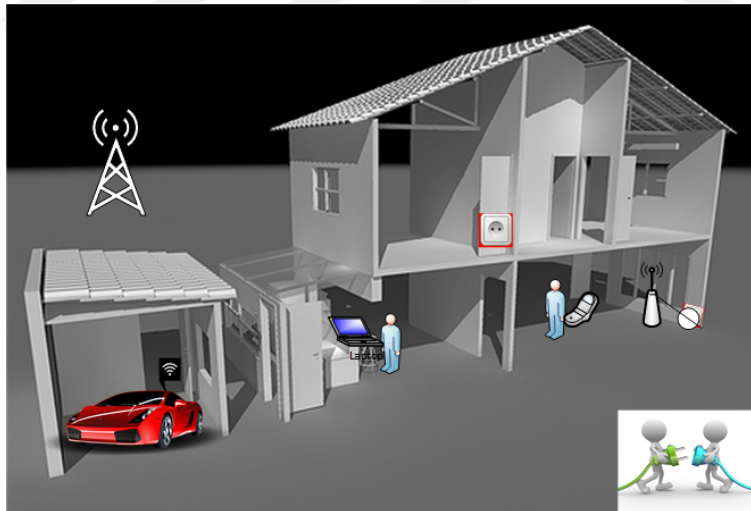
3.3.2 Quality of Service and Experience

Channel quality may vary in time and frequency. In milli-meter-wave (mmWave) band small cells, gNBs are equipped with multi-user, multiple input, multiple output (mu-MIMO) antennas, and user mobility is low, one may assume dynamic channels (due to the high attenuation level in mmWave band) while the channel quality does not vary considerably in time [161]. In this case, user multiplexing over different carriers is a smarter option compared to time-domain channel scheduling. Depending on the physical layer dynamics, the radio link control has to support segmentation and concatenation of the frames. This is a clear requirement for a cross-layer design.

Moreover, multi-homing techniques can also be employed for enhancing QoS [162], hence schedulers also have to deal with the reliability of connections and cross-link interference management, which can increase the processing load in the network. Wireless signals are considerably attenuated while penetrating inside the buildings



(a) Initially, the femto BS is operational on the first floor and users, instead of using outdoor BS, connect to the mobile network through the femto BS that can enhance QoS and conserve energy.



(b) The household decides to move the access point to the ground floor which causes an uncontrolled BS failure for some time.

Figure 3.1: A scenario where the household is able to change the location of a femto-cell deployed inside the house.

in mobile networks. The attenuation substantially decreases the SINR, and consequently, the achievable data rates. Instead of outdoor deployments, indoor small cells may employ lower power levels and provide higher data rates compared to outdoor BSs. This scheme reduces energy consumption, improves the quality of experience (QoE), employs the spectrum efficiently, facilitates the use of licensed bands for home networking, lowers the level of electromagnetic radiations, minimizes the costs for the mobile operator and provides true ubiquity and coverage for subscribers. However, operators lose their control over BS deployment. As an example, there is an indoor Femto BS deployed in a house, as shown in Figure 3.1a, the location of the Femto BS which is changed based on user decision. Furthermore, this deployment change causes uncontrollable interference to neighboring houses after the BS becomes operational at its new location. Therefore, by implementing adaptive density algorithms, the density of active BSs can be estimated frequently by leveraging multi-access edge computing (MEC) utility in order to maintain and enhance QoS (higher throughput, lower delay, interference, outage and etc.) in future networks. In [58], the BS distribution for different cities are modeled, and they claim the proposed model can be used to prevent coverage holes and interference in the network.

3.3.3 Modulation Techniques

In the next generation of mobile networks, by employing multi-carrier modulation, we can immune our system to fading due to the simultaneous transmission of data over multiple paths (multipath fading), which can also prevent cross-link interference during communication among cells. However, when multi-carrier modulation is employed, simultaneous transmission over sub-carriers may lead to greater deviations in instantaneous signal power and push amplifiers into the non-linear regions. This phenomenon leads to a larger amount of power consumption and dramatically increases the costs of amplifiers. Moreover, frequency selectivity fading will lead to higher bit error rates and degrade the quality of the channel [163]. In order to cope with these problems, density aware small cells are adequate candidates since the terminal-to-base distances in small cells are shorter, which can reduce the average transmit power and cost of amplifiers. Typically, less frequency selectivity is experienced in small cells [164]. Additionally, to combat frequency selectivity, cyclic-

prefix insertion can be employed in multi-carrier modulation, and the length of the prefix depends on the channel delay spread, which can be affected by BSs density variations. Therefore, cyclic-prefix can be adapted to the network density to prevent inter-symbol interference in the network [204]. Moreover, choosing an appropriate modulation coding scheme (MCS) is vital for satisfying 5G networks' requirements, such as ultra-reliable low-latency communications (URLLC) and enhanced mobile broadband (eMBB). Because, in URLLC communication signals need to be interpretable quickly, which require lower MCS, while in eMBB communications, a high number of bits need to be coded for each transmission to achieve high throughput in the network. Therefore, MCS in the future networks needs to be tuned not only by considering the received SINR value (like LTE) but also it needs to be adapted to the BSs density [165, 166].

3.3.4 Ubiquitous Coverage and Connectivity

In future networks, UEs have different requirements and expect to receive service everywhere. Therefore, future networks need to be equipped with a flexible network coverage and topology. The topology and coverage of the dynamic networks must be controlled since it significantly impacts the performance in terms of capacity, delay, and resilience of the network under node and link failures. The topology depends on many controllable parameters and uncontrollable factors. Interference, attenuation, environmental parameters such as obstructions, especially for mmWaves, multipath propagation effects, fading, and noise, can be considered as uncontrollable factors which impact the link quality, and consequently the topology. These uncontrollable factors produce time- and space-variant links that are not predictable in advance. Cell mobility or presence may or may not be a controllable parameter that may sporadically cause blind spots or redundant coverage. The transmit power, antenna directivity, tilt, or antennae count are the controllable parameters that can be used to change the network topology as required to make the network adaptive to density changes. Topology and coverage control decisions should be given autonomously based on the estimated density by BSs or by a MEC entity. MEC entities have a broader perspective over network topology in comparison to BSs facilitating decentralized optimizations. For instance, in [42, 142], authors by adapting the transmit power of BSs to the

network density, managed to enhance the network capacity and increase the throughput while coverage holes are prevented. Future networks guarantee the ubiquitous connectivity in case of a disaster, which causes a dysfunction of the network infrastructure [167]. At this point, with the help of device-to-device communication (D2D) and integrated access-backhaul (IAB) opportunity, BSs can form an ad hoc network. They establish a dynamic infrastructure to backhaul traffic to the core of the network as we show in Figure 3.2 in case of a network failure to sustain communication and enhance reliability through mobile BSs in the network [167, 168]. As claimed in [168, 169], in D2D communications, an optimal threshold value for density of BSs is required to enhance the network performance.

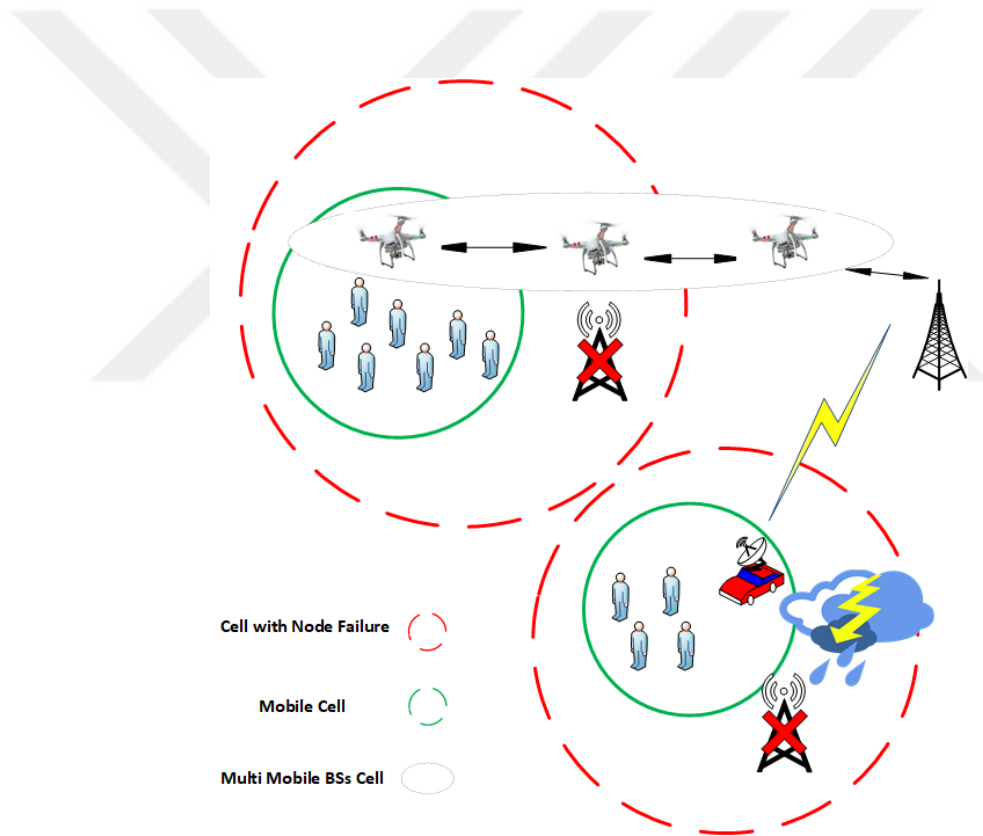


Figure 3.2: Mobile or stationary BSs may form an ad hoc infrastructure to backhaul traffic to the core network; for example, when a stationary BS fails as we exemplify here.

3.3.5 Mobility Management of Cells

In stationary networks, coverage is restricted to the range of BSs. However, by employing mobile BSs, network infrastructure will also be dynamic, which can enhance the network capacity, throughput, and coverage in future networks [118, 205]. For instance, flying BSs can form an ad hoc network and establish a dynamic infrastructure to backhaul traffic to the core network, as we show in Figure 3.2 in case of a network failure to sustain communication and enhance reliability through mobile BSs in the network. Although the implementation costs, maintenance, and the battery requirements of drone networks currently are a considerable challenge, the availability of cheap commodity hardware in the future presents a new avenue for provisioning such networks [134]. In particular, with the advent of Google's Sky Bender¹ and Facebook's Internet drone², drone empowered small cell networks (DSCNs) can be considered as a solution in future networks. Due to lower computational requirements and light payload, implementing drone cells can provide a lower CAPEX (in comparison with stationary BSs) and OPEX (with respect to energy consumption and maintenance) for network operators [133]. Due to the BSs' mobility, not only the users but also the BSs have to be tracked, and their locations have to be registered. Motion and deployment planning, handover management, and new (dynamic) location area concepts are required and can be considered as open research challenges. Even when the users are stationary, handovers may be necessary when the BSs move. One of the promising solutions for maintaining QoS in dynamic mobile networks and reducing handovers is employing a user-centric mechanism such as virtual cells where UEs can be connected to more than one BS [170]. In dense deployments, UEs may camp on multiple base stations simultaneously, and dual-connectivity, concurrent multi-path transfer or multi-homing may be possible. At this point, accurate estimation of location plays a vital role in cooperative mobile BSs. In current networks, location estimation methods such as the GPS are mainly used to calculate the coordinates of nomadic communication terminals and usually is sufficient to determine nodes' locations. In case GPS is not available, by employing proximity-based techniques or beacon nodes, we can estimate the nodes' coordination. Due to various mobility models

¹ <https://www.theguardian.com/technology/2016/jan/29/project-skybender-google-drone-tests-internet-spaceport-virgin-galactic>

² <https://www.theguardian.com/technology/2017/jul/02/facebook-drone-aquila-internet-test-flight-arizona>

of cells on wings or wheels, we need a highly accurate location estimator with a small delay. GPS has 10 to 15 m error in location estimation. The location information can be received with one second, which may not be applicable when multiple mobile BSs is employed, since it can cause a collision among them under fast mobility or affect the channel conditions among them. To reduce the estimation error, assisted or differential GPS (AGPS or DGPS) can be used that can enhance the accuracy of estimation for about 10 cm by employing ground-based reference points [171, 172]. To estimate location faster by equipping UAVs with an inertial measurement unit (IMU), which can be calibrated by the help of GPS, the location of mobile BSs can be retrieved faster and with higher accuracy [173].

3.3.6 Reliable Communication

Requirements for reliable end-to-end communication, availability of resources, lasting connectivity, and seamless handover can be addressed by employing multi-homed transport protocols and dual-connectivity not only in the control plane but also in the user/data plane. Multi-homing and dual-connectivity in the user plane ease the mobility management burden [174, 175]. In dense deployments, UEs may camp on multiple BSs at the same time. Reliable end-to-end communication requirements can then be addressed by employing multi-homed transport protocols not only in the control plane but also in the user/data plane. Cell discovery, security, access scenarios have to be tackled in dynamic networks when multi-homing is employed. Future dense networks have various types of wireless technologies such as LTE-Advanced, LTE, 3G, WiMAX, Satellite, WiFi, ZigBee, and Bluetooth. In these networks, tablets, IP-Cameras, laptops, sensors, smartphones, game devices, wearable devices, and other IP-enabled devices located on buses, aircraft, trains, satellites, etc. define a different application and user requirements. With the evolution of densification and mobility, which is the binding nature of the future networks, in addition to dynamically changing user preferences and QoS requirements, some challenges may arise, such as availability of resources, fault tolerance, lasting connectivity, and seamless handover [176, 177]. These developments in wireless communication systems equip users to concurrently receive content through multiple radio access technologies (RAT) for homogeneous or heterogeneous network environments. To do so, having a power-

ful and fast (low delay) processing unit such as MEC close to BSs can enhance the interface selection accuracy within a short time. Multi-homed protocols meet these requirements that can be implemented in the network communication stack. Multi-homing can use multiple network paths simultaneously to provide the lasting connectivity and the reliability of user requirements [178]. As demonstrated in [177], the transport layer multi-homed protocol has a better solution in order to provide reliable handover and connectivity. However, as we presented in Figure 3.1 and Figure 3.2, the density of BSs may fluctuate during each time slot. Therefore, future multi-homed algorithms need to consider the density of active BSs into their models to provide a reliable communication path in the network [179].

3.3.7 Scalability

In one-cell frequency reuse, the same time-frequency resources can be reused in neighboring cells. To increase the network capacity, operators can employ IAB, where the same radio technology standard is used for backhaul and access communications [180]. Although this approach eases network deployment and increases spectral efficiency, it may also cause significant variations in SINR due to a high amount of interference. Enhanced inter-cell interference control (e-ICIC) is a solution to this problem that has to be density-adaptive since BS topology changes in dynamic networks and the type received interference will be dynamically changed as it is shown in Figure 3.3. In the next generations of mobile networks, to fulfill the UEs requirement, different numerologies need to be employed [206]. However, by using mobile BSs, cells with different numerologies can travel in the network, which can cause Inter-Numerology Interference (INI) among cells [181]. Therefore, future interference cancellation models need to consider the variation of BSs numerologies with respect to the density of active BSs in time and space. In non-terrestrial networks (NTN), airborne or space-borne BSs are used for transmission. NTN may require delay-tolerant networking (DTN) protocols. When backhauling is not possible, mobile BSs may have to manage the functions of the core network themselves. Lightweight evolving packet core (lightweight-EPC) and DTN may have to be considered for BSs on wheels or wings. Furthermore, location area planning cannot be stationary anymore since the infrastructure becomes dynamic. Interference manage-

ment models will be affected by mobile BSs since the cell layout will dynamically change by the movement of BSs. In such networks, the dynamicity of frequency reuse is high and cannot be handled by current interference management models. Therefore, adaptive interference management and resource allocation models for dynamic networks with mobile BSs are needed.

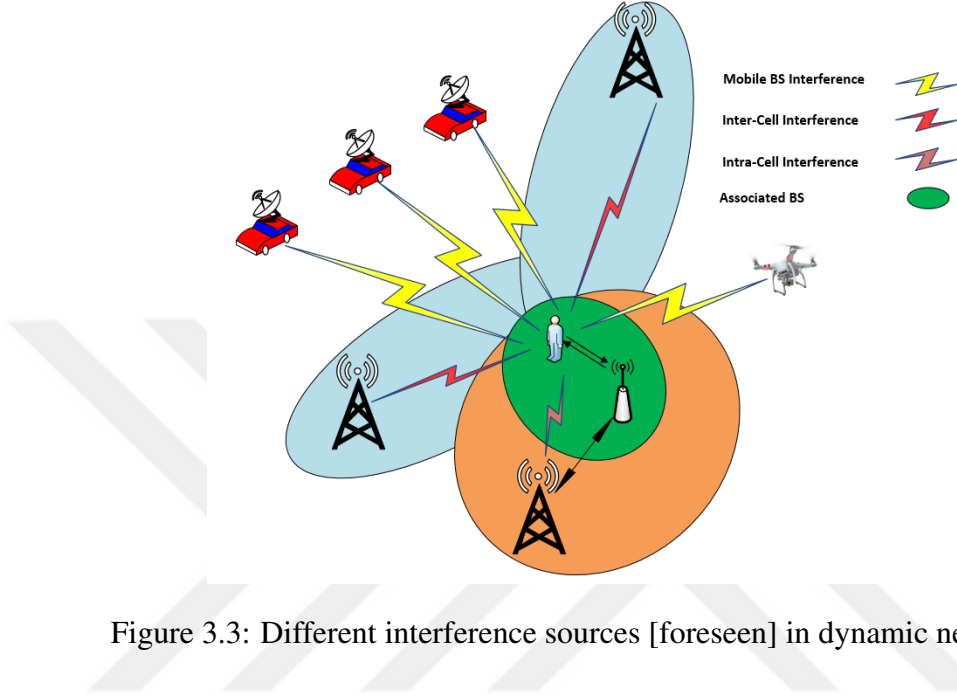


Figure 3.3: Different interference sources [foreseen] in dynamic networks.

3.3.8 Antenna Type Selection

The antenna structure is another vital constraint for an efficient dynamic network. In a dynamic network, in case of using a more powerful radio signal to transmit data to longer destinations, although the coverage range is expanded, the link variation and loss can also increase too. Choosing an appropriate antenna type is another parameter that can affect the QoS in the dynamic networks. On the one hand, because BSs' locations can change frequently, by choosing omnidirectional antennas, there is no need to access nodes' locations, which can ease the communication in the network [182]. On the other hand, directional antennas can transmit signals to a more considerable distance in comparison with omnidirectional antennas, which can reduce hop count and latency in the network. The capacity of the network can also be enhanced by using directional antennas, which have higher spatial reusability with respect to

the omnidirectional antennas. However, for moving topologies using directional antennas can be challenging [183]. Therefore, choosing an appropriate antenna in the dynamic networks is another important constraint which is needed to be evaluated for the future networks. By employing density-adaptive algorithms, the number of antennas by considering density of active BSs can be optimized. By using beam-forming techniques, density of BSs can be optimized in a way that interference is reduced, and overall system throughput is enhanced.

3.3.9 Dynamic (in-band) Backhauling

By introducing mobile BSs for future networks, channel models have to be revised. For cells on wings, air-to-ground, ground-to-air and air-to-air, channels have to be studied and modeled accordingly. The mobility of BSs can cause new challenges such as reflections from the ground (for drone cells), variations of drone attitude, considering changes in weather conditions for different altitude, environmental clutter, interference from other BSs in three dimensions (possibly four including time), and jamming by hostiles. All these additional constraints have to be evaluated in the channel modeling of BSs [207, 208, 209]. With the help of mobile BSs, there is a considerable potential for relay BS where nomadic nodes can be used to reduce the congestion in backhaul-links and provide higher capacity and faster communication in the network. Moreover, in-band (converged access/backhaul) or out-of-band relaying can be employed. The trade-offs between these approaches need to be evaluated [210]. Additionally, in 5G networks for increasing the network capacity, and provide reliable, secure, and lasting services, mmWave and massive multiple-input multiple-output (MIMO) can be considered as a solution [184]. This paradigm shift is analyzed in [185], in terms of network secrecy and network connection outage by demonstrating how base station density, mmWave small cells, and mu-MIMO affect each other through analytic models considering the base station density. They prove that if base station density is higher, then mu-MIMO-enabled networks along with mmWave small cells, dramatically decreases the network outage probability. Therefore, due to dynamicity of mobile BSs, employing the density of BSs in channels' models play a vital role for achieving accurate and adaptive models in the next generation mobile networks.

3.3.10 Low Latency

Due to the tremendous pace of increasing multimedia services, current network link capacity and bandwidth cannot satisfy the growth of users' demands. As it is mentioned previously, one of the main concerns in the dynamic networks is reducing the delay and response time in the network [186]. For instance, in delay-sensitive applications such as reconnaissance, packets need to be delivered within a specific delay bound. When multiple mobile BSs (such as drone BSs) are deployed together to provide coverage, communication delay among those BSs needs to be low to avoid any collisions among them. However, current protocols that are developed for mobile ad-hoc networks may not be applicable to flying ad-hoc networks of BSs [36]. To achieve this goal, network operators, by applying mobile content caching in the intermediate network infrastructures, reduce duplicate data and response time in the network [187, 188]. However, one of the main issues of caching in the dynamic network is to decide where the appropriate place for caching is [189]. In the current networks, by implementing caching toward the network edge, the amount of redundant data and delay can be reduced significantly. However, due to the mobility of infrastructures in the dynamic network, future networks need to be equipped with content-centric networking (CCN) architecture [190]. The main concern in CCN is to distribute caching in every network infrastructure, even to UEs, which can ease the data access and reduce the response time in the dynamic networks. When UEs request particular data in CCN, an interest packet will be transmitted to its neighbors, and the requested data can be delivered from the caching store of any node in the network. If the requested data is not available at neighbors, routers propagate interest packet in the network and push the cached data toward the requester. However, due to the universal distribution of caches in the network, cooperative policies need to consider diversity, freshness, number of replications, and their locations in the network topology. Moreover, by employing density of BSs as an optimization parameter in routing and caching techniques, the amount of time required for transmitting the cached data to the destination can be reduced by optimizing number of active BSs. The size of required cached dataset in the network can also be optimized which can decrease the transmission load and bandwidth needed in the network.

3.3.11 Energy Efficiency and Green Operations

Small cells may reduce CO₂-equivalent gas emissions per second. However, in ultra-dense networks, the total sum may not be negligible. Furthermore, the new dimension of energy efficiency research will be trying to reduce the power consumed for the mobility of BSs. Energy consumption, CO₂-equivalent gas emissions, and the impact of the battery-driven operation of mobile BSs have to be carefully investigated. By increasing the density of small cells, and maximizing the energy efficiency, BS density needs to be adapted and optimized by considering the overall network condition. On the other hand, the network needs to be smart enough to maintain QoS when the density of base stations dynamically changes [160]. For instance, by turning off a BS in a heterogeneous network, its traffic load needs to be adaptively handled by its neighbor cells to prevent coverage holes in the network. In [142], authors introduced a density-adaptive algorithm which can jointly enhance energy efficiency by adapting the density of BSs to network condition while coverage and throughput are enhanced by adapting BSs' transmit power to the effective density of BSs.

3.3.12 Management of Dynamic Architecture

Software-defined networking (SDN) and network function virtualization (NFV) are two distinct concepts that may help implement dynamic networks [191]. The integration of SDN and NFV can be used to optimize resource allocation in the network, while centralized and stationary resource allocation may waste valuable resources [192]. Through mobile edge computing, hybrid approaches may be developed. End-to-end slicing will significantly be more complicated than the present approaches since to-be-solved optimization problems morph with a higher frequency [193, 194, 211]. One should also not forget the scalability requirements. End-to-end slicing and limited computation resources' sharing are important challenges of the future networks. Cloud radio access network (C-RAN) is a novel mobile network architecture with joining the processing resources of the base-band unit in a pool, and virtualizing base-band units with the help of SDN and NFV [193]. C-RAN enables the aliasing of the limited computation resources, and can not be used from the other nodes in traditional radio access network (RAN) architecture on demand. For

enhancing interference management and reduce the power consumption, C-RAN can dynamically allocate radio resource heads (RRHs) by considering the network condition. In future networks, the enabling of such a feature introduces the concept of cloudification. Techniques such as coordinated multipoint (CoMP), carrier aggregation, and MEC, and their hybrid approaches may be developed for the enhancement of the joint resource usage at centralized baseband units.

Self-organizing networks (SONs) have many functions (such as energy efficiency (EE), coverage and capacity optimization (CCO), mobility load balancing (MLB), etc.), which can enable BSs to adapt themselves automatically to the network condition. However, these functions may conflict with each other if the density of BSs is not considered. For instance, by increasing EE without considering BSs' density, CCO functionality may negatively be affected due to the reduction of SE in the network. In order to increase SE to its maximum level, BSs' density needs to be optimized [131]. Moreover, SE will be increased when the density of BSs is optimized, and in case of over-deployment SE will be degraded drastically [131]. Therefore, by optimizing the density of BSs, EE and CCO can be enhanced simultaneously. In [195], authors present an energy-efficient mechanism by considering the density of BSs and controlling the transmit powers for a dynamic SON. As it is shown in [130], by evaluating the density of BSs, a threshold value for the minimum received SINR in each cell can be obtained, which is used for optimizing coverage, energy consumption and SE in the network. Thus, by employing the density of BSs in SON, the possible conflicts among SONs' functions will be prevented.

3.3.13 Transmit Power Adaptation

Optimizing downlink power allocation is another critical parameter that plays a vital role in enhancing throughput and user satisfaction in the network. On the one hand, if the power is excessively allocated in BSs' downlink channel, it can cause interference among neighboring cell, which can reduce the QoS and throughput in the network. On the other hand, degrading too much the downlink power can cause coverage holes and reduce the throughput in the network. Therefore, the downlink transmission power needs to be chosen wisely, and it needs to be adapted to the

density of BSs in dynamic networks. In [130], by employing MEC in the network architecture, the minimum required received SINR for maintaining QoS in the network with respect to the density of active BSs is calculated. The obtained value will be transferred to BSs, and BSs adapt their transmit power in a distributed manner to reduce the interference in the network while the overall throughput is enhanced. For density-aware mobile networks, cell zooming is a key concept regarding with preserving coverage, controlling network outage, and improving the energy efficiency [196]. Adapting transmit power based on the effective density of base stations is one of the dynamic solutions for cell zooming. To control the network coverage and outage, changing the transmit power of each base station depending on the base station density can be a handy solution as clearly illustrated in [196]. We conduct Monte Carlo simulations by leveraging the outage and transmit power models proposed in [196] to clearly observe the impact of the network density on the network outage and the transmit power of base stations. The simulation parameters are presented in Table 3.5. In our simulations, we randomly deployed a set of base stations and user equipment as a three-dimensional network. In each run, a UE is randomly selected as a reference point, and received signal strength values are collected by this UE from its closest base station. If the collected RSS value is less than a threshold value, this run is considered as an outage. We compute the ratio of simulation runs that yields outage to the total number of runs as the outage probability. The simulation results are compared with the provided analytic model for the network outage based on the actual density. As can be seen in Figure 3.4, the density of BSs needs to be higher for the network with lower transmit power to achieve the same outage probability in two networks equipped with BSs that have different transmit power levels (10 mW and 20 mW). Additionally, as we explained in Table 3.1, when BS density reaches the transition phase, increasing the density of BSs will not enhance the outage probability anymore, and it can increase the interference and the energy consumption in the network. As can be seen in Figure 3.4, to achieve the same outage probability in case of different transmit power levels, the density of BSs in the network with lower transmit power needs to be higher. Therefore, by considering density-aware approaches, we can reach an adaptive and flexible model for dynamic networks where BS density and BS transmit power can be varied in each time slot.

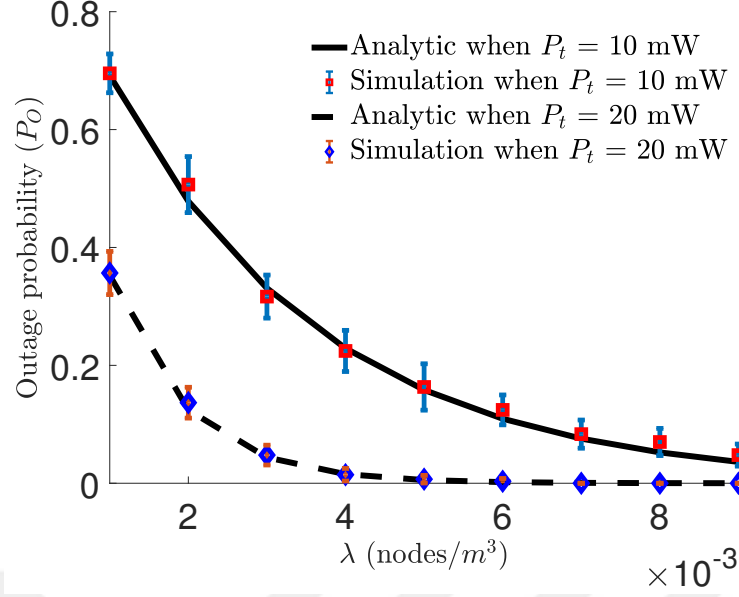


Figure 3.4: Impact of BSs density (λ) (nodes/m³) on the probability of network outage (P_O) when the transmit power of base stations (P_t) is changing.

3.3.14 Interference Management

In future networks, high-speed and ubiquitous connectivity will be a leading demand that can be satisfied by densification. Network densification provides higher capacity by performing spatial reuse and less congestion with offloading. However, interference, depending on the spatial distribution of base stations, will be a significant problem to be tackled [199]. Density-aware interference management will increase link capacity and spectral efficiency in dynamic networks [200].

In 4G mobile networks, if a UE is located at cell edges, it can receive signals from multiple contiguous cells. Inter-cell interference may originate from various types of BSs. Different UEs can also interfere with each other, as shown in Figure 3.3. What will be of notable importance is the interference from nomadic or mobile cells in future networks. In Figure 3.3, we present a scenario where a cell on wheels (mobile BS) interferes with a UE. This type of interference is the most challenging if centralized solutions are to be employed [200, 201, 202].

Mobile operators may control interference at three levels: at the RAN, between RAN

Table 3.5: The nomenclature for symbols, notations, values and units of the simulations' parameters.

Parameter	Default Value	Units	Ref
Actual density, λ	[0.001,0.003]	nodes/ m^3	[196]
Path-loss exp. γ	$1.5 \leq \gamma \leq 2$		[81]
Reference distance, r_0 ,	1	m	[55]
Transmit power, P_t	[10,100]	mW	[142]
Simulated outage probability, P_O	[0,1]		[196]
Nearest neighbor index, $k.n$	6		[196]
radius, R	300	m	[196]
K	-40.046	dB	[196]

and UE, and within UE.

In coordinated multi-point operation, BSs have to synchronize with each other over the X2 interface (the signaling interface which is used between eNodeBs) to transmit the same information to edge terminals. In this case, inter-cell interference becomes a constructive phenomenon which is regarded and processed by the terminals using techniques to combat multipath fading [198]. With this approach, the broadcast is increased more in small cells in comparison to macro cells.

Network density is used as an optimization parameter in [148] to enhance network capacity. Authors consider the expected link rate, which depends on both user association and interference distribution, as a function of network density. Interference and network throughput models based on BSs' density are also presented to clarify the trade-off between the density of BSs and network throughput or interference. By densification, network throughput will increase until the BSs' density reaches a threshold. Crossing the threshold degrades throughput because of the high acceleration of interference and increases service disruption due to large numbers of handovers. High link capacities or high SINRs do not always guarantee high throughput in a network. Under congestion, the performance can become low. That is why a UE may not connect to a BS even when it provides the highest RSS. It is shown that a robust and optimized network density estimator is an essential requirement for maximizing the

network capacity [148].

Different or the same frequency bands can be used by femtocells as macro cells do. However, employing co-channel femtocells results in inter-cell interference with their adjacent macro cells, which can reduce the performance of cell-edge UEs. An adaptive solution is presented in [197] for reducing the downlink interference caused by femtocells. That solution exploits the orthogonal fractional frequency reuse (FFR) for radio resource allocation and FFR resource hopping based on the femto-BS density and locations. If the density of femto-BSs near the macro BS is high, then femto-BSs should use orthogonal sub-channels based on the FFR method proposed. If the density of femto-BSs is low, they should choose a sub-channel randomly for a while and then hop to other sub-channels. However, such an approach is not sufficient to avoid inter-macro-cell interference in the case of high femto-BS density. The analysis of the impact of the femto-BS density shows that the density of femto-BSs should be considered to successfully combat interference [197].

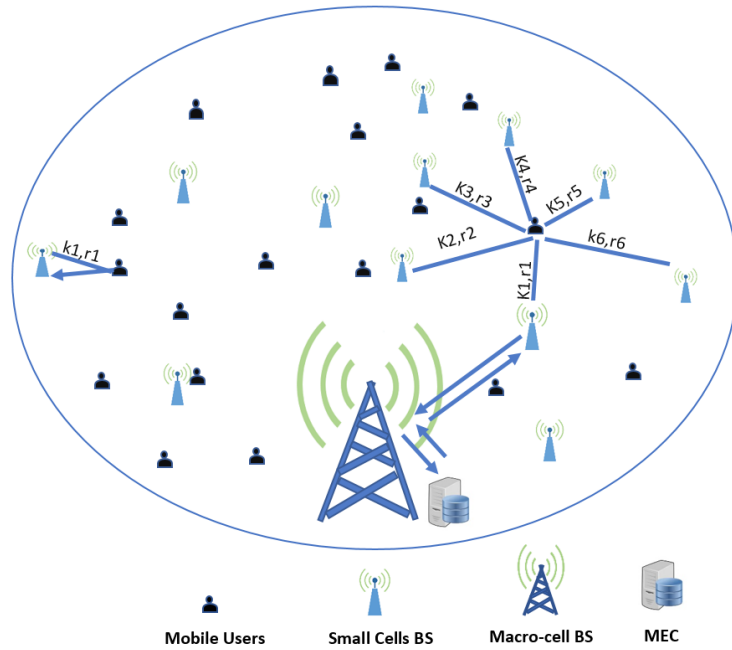
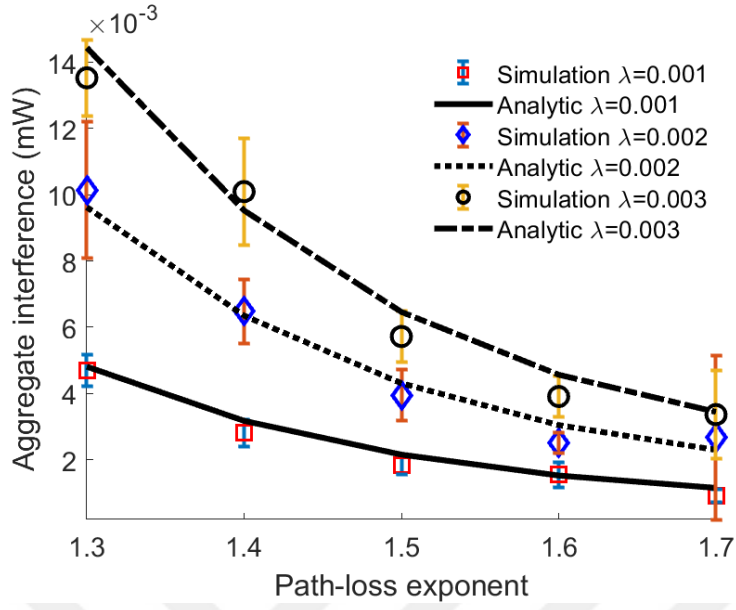
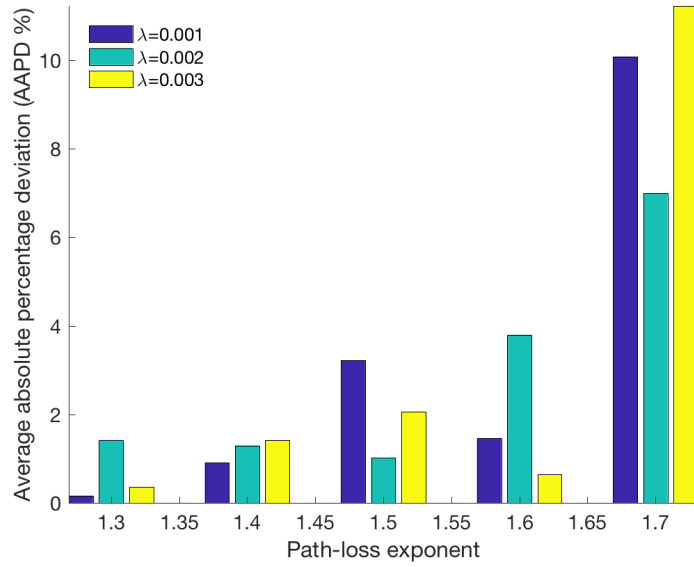


Figure 3.5: A cellular network scenario including a set of base stations, user equipment and a macro-cell for backhauling.

As a simple back-of-the-envelope calculation, we consider a network where the base stations are randomly deployed with an effective density of λ nodes/m² in a two-



(a) Aggregate interference (mW)



(b) AAPD (%)

Figure 3.6: Impact of path loss exponent γ and density λ on aggregate interference from all nodes.

dimensional Euclidean space as illustrated in Figure 3.5. This corresponds to the 2-D Poisson point process. The joint probability density function (PDF) of random distances from a randomly selected reference point up to the n^{th} nearest neighbor is given in [212] as $f_{\mathbf{R}_n}(r_1, r_2, \dots, r_n) = e^{-\lambda \pi r_n^2} (2\pi\lambda)^n \prod_{i=1}^n r_i$. We consider the simple path-loss model; the received signal power by a randomly positioned user equipment from the k^{th} nearest base station that is r_k meters away is $x_k = K (r_0/r_k)^\gamma$, where γ is the path-loss exponent, K accounts for the attenuation factor at r_0 , the impact of non-distance-related factors and the transmission power. The mean of the received interference power from the closest n base stations to a randomly located UE is then

$$\mu_n = \frac{2K(\pi\lambda)^{\gamma/2}\Gamma(n+1-\frac{\gamma}{2})}{(2-\gamma)\Gamma(n)}, \quad (3.1)$$

where $\Gamma(\cdot)$ is the Euler gamma function and $\gamma < 2$. Unfortunately, we could not derive a closed-form formula for the PDF of the aggregate interference in this formulation. In large scale networks, the aggregate interference from a huge number of interferers approaches to

$$\mu_n = \frac{2Kn(\pi\lambda/n)^{\gamma/2}}{(2-\gamma)}, \quad (3.2)$$

by using Stirling's approximation of the quotient of gamma functions. We present aggregate interference in Figure 3.6 that are validated by Monte-Carlo simulations implemented in Matlab. In the simulations, a set of base stations are uniform randomly deployed in a circular field with the chosen density. As shown in Figure 3.5, the processing power of BSs can be enhanced by equipping the network with MECs. For instance, in this scenario the density of BSs can also be obtained by a density estimator model deployed in MEC [42]. The simulation parameters are presented in Table 3.5. The downlink received signal strength for a randomly located UE is computed following the simple-path loss model. We fix $K = -40.046$ dB including the transmit power. Figure 3.6a depicts that for the same path-loss exponent, when the density of BSs decreases, aggregated interference also diminishes because of lower received power. When the network conditions such as channel quality are harsh, we can deploy more base stations to enhance the QoS. Aggregate interference grows up by increasing the density, as shown in Figure 3.6a. The convergence is only possible when $\gamma < 2$. As the path-loss exponent increases, the aggregate interference will drop as expected. The average absolute percentage deviation (AAPD %) of the analytic aggregate interference results from those of the simulations are shown in Figure 3.6b.

As the path loss exponent goes to 2, the AAPD values increases and gets closer to 10%-15% range. Since this model leverages the average received signal strength, the accuracy of the results is subject to the positions of the nodes, and the topology. If the user is near to the middle, then the accuracy of the results will be higher. However, if the user or the nodes at the corner of the topology, then the accuracy of the results will degrade. These results provide us an intuition about how UE's downlink capacity changes as the density of the network increases. Practical issues such as shadowing, fading, transmit power adaptation have to be addressed for dense networks to draw adequate conclusions.

All in all, one size protocols that are statically configured will not fit all scenarios in dynamic networks. Robust interference management, coverage control and SON techniques that take mobile cells into account have to be developed. Such approaches may increase the cost of control. Backhauling from cells on wheels or wings to the infrastructure may increase the load on and the cost of transport networks. Traffic from mobile cells may overload the whole system if not controlled. Topology control and resource allocation become a very important challenge that cannot be easily addressed with the present inflexible management planes.

3.4 Conclusion

With the invent of mobile BSs such as drone cells, not only the user's devices but also the elements in the infrastructure of the network has also become mobile, introducing many novel and not-addressed challenges. A flexible and density-adaptive mobile communications architecture is required. However, there is a significant research gap between state of the art and the ambition of achieving a self-organized, adaptive, and flexible networking architecture. In this thesis, we present this gap by presenting the paradigm changes in mobile communications and the consequences thereof. The existing architectures have severe limitations and shortages to be able to address the introduced paradigm changes. We stress in this thesis that density-aware and -adaptive networking is crucial in future networks by presenting a qualitative and quantitative analysis of the impact of density on network performance. We also categorized different density estimators to illustrate how the density of BSs can be

obtained in dynamic networks. We investigate opportunities can be achieved, and challenges can be faced by adapting the density of BSs in the current mobile and wireless networks to maintaining and improving quality of service and experience, latency, energy efficiency, resource management, interference management, mobility management, etc. in a comprehensive manner. We also evaluate how the density of BSs can be leveraged in the density adaptive solutions by providing a novel aggregate interference technique that can control the interference based on the density changes in dynamic networks. With the light of the comprehensive analysis and results for the density-aware and -adaptive solutions, the density can be as an opportune and a practical solution which should be considered in network communication stack to increase the network performance in addition to reducing the energy consumption and resource wastage at run-time.



CHAPTER 4

NETWORK DENSITY ESTIMATORS

In this chapter, we present the system design of our proposed network density estimation methods for different case studies of wireless networks including ad hoc networks, cellular networks, and flying ad-hoc networks. We propose three network density estimators, which are applicable in any wireless network. However, there are some constraints which are related to the dimension and structure of the network: The distance matrix-based density estimator is operational for two-dimensional networks, and the network should be organized in a clustered manner. Therefore, we design a case study including clustered ad hoc network for the implementation of this density estimator. Any kind of wireless network containing these features can utilize this network density estimator. Other density estimators which are interference-based density estimator and multi-access edge cloud-based density estimator are operational in three-dimensional wireless networks. Therefore, we apply this density estimators by designing cellular network and flying ad hoc network case studies.

4.1 Density Estimation in Ad Hoc Networks

In this thesis, we propose a novel cluster density estimator in random ad hoc networks by employing distance matrix. We assume a scenario based on a clustered ad hoc network where the leader of a cluster can perform the estimator.

4.1.1 Distance Matrix-based Density Estimator

Assume N nodes move freely in a mobile ad hoc network and the mobility models (directions, speed, acceleration) of nodes are not known in advance. By exchanging

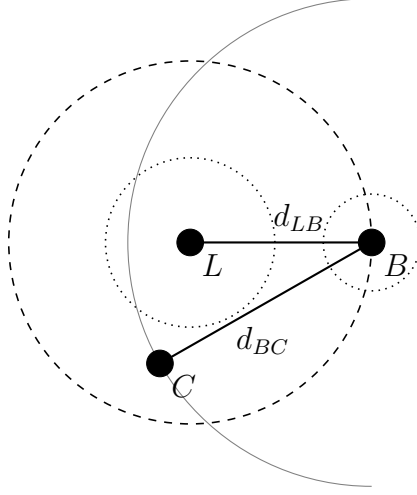


Figure 4.1: The illustration of the proposed density estimator. Three nodes in a randomly deployed ad hoc network, namely, the leader node L , the most distant node to the leader B and B 's most distant node C are shown. We use the distances to compute the effective area and assume that the leader knows the total number of nodes in the cluster.

some control packets, nodes are able to measure the received signal strengths (RSS) or propagation delay that can be used to estimate the transmitter-to-receiver distances. Let $\mathbf{D}_{N \times N}$ represent the distance matrix where its element d_{ij} is the distance between node $i = 1, 2, \dots, N$ and node $j = 1, 2, \dots, N$. A node in the set of N nodes, say node L in Figure 4.1 is designated as the leader. We aim at quantifying the density of the cluster, $\hat{\lambda}$ nodes/m².

We assume the leader is able to construct $\mathbf{D}_{N \times N}$ using some method as discussed in Section 4.1.1. In fact, we do not require the whole matrix, we will be using only two rows of it. Let d_{ij} and \tilde{d}_{ij} be the actual and estimated distances between node i and j . We assume normally distributed measurement errors (or noise, ϵ_{ij}) with zero mean and standard deviation σ ; therefore, $\tilde{d}_{ij} = d_{ij} + \epsilon_{ij}$.

As an example, we present three out of N nodes in Figure 4.1 in a randomly deployed ad hoc network, namely, L , B and C . The density estimator works as follows. The leader L determines the distance to its distant neighbor using the distance matrix, let its node identifier be B , and the distance be d_{LB} . This means that all the nodes reside in the circle centered at L 's position with radius d_{LB} as shown in Figure 4.1. Then,

B determines its most distant neighbor, say C where the distance between B and C is d_{BC} . Notice that, all other nodes have to be in the intersection area of circles centered at L and at B with radii d_{LB} and d_{BC} since these are the most distant nodes. The measurement errors may impact this argument; we will analyze the effect in the sequel. After these two steps of computations, we have computed the effective area in which all the nodes reside and we assume the leader can estimate the cluster density since it knows the total number of nodes in the cluster. Nodes may be mobile. However, we assume the relative positions of nodes to each other does not change throughout the period of computation.

Algorithm 1 Density estimator

Let L represent the node index of the leader

$[d_{LB}, B] = \max(\mathbf{D}(L, :))$ \triangleright max function returns the distance to the farthest node and its index

$[d_{BC}, C] = \max(\mathbf{D}(B, :))$

$D(i, i) = \infty$, for $i = 1, 2, \dots, N$ \triangleright Distance of nodes to themselves are set to infinity to compute min next

$[d_{LU}, U] = \min(\mathbf{D}(L, :))$ \triangleright min function returns the distance to the closest node and its index

$[d_{BV}, V] = \min(\mathbf{D}(B, :))$

if $d_{LB} + d_{LU} > d_{BC}$ **then**

 Compute $A_T = A(d_{LB}, d_{LB}, d_{BC}) - A(d_{LB}, d_{LU}, d_{BC}) - A(d_{LB}, d_{LB}, d_{BV})$ \triangleright where $A(., ., .)$ is as defined in (4.1).

else

 Compute $A_T = A(d_{LB}, d_{LB}, d_{BC}) - \pi d_{LU}^2 - A(d_{LB}, d_{LB}, d_{BV})$

end if

 Compute $\hat{\lambda} = \frac{N-2}{A_T}$ nodes/m²

The area $A(d, r, R)$ of the intersection of two circles, where the distance between the centers, the radii of the two circles are represented with d, r and R respectively, can be computed as [213]:

$$A(d, r, R) = r^2 \cos^{-1} \left(\frac{d^2 + r^2 - R^2}{2dr} \right) + R^2 \cos^{-1} \left(\frac{d^2 - r^2 + R^2}{2dR} \right) - \frac{1}{2} \sqrt{(d+r-R)(d-r+R)(-d+r+R)(d+r+R)} \quad (4.1)$$

We may exploit two other facts in this model. L and B may compute the distance to their closest neighbors, say U , and V . Computing the distance to the closest nodes indicate that there are no other nodes within the circles centered at L and B with radii d_{LU} and d_{BV} . We may enhance the resolution of the effective area and consequently the accuracy of the estimator by subtracting the areas of these circles from the above explained intersection area. In the last step of the algorithm, we subtract 2 from the total number of nodes in the cluster since the areas where these two nodes (L , and B) reside are not included in the effective area computation. The overall procedure for the proposed density estimator is presented in Algorithm 1. We will show in the next section that this estimator is not only simple but also very accurate.

Distance Estimation and Errors

The estimation of distances in wireless networks can be carried out in various ways. Existing approaches are to use the received signal strength (RSS), signal-delays such as time-of-arrival (ToA), or hop count. Most of the methods rely on some anchor nodes that know their coordinates or able to determine them by GPS [2] [214]. RSS is a function of the transmitter-to-receiver distance. Therefore, RSS can be employed to estimate the distances in wireless networks, albeit it is a mediocre estimator. Shadowing, multipath fading and many other environmental factors affect the quality of signals. As a consequence, spatio-temporal changes in link quality have a huge impact on the distance estimation. The impact of shadowing on distance estimation is presented in [215]. Chitte *et al.* conclude that the maximum likelihood estimation of distance is an inefficient problem and there is a unique unbiased estimator whose variance increases exponentially with noise power. When orthogonal frequency division multiplexing is employed, channel state information (CSI) provides a larger amount of information than RSS. Applications of CSI to localization and ranging is reviewed by Yang *et al.* in [216]. A thorough survey of distance estimation based on ToA of signals is presented in [217]. The measurement errors are mostly due to obstructions on the transmitter-to-receiver path that generates non-line-of-sight conditions. Interference and imperfections of the equipment are the additional sources of errors in general.

Complexity of the Algorithm

Firstly, the algorithm requires the distance from the leader L to the most distant node B and its index. Secondly, the distance to C (the most distant node to B) is required. We need not compute the whole distance matrix \mathbf{D} . At the link layer of communication stack of any ad hoc network, nodes employ some neighbor discovery technique to determine their local topology. We assume at this phase, nodes are able to compute the distances to their neighbors as well. The estimated distance vectors are to be conveyed to the leader in the sequel. Then, the leader is able to estimate the cluster density with simple mathematical operations in constant time, $\mathcal{O}(1)$. To reduce the messaging complexity, leader may determine the identity of node B first and then send a unicast message to acquire its distance vector.

4.1.2 Other Estimators

We compare our proposal with the RSS-based estimator presented in [54] and the estimator proposed in [214] that is based on the distances to the closest neighbors.

4.1.2.1 RSS-based Collective Distance Estimator

Assume each node can measure RSSs from its neighbors in a collective fashion in a field [54]. Distance estimation is done by using these measurements including multiple observations between two nodes. By using the simple path-loss model we can calculate estimated distances (d_j values) by using these RSSs. After (d_j values) are obtained among each pair nodes, $\widehat{\lambda}_C = T/(\pi \sum_{j=1}^n d_j^2)$ is performed to find the density. T is the summation of the connectivity degrees (k_j), and it can be obtained from $T = \sum_{j=1}^n k_j$.

4.1.2.2 Kendall's Distance Estimator

In 2.26 of Kendall's book, Geometric Probability [214], the estimator is explained as follows. Assume that y_1, y_2, \dots, y_n are n measurements of the square of the distances

to the closest neighbors. In the implementation, we assume that all the nodes in the network measure the square of the distances to their closest neighbors and convey this information to the leader of the cluster. Using these measurements, the leader can compute $Y = \sum_{i=1}^n y_i/n$. It is shown that the expected value of $\mathbb{E}[Y] = 1/(\pi\lambda)$. Therefore, $\hat{\lambda}_K = 1/(\pi Y)$.

4.2 Density Estimation in Cellular Networks

As demand for mobile communications increases, cells have to become smaller to efficiently use the scarce spectrum and to increase capacity, and small-cell networks will hereby emerge. They may be large in scale and highly dynamic resembling ad hoc networks due to the moving base stations. The variations in the density of the small cell networks impact the quality of service and introduce many novel challenges such as coverage control. We propose two novel base station density estimators, the interference-based density estimator (IDE) and the multi-access edge cloud-based density estimator (CDE) in a three-dimensional field. The estimators employ received signal strength measurements. We validate these two density estimators by using Monte-Carlo simulations. Furthermore, by leveraging these density estimator results, we analyze the impact of density on network outage in cellular networks and propose a density-aware cell zooming technique in Chapter 5. According to the observations, base station density affects network coverage significantly. Received signal strength-based density estimators can easily be implemented and applied in the network communication stack although they are more prone to the large and small scale fading. Under favor of the density-aware cell zooming method, the network outage can be managed dynamically by adapting the transmit power, which provides a self-configurable and -organized network.

4.2.1 System Model

In an m -dimensional Euclidean space, we assume that a large number of nodes (base stations and UEs) are distributed uniform randomly [218, 219]. It is assumed that the random variables indicated the number of nodes deployed in any disjoint Borel set

A_1 and A_2 are independent and follow a Poisson distribution with a mean density λ nodes per unit m -volume. The derivation of the distance distribution to k^{th} nearest neighbor for any dimension in uniformly random networks is investigated clearly in [218]. Therefore, node positions form an m -dimensional homogeneous Poisson Point Process [218, 219, 220].

By taking one of the user equipment (UE) in the uniform randomly deployed cellular network as the reference node (receiver), let's denote the distance of the reference node to its k^{th} nearest neighbor r_k with the random variable \mathbf{R}_k . The PDF of \mathbf{R}_k is

$$f_{\mathbf{R}_k}(r_k) = e^{-\lambda c_m r_k^m} \frac{m(\lambda c_m r_k^m)^k}{r_k \Gamma(k)}, \quad (4.2)$$

where $c_m r_k^m$ is the volume of the m -dimensional ball with radius r_k [220]. The coefficient c_m is defined as

$$c_m = \begin{cases} \frac{\pi^{\frac{m}{2}}}{(m/2)!}, & \text{for even } m \\ \frac{\pi^{\frac{m-1}{2}} 2^m (\frac{m-1}{2})!}{(m)!}, & \text{for odd } m. \end{cases} \quad (4.3)$$

where Γ is the gamma function interpolating the factorial function [221]. For example, $\Gamma(k)$ equals to $(k-1)!$. When $m = 1, 2$ or 3 c_m is $2, \pi$ and $4\pi/3$, respectively. For instance, a vehicular network on a road can be modeled in one dimensional space where $m = 1$ and $c_m r_k^m = 2r_k$ m. If it is in two dimensional, then $m = 2$ and $c_m r_k^m = \pi r_k^2$ m² are considered. Distribution of unmanned aerial vehicles in space may require a three dimensional model, where $m = 3$ and $c_m r_k^m = 4\pi r_k^3/3$ m³.

We assume that a large number of many base stations are deployed in a cellular network and the positions of BSs follow uniform random distribution in the three-dimensional Euclidean space with density λ (nodes/m³). We exploit the simple path-loss model; the received signal power x_k of a BS from its k^{th} nearest neighbor that is r_k meters away is $x_k = C P_t \left(\frac{r_0}{r_k}\right)^\gamma$ where $\gamma \leq 3$ is the path-loss exponent, C accounts for the attenuation factor at a reference distance of r_0 meters and the impact of non-distance-related factors such as antenna gains, calculated by using $G_t G_r ((300 \times 10^6 / f) / (4\pi))^2$, where G_t is the transmitter receiver antenna gain in dB, G_r is the receiver antenna gain in dB, and (f) is the frequency with value of 2400×10^6 Hz. For simplicity we set $r_0 = 1$ m; then $x_k = C P_t r_k^{-\gamma}$. The transmit power of base

stations is represented as P_t . The received signal strength with the random variable P_k is a function of R_k . For the sake of generality, the probability density function of P_k calculated using above PDF of R_k and the simple path-loss model is

$$F_{P_k}(x_k) = \frac{m\lambda^k r_0^{mk-1} c_m^k \left(\frac{x_k}{CP_t}\right)^{k\left(\frac{1-m}{\gamma}\right)} e^{-\lambda c_m r_0^m \left(\frac{x_k}{CP_t}\right)^{\frac{-m}{\gamma}}}}{\Gamma(k)}. \quad (4.4)$$

Although we assume moving base stations, we suppose that the locations of base stations and user equipment do not change dramatically during the measurement period. The estimator can compute the estimate over a single slot that can be very short. Therefore, the network can be considered stationary throughout the estimation period. This system-level model is based on a generalization of Winner II channel models following a stochastic approach and statistical distribution, which can be used for indoor and outdoor scenarios [81]. Moreover, we assume that a dedicated control channel is only implemented by BSs, therefore the interference from different UE is not considered in this work. In a coordinated fashion, we assume that UEs can receive signals only its corresponded base stations.

4.2.2 Network Density Estimators

In this work, we concentrate only on the density of base stations that is called as network density; we do not deal with the density of users. The received signal strength (RSS) of signals transmitted by BSs and measured by user equipment (UE) is highly correlated to the density of base stations. Therefore, we construct two techniques for estimating the network density using the RSS measurements of UEs. Firstly, we present a novel estimator that uses the aggregate interference from the nearest N base stations. This estimator is called as the interference-based density estimator. Secondly, we revert an early density estimator developed for two-dimensional ad hoc networks and adapt it to the mobile networks where multi-access edge cloud computing (MEC) is employed. Hence, we call it as the MEC-based density estimator.

4.2.2.1 Interference-based Network Density Estimator (IDE)

By selecting a random position as the location of a reference UE, let's denote the distance of the UE to the k^{th} nearest base station r_k with the random variable \mathbf{R}_k . Based on the system model presented in Section 4.2.1, the joint probability density function (PDF) of the distances of the randomly selected reference point to the first N BSs, $\mathbf{r} = (r_1, r_2, \dots, r_N)$ denoted with the random variables $\mathbf{R} = (R_1, R_2, \dots, R_N)$ as derived from [219] is

$$f_{\mathbf{R}}(\mathbf{r}) = e^{-\frac{4}{3}\pi\lambda r_N^3} (4\pi\lambda)^N r_1^2 \dots r_N^2 d\mathbf{r}.$$

Assume that all these N base stations transmit a signal at the same time. The expected value of the aggregated interference measured by a UE located at a random point then becomes

$$\begin{aligned} \mu_I &= \int_0^\infty \int_0^{r_N} \dots \int_0^{r_2} \sum_{i=1}^N C P_t r_i^{-\gamma} f_{\mathbf{R}}(\mathbf{r}) d\mathbf{r} \\ &= \frac{3C P_t (4/3\pi\lambda)^{\gamma/3} \Gamma(N - \gamma/3 + 1)}{(3 - \gamma)\Gamma(N)}, \end{aligned} \quad (4.5)$$

where $\Gamma(\cdot)$ is the gamma function, and $\gamma < 3$.

In the Interference-based Density Estimator method, each UE measures the aggregate interference from the nearest base stations and report these measurements to their associated base stations. In the coverage of each base station, there will usually be a large number of UEs, say M . The base station will average the aggregate interference measurements of UEs and then will estimate the network density as

$$\hat{\lambda}_{\text{IDE}} = \frac{1}{4\pi} \left(\frac{\bar{\mu}_I (3 - \gamma)\Gamma(N)}{3^{1-\gamma/3} C P_t \Gamma(1 + N - \gamma/3)} \right)^{3/\gamma}, \quad (4.6)$$

where $\bar{\mu}$ is the average of aggregate interference measurements by M UEs. In IDE, all base stations can estimate the network density in a local fashion with the assistance of the UEs in their coverage areas. One can enhance the performance of $\hat{\lambda}_{\text{IDE}}$ by averaging the individual estimates of base stations. Although, we call it interference, BS generates collusion of signals intentionally to let UEs take samples.

4.2.2.2 Multi-access Edge Cloud Based Network Density Estimator (CDE)

We present the multi-access edge cloud-based density estimator (CDE) as the second estimator model. In CDE, we assume that user equipment measure the received signal strength (RSS) of pilot signals transmitted by base stations at various non-overlapping time slots and send these measurements back to their associated base stations. Then, the base stations convey these measurements to a multi-access edge computing (MEC) entity. Afterwards, the MEC employs these measurements to estimate the network density. We modify the two-dimensional model proposed in [55] to fit it into the three-dimensional Euclidean space. In this section, we present the theoretic basis of the maximum likelihood density estimator $\hat{\lambda}_{\text{CDE}}$ where the actual density is λ in nodes/m³.

By selecting a random position as the location of a reference UE let's denote the distance of the UE to the k^{th} nearest base station r_k with the random variable \mathbf{R}_k . The PDF of \mathbf{R}_k [55] is

$$f_{\mathbf{R}_k}(r_k) = e^{-\frac{4}{3}\pi\lambda r_k^3} \frac{3(\frac{4}{3}\pi\lambda r_k^3)^k}{r_k \Gamma(k)}. \quad (4.7)$$

We represent the received signal power from the k^{th} base station x_k with the random variable \mathbf{P}_k which is a function of \mathbf{R}_k considering the system model presented in Section 4.2.1. Then, the cumulative distribution function (CDF) of \mathbf{P}_k [55] becomes

$$F_{\mathbf{P}_k}(x_k) = \frac{\Gamma\left(k, \frac{4}{3}\pi\lambda x_k^{-3/\gamma} \left(\frac{1}{CP_t}\right)^{-3/\gamma}\right)}{\Gamma(k)}, \quad (4.8)$$

where $\Gamma(a, z) = \int_z^\infty t^{a-1} e^{-t} dt$ is the incomplete gamma function [55], when we consider the model for three-dimensional deployment of base stations and user equipment.

Let x_i denotes the RSS of a pilot signal transmitted to a UE by its k_i^{th} nearest base station, and (4.8) is the CDF of x_i . After n RSS samples x_1, x_2, \dots, x_n and the corresponding neighbor proximity indexes k_1, k_2, \dots, k_n are collected by UEs collectively *from non-overlapping regions*, UEs convey these measurements to the MEC over base stations. Then, the MEC can compute the maximum likelihood estimator, $\hat{\lambda}$. We assume the node distribution of base stations in the m -dimensional space follows a homogeneous Poisson point process (PPP); and the RSS measurements are

independent since they are collected from non-overlapping regions. As in [20, 55], the maximum likelihood density estimator becomes

$$\hat{\lambda}_{\text{CDE}} = \frac{K - 1}{\frac{4}{3}\pi \sum_{j=1}^n \left(\frac{x_j}{P_t C}\right)^{-3/\gamma}}, \quad (4.9)$$

where $K = \sum_{j=1}^n k_j$. The unit of density is nodes/m³. $\hat{\lambda}_{\text{CDE}}$ is an unbiased estimator and its variance goes to zero as more and more samples are collected from the field. Therefore, the number of collected samples impact K which in turn significantly impacts the accuracy of the estimator $\hat{\lambda}$. It can be seen that the different dimensions have different c_m and m values [55, 218]. Then, we can generalize the estimator as follows:

$$\hat{\lambda}_{\text{CDE}} = \frac{K - 1}{c_m \sum_{j=1}^n \left(\frac{x_j}{P_t C}\right)^{-m/\gamma}}.$$

4.3 Density Estimation in FANETs

The variations in the density of the flying ad hoc networks impact the quality of service, and introduce many challenges. In this thesis, we present a novel density-aware technique to increase and stabilize channel utilization for flying ad hoc networks (FANET).

Assuming that a FANET consists of a number of UAVs as uniform randomly deployed with a density of λ (nodes/m³). DASAP is used as a communication protocol between UAVs by taking advantage of the slotted ALOHA protocol just with a dynamic channel access probability. It is assumed that time is divided into a number of slots. The channel access probability of each UAV may initially be set randomly. We may assume that each UAV can make this initialization by itself or a base station in this FANET may distribute the initial parameters of DASAP via broadcasting. In this network, since at the beginning of each time slots, two kinds of UAVs which may be determined in a probabilistic manner, the transmitting UAVs generates random signal, and then each of estimating UAVs can measure the noise power on the channel. The estimating UAVs can estimate the density of UAVs by measuring the channel power. In order to determine the network density, UAV executes interference-based network density estimator as explained in Section 4.2.2.1. The estimating UAVs can now update their channel access probability based on the effective density value.

One of the design questions in this analysis is that should we estimate the UAV density at the beginning of each time slot? In other words, what should be the number of optimal Estimation mini-slots? By considering DASAP, we can claim that we need to reserve a portion of each time slot for the estimation, since we need to update the channel access probabilities depending upon the effective network density. According to the system design, at each time some of the UAVs are selected estimating UAVs and some of them are chosen as transmitter UAVs. Only the subset of estimating UAVs can update their channel access probability according to their estimated density value. Therefore, we observe that for a stabilized channel access probability, we divide the required number of time slots to be sure that each of UAV change its access probability by determining according to its effective density measurement. In addition, at each time slot, the network topology is changed. Since we are proposing an approach for FANETs, we should consider a highly dynamic network topology. This perspective also encourages to make estimation at the beginning of each time slot.

CHAPTER 5

DENSITY-AWARE NETWORKING APPLICATIONS

This chapter discusses the density-aware and -adaptive protocols and network parameters proposed in this thesis. There are three categories for density-adaptive models. The first one is called density-aware network outage for two-dimensional and three-dimensional networks. The second one is the density-aware transmit power adaption method which is designed as different dimensions. Finally, we discuss the density-adaptive dynamic channel utilization method for flying ad hoc networks.

5.1 Density-aware Network Outage

We propose network outage models which utilize the network density as an optimization parameter.

5.1.1 Network Outage in Two-Dimensional Wireless Networks

Assume a two-dimensional clustered ad hoc network where nodes are uniformly randomly deployed with an effective density of λ nodes/m². Let x_k refer to the RSS of a packet measured by a randomly located reference node from the k^{th} closest neighbor that is r_k meters away. By considering the simple path-loss model, the RSS will be $x_k = K P_t \left(\frac{r_0}{r_k} \right)^\gamma$ where K is the fading factor at $r_0 = 1$ m that accounts for the effect of non-distance-related aspects, P_t is the transmit power and $2 \leq \gamma \leq 7$ is the path-loss exponent.

Consider a random node as the reference node in a clustered ad hoc network, and let r_k represent the distance of that node to the k^{th} closest node that is represented

with the random variable \mathbf{R}_k . The RSS of a packet sent from the k^{th} closest node to the reference node, x_k is represented with the random variable $\mathbf{P}_{\mathbf{I}_k}$ that is a function of \mathbf{R}_k . This channel model considers only path loss; shadowing or fading are not considered. Then, the CDF (Cumulative Distribution Function) of $\mathbf{P}_{\mathbf{I}_k}$ [55] is defined as

$$F_{\mathbf{P}_{\mathbf{I}_k}}(x_k) = \Gamma \left(k, \pi \lambda \left(\frac{K P_t}{x_k} \right)^{2/\gamma} \right) / \Gamma(k).$$

In this thesis, we consider outage probability as the probability (P_O) of the strength of the signals transmitted by the closest neighbor of the reference node (i.e., $k = 1$) being smaller than a threshold, T . Based on this definition, the outage probability can be calculated as

$$P_O(\lambda) = F_{\mathbf{P}_{\mathbf{I}_1}}(T) = e^{-\pi \lambda (K P_t / T)^{2/\gamma}}. \quad (5.1)$$

5.1.2 Network Outage in Three-Dimensional Wireless Networks

By considering the PDF of \mathbf{R}_k (4.7) and the CDF of \mathbf{P}_k (4.8), we present the outage probability as the probability (P_O) of the received power of the signals transmitted by the closest base station (i.e., $k = 1$) and measured by the randomly located reference user being below the receiver sensitivity, T . Based on this definition, the outage probability becomes

$$P_O(\lambda) = F_{\mathbf{P}_{\mathbf{I}_1}}(T) = e^{-4/3 \pi \lambda (C P_t / T)^{3/\gamma}}, \quad (5.2)$$

where T is the receiver sensitivity (threshold) that is the minimum required received signal strength to intelligibly decode the signals [222]. (5.2) is different from its two-dimensional representation proposed in [144]. The dimension of the solution changes the network outage model. This network outage model analytically indicates that the outage probability and the base station density are two important interactive parameters. The network outage is also influenced by the path-loss exponent, transmit power of base stations and the minimum power requirement which is the threshold value as experimentally demonstrated in Section 6.2.2.1. The PDF decreases with $e^{-(C P_t / T)^{3/\gamma}}$ when P_t increases, the outage probability becomes zero. When T increases the expected value will be 1. The PDF of received signal strength (4.4) will affect the outage probability. If P_t increases the received signal strength will be increases, which means more and more UE can receive the message with a higher RSS.

In this formulation, we suppose that there is a robust interference cancellation technique implemented in the system. That is why we consider only the received signal strength instead of signal-to-interference-plus-noise ratio (SINR) [20].

5.2 Density-aware Transmit Power Adaptation (DTPA)

We suggest cell-zooming methods based on the network density and transmit power adaptation for different dimensional networks.

5.2.1 Transmit Power Adaptation in Two-Dimensional Wireless Networks

Let network designer designate the required outage probability, P_O^* as a design parameter. Assume that each node can distributively estimate the density of the cluster it belongs to for computing outage as in (5.1). Nodes can adapt their transmit power to the estimated density $\hat{\lambda}$ in a dynamic fashion for overcoming energy consumption and coverage problems by

$$P_t^* \geq \frac{T}{K} \left(\frac{-\log(P_O^*)}{\pi \hat{\lambda}} \right)^{\gamma/2}. \quad (5.3)$$

During the estimation of density P_t will be considered as fixed.

5.2.2 Transmit Power Adaptation in Three-Dimensional Wireless Networks

Let's assume that the base stations located in a cellular network has an ability to estimate the network density. Then the adaptation of their transmit power levels using (5.2) would be possible in order to satisfy a provided outage probability level in a decentralized or distributed fashion [20]. Using (5.2), the transmit power has to be adapted to its minimized value

$$P_t^* \geq \frac{T}{C} \left(-\frac{3 \log(P_O^*)}{4\pi \hat{\lambda}} \right)^{\gamma/3}, \quad (5.4)$$

where the required outage probability P_O^* is a network design parameter set by the network operator and $\hat{\lambda}$ is either IDE or CDE. We assume that using some technique,

IDE or CDE, base stations estimate the density of the network. Then, they employ the estimated density $\hat{\lambda}$ to set their transmit power using (5.4).

With the help of the transmit power adaptation technique, we can choose the minimum required power instead of a constant or pre-configured value to manage the coverage area of the network. After, updating the value of minimum required power, namely receiver sensitivity, transmit power of base stations can be updated based on the effective network density measurements and the required outage probability provided by network operators. This adaptation provides us energy efficient network configuration.

Although many phenomena and impairments that affect the received signal strength are not included, this model is very practical as a result of its simplicity. Many users in a cell may independently measure the received signal strength. These measurements may be transmitted to a mobile edge computing (MEC) entity, and fusion of the results may be exploited by the MEC and base stations to decrease the impact of fading and shadowing. By means of the user equipment signal strength measurements, base stations will be able to arrange their transmit powers immediately bounded with the time period of the density estimation. A simple and fast density estimator will be very rewarding for this matter. Hence, we suggest two novel three-dimensional density estimators.

All these models need to be validated. In Chapter 6, we validate these models by using Monte Carlo simulations and leverage them to demonstrate their applications and analyze the outcomes for different scenarios.

5.3 Density-aware Channel Utilization in FANETs

In this section, we introduce density-aware slotted ALOHA protocol which provides a dynamic random access and optimized channel utilization. To perform the proposed technique, we assume a scenario based on flying ad hoc networks. This protocol takes advantage of interference-based density estimator.

5.3.1 System Model

In this thesis, we propose a novel density-aware MAC protocol design based on slotted ALOHA with a dynamic channel access probability which is called Density-aware Slotted ALOHA Protocol (DASAP). Consider a random flying ad hoc network that employs slotted ALOHA over a single channel. We divide the time into a number of slots. The structure of a time slot is illustrated in Figure 5.1 which includes two mini-slots: The first mini-slot denominated as Estimation mini-slot for estimation procedure which starts from the beginning of the corresponding time slot, and in the second mini-slot UAVs can make packet transmission based on a dynamic channel access probability, p . A sample link layer frame divided into n time slots is displayed in 5.2. We assume that each of the time slots are equal in length. At the beginning of each time slot UAVs randomly determine whether or not to transmit a pseudo-random signal in the Estimation mini-slot with a predetermined constant transmission power level. With considering the Poisson point-process assumption, the transmitting UAVs are randomly determined with probability, p_s . That we call as the selection probability. Those UAVs that do not generate noise signal power on channel and estimate the density of UAVs, determine their individual channel access probabilities with the estimated density and in the data transmission slot transmit their packets according to the computed channel access probabilities. In other words, by obeying the selection probability p_s , UAVs are selected as transmitting or estimating UAVs in a probabilistic manner. Figure 5.3 shows the generated signals from transmitting nodes, and estimating nodes in these time slots. In Figure 5.3, two different Estimation mini-slots are displayed. In these two of mini-slots, the changing distribution of UAVs are also illustrated.

We assume that the UAVs are randomly deployed with a density of Λ nodes/m³ in a three-dimensional volume. The effective density of the transmitting (active) UAVs at the designated control slot becomes $\lambda = p_s \Lambda$, where p_s is the selection probability mentioned in Section 5.3.1.

We assume that the locations of the UAVs do not change significantly throughout the Estimation mini-slot of a time slot and the network can be considered stationary during the estimation process. Since the estimator does not require any communication,

and it can compute the estimation result over a single slot that can be very short, i.e., stationary assumption is valid. A subset of the UAVs *randomly* access the channel at Estimation mini-slot, therefore the uniform randomness assumption is not violated.

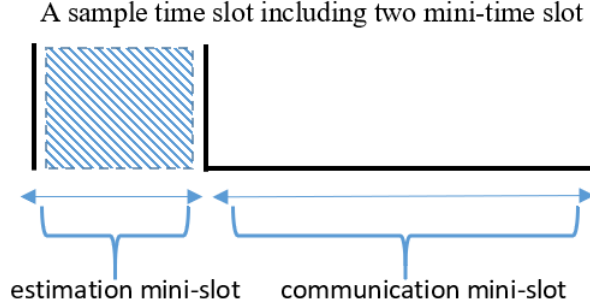


Figure 5.1: The first mini-time slot called **estimation mini-slot** to perform the estimation of the UAV density (nodes/m³). Some of the UAVs are selected based on a selection probability as estimating UAVs, and others will be assigned as transmitting UAVs. The estimating UAVs can determine the effective UAV density by total signal strength on the estimation mini-slot from the transmitter UAVs in its communication range. Then, estimating UAVs use the estimated density by the selection probability to obtain the whole network density. The second mini-time slot named as **communication mini-slot** where UAVs can transmit their packets based on the dynamic channel access.

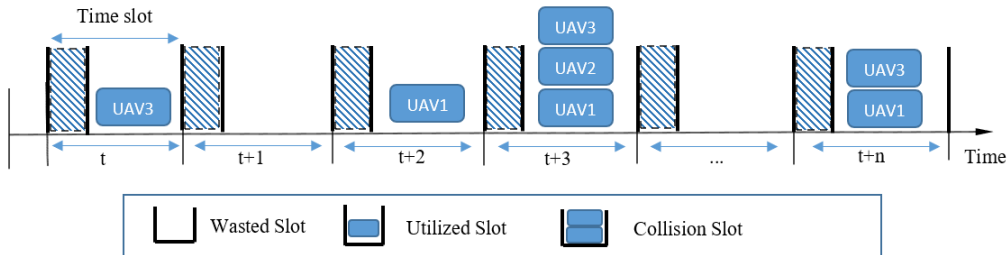


Figure 5.2: A MAC frame example with three UAVs and n time slots. Each of the UAVs send several packet replicas. Slots t , and $t + 2$ are successful transmissions. Slots $t + 3$, and $t + n$ are collided on the other hand slots $t + 1$ is a wasted slot.

The inactive UAVs (i.e., those that do not generate a signal) only measure the signal power on the channel in the Estimation mini-slot without trying to decode the signals intelligibly. Let us represent the accumulated power of the signals sampled by a

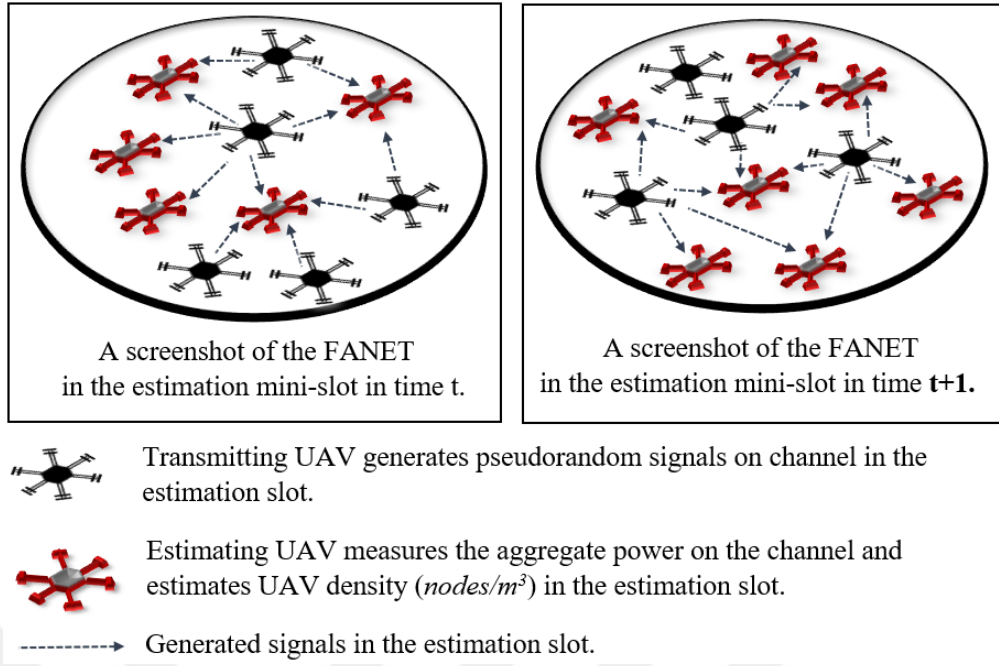


Figure 5.3: Two sample scenarios in two estimation mini-slots. For the sake of simplicity, we present estimating and transmitting UAVs as different view-design. In the fact that, UAVs designate themselves independently and randomly with probability p_s as transmitting or estimating nodes locally. Communication between UAVs is performed within the boundaries of corresponding UAV communication range.

node using received signal strength, which is not active in that slot, with the random variable $\mathbf{P_I} = \sum_{k=z}^{\infty} \mathbf{P_{I_k}}$. The expected value of $\mathbf{P_I}$ is represented as μ_I as explained in Section 4.2.2.1.

5.3.2 Further Assumptions

We present the measurement of aggregate power using RSSs in Section 4.2. Our further assumptions:

Assumption 1: All nodes have a packet to send, and all packets have the same priority. The frame size is fixed.

Assumption 2: The distribution of nodes is following the three-dimensional homogeneous Poisson point process with a deployment spatial density λ (nodes/m^3).

Assumption 3: The simple path-loss model is leveraged; the received signal power x_k of a UAV from its k^{th} nearest neighbor that is r_k meters away is $x_k = KP_t \left(\frac{r_0}{r_k}\right)^\gamma$ where $\gamma \leq 3$ is the path-loss exponent, C accounts for the attenuation factor at a reference distance of r_0 meters and the impact of non-distance-related factors such as antenna gains [223].

Assumption 5: Each of UAVs can send their packets at the beginning of the Communication mini-slot. Moreover, a packet fits in a single Communication mini-slot.

Assumption 6: UAVs can measure the channel energy caused by the UAVs trying to generate a noise, and have some computational power to perform the estimation process.

Assumption 7: Each UAV has a synchronized time and knows at the beginning of the time slot.

5.3.3 Updating The Channel Access Probability

In DASAP, all UAVs can estimate the network density in a local fashion and can change its access probability based on this measurement. Since our proposed method is based on slotted ALOHA protocol, and our aim is to obtain a channel access probability and maximize the channel utilization of slotted ALOHA, we need the number of UAVs (N) within the communication range. Slotted ALOHA protocol achieves maximum channel utilization if channel access probability is selected as $p = 1/N$. Hence, we need Estimation mini-slot to determine this parameter and adapt the channel access probability p . To update the probability of channel access, we utilize a moving average approach as presented in (5.5) to take advantage of the previous values of the access probabilities. The channel access probability (p_{t+1}) of a UAV at time slot $t + 1$ is exponential moving average which provides the usage of the trending values and the current values of p in a weighted approach:

$$p_{t+1} = (\alpha) \frac{1}{\widehat{\lambda}(4/3)\pi r_c^3} + (1 - \alpha)p_t, \quad (5.5)$$

where α is a smoothing factor with a range between 0 and 1, and r_c is the maximum communication range of a node. Our aim is to reach the maximum utilization in

slotted ALOHA protocol. In SAP, the value of N , number of UAVs, can not know. However, with this approach we can obtain the number of UAVs in a volume and use this information to provide the new channel access probabilities (p_{t+1}) of each node.

5.3.4 Other Proposals

There exist two approaches that we compare them with our proposals. One of them is the theoretic slotted ALOHA protocol, and the other one is the stabilized slotted ALOHA protocol.

5.3.4.1 Slotted ALOHA Protocol (SAP)

SAP can be utilized as a communication protocol in a FANET. Assume that the channel access probability for UAVs are initialized with a constant and fixed probability value randomly. It is also assume that time is divided into slots. At the beginning of each time slot, backlogged UAVs try to transmit their packets on the channel. If there are more than one or none packets transmitted, then UAVs should wait a time slot to make a re-transmission based on the channel access probability or if there is only one packet on the channel during the slot, then this means that the packet is successfully delivered to the destination by using the same shared medium. Slotted ALOHA protocol has a constant channel access probability which is a disadvantage of this protocol.

5.3.4.2 Stabilized Slotted ALOHA Protocol (STSAP)

There is a need to avoid the weaknesses of the slotted ALOHA protocol by changing the channel access probability in a dynamic fashion. One of the possible solutions is changing the access probability by observing the result of the attempt at the beginning of a time slot. If the attempt is successful then the channel access probability is increased. However, if the transmission is collided then the access probability can decrease. UAVs need to stabilize the change of the channel access probability. Thus, STAP is defined as stated in Algorithm 5 [224, 225, 226].



CHAPTER 6

VALIDATION AND EXPERIMENTAL RESULTS

This chapter is to validate both density estimators and density-aware and -adaptive analytic models. Different types of simulations are conducted based on Monte-Carlo simulations to verify the models and to show the significant importance of density in case of network performance.

6.1 Validation of Density Estimators

In this section, we present the simulation details for the validation of the distance matrix-based density estimator, interference-based density estimator, multi-access edge cloud-based density estimator.

6.1.1 Validation of Density Estimator for Ad Hoc Networks

We validated the proposed estimator using Monte-Carlo simulations. In a circular field of interest a set of points following the deployment density λ nodes/m² are selected uniform randomly; i.e., spatial Poisson point process with intensity λ . Algorithm 1 is applied and $\hat{\lambda}$ is computed. The simulations are repeated 50 times and the averages are presented.

Performance of the Estimator

The relative standard deviation ($RSD=100\sigma_{\hat{\lambda}}/|\mu_{\hat{\lambda}}|$) of the estimator for various deployment densities is shown in Figure 6.1 when we assume no errors in the mea-

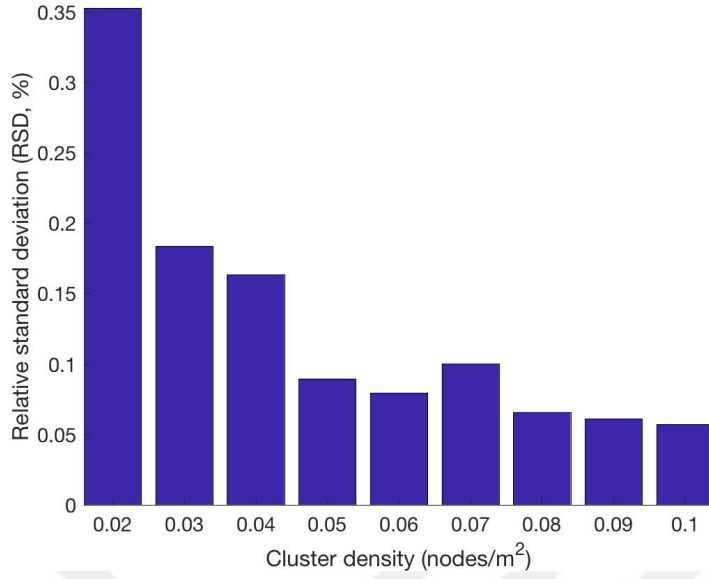


Figure 6.1: The relative standard deviation (%) of the estimator for various cluster densities where $\sigma = 0$; i.e., no error in the measurements.

surements ($\sigma = 0$). In dense clusters, a larger number of nodes are considered for the computation which reduces the variation in the estimator. Therefore, as density increases the RSD of the estimator drops as can be seen in Figure 6.1.

There will always be distance measurement errors because of multi-path fading, shadowing, and obstructions in the environment [215]. In this work we assume normally distributed error with zero mean and standard deviation σ . The impact of σ on the average absolute percentage deviation, $AAPD = (100\hat{\lambda} - \lambda)/\lambda$, is presented in Figure 6.2. An accurate method for distance estimation will enhance the quality and accuracy of the proposed density estimator as can be seen in this figure. As the errors in the distance measurements increase, the AAPD of the proposed estimator increases.

We compare our proposal $\hat{\lambda}$, Kendall's $\hat{\lambda}_K$, and the cooperative $\hat{\lambda}_C$ estimator based on the AAPD from the actual density as shown in Figure 6.2. The AAPD increases as the measurement errors increase for all estimators. However, the deviation of $\hat{\lambda}_K$ is larger than that of $\hat{\lambda}$ always and the AAPD of $\hat{\lambda}_K$ explodes while the AAPD of $\hat{\lambda}$ increases steadily. The proposed method provide more and more accurate results although the errors are increasing. $\hat{\lambda}_C$ may not provide distinctly accurate results because of uncertainties of RSS, the Kendall's AAPD results are always soaring while

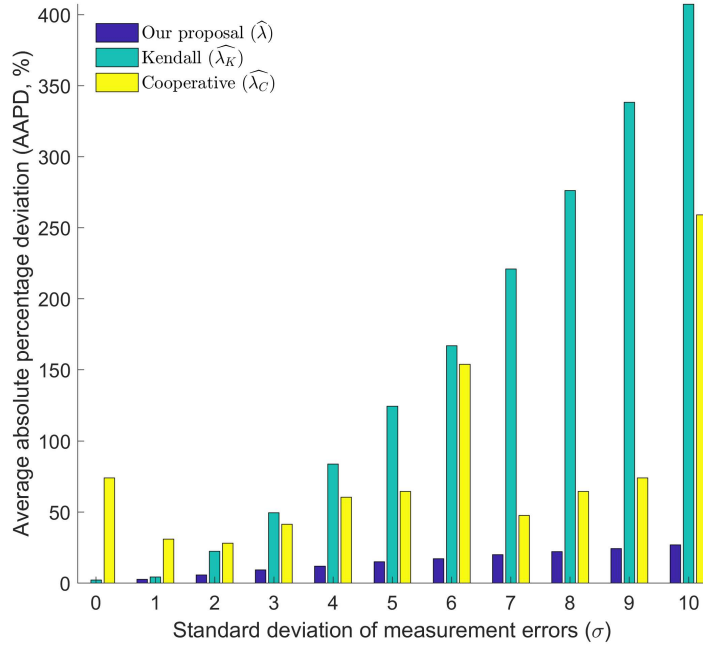


Figure 6.2: The comparison of the estimators based on average absolute percentage deviation (AAPD) where $\lambda = 0.05$ nodes/m².

the measurement errors are increasing.

6.1.2 Validation of Density Estimator for Cellular Networks

In this section, we present the simulation results for validating IDE and CDE.

6.1.2.1 Simulator Design

These network density estimators are validated by Monte-Carlo simulations implemented using Matlab. In the simulations, a number of base stations and UEs are uniform randomly deployed in a three-dimensional Poisson process in Matlab. For each run of the simulator, the locations of BSs and UEs change randomly. We assume that UEs can measure the RSS from their closest base stations. Table 6.1 presents a summary of symbols and the parameters which are considered during the validations of two estimators. Actual density, λ , is the deployment density, which is the number

Table 6.1: The symbols, notations, values and units of the 3-D simulation parameters for cellular networks.

Parameter	Default Value	Units	Ref
Actual density, λ	[0.0001,0.003]	nodes/ m^3	[20]
Estimated (effective) density, $\hat{\lambda}$	(4.6) or (4.9)	nodes/ m^3	
Sparse deployment, λ_S	0.0005	nodes/ m^3	[20]
Dense deployment, λ_D	0.0015	nodes/ m^3	[20]
Ultra-dense deployment, λ_U	0.003	nodes/ m^3	[20]
Path-loss exp. γ	$0 \leq \gamma \leq 6$		[81]
Reference distance, r_0 ,	1	m	[55]
Transmit power, P_t	[10,100]	mW	[142]
Adapted transmit power, P_t^*	(5.4)	mW	
Threshold (Receiver sensitivity), T	5×10^{-13}	mW	[20]
Required outage probability, P_O^*	[0,1]		[20]
Simulated outage probability, P_O	[0,1]		[20]
Analytic outage probability, P_{O_A}	[0,1]		[20]
Nearest neighbor index, k	$[1, \infty)$		[20]
Max. nearest neighbor index, N	$[1, \infty)$		[20]
C	10^{-5}		[20]

of UEs and BSs divided by the volume (m^3). The estimated (effective) density, $\hat{\lambda}$, is the computed density value after applying one of the density estimators in a network. Sparse deployment, λ_S , dense deployment, λ_D , ultra-dense deployment, λ_U show different deployment density for different network scenarios [20]. Path-loss exponent, γ , is the coefficient for the path-loss model in the range between 0 and 7, which is already determined as empirical values for different indoor and outdoor scenarios [54]. r_0 is the reference distance in the far-field of the antenna, which is selected as 1 m for simplicity. We assume that the random distances in the network are generally larger than the reference distance. P_t is the transmit power for base stations which is selected up to the 20 dbm considering the small cell requirements [20]. P_t^* is the transmit power for base stations adapted by the proposed model (5.4). T is calculated by $T = CP_t r_c^\gamma$, where r_c is the maximum communication range. This

threshold value for the network outage model, which is the receiver sensitivity, and it provides the minimum power requirement to receive a signal [20]. P_O^* is the required outage probability which is provided by the network operator. P_O is simulated and calculated by performing the proposed model (5.2). P_{O_A} is calculated by using the CDF of the network outage model (4.8). The nearest base station neighbor for a UE is represented as k which is in range of $[1, \infty)$ for a model based on Poisson Point Process. N is the selected maximum value of the nearest base station index. Moreover, C is a constant originated from non-distance-based factors and antenna gain, which is calculated as explained in Section 4.2.1. The results are the averages of 10^4 runs.

6.1.2.2 Validation of the Interference-based Network Density Estimator (IDE)

To validate the IDE, base stations are assumed to be randomly deployed with various densities from sparse networks to dense networks in a spherical simulation environment with a radius of 250 meters. A randomly selected point designates the location of a UE. We assume that this UE measures the aggregate signal power from the first six base stations closest to it; $N = 6$. The averages of 10^4 simulation runs are compared to the results of the analytic model (4.5) presented in Section 4.2.2.1 under the same set of parameter values.

Figure 6.3 show the simulation and analytic results based on different path-loss exponent (γ) values and various densities. As can be seen in Figure 6.3, the simulation results validate μ_I in (4.5). The accuracy of the results decreases as the environment gets harsher, i.e., when path-loss exponent becomes larger. In harsh environments with a large γ , only the overall strength of the signals become smaller. The errors in the channel model such as deviations in the γ estimates will significantly impact the density estimators.

We define the average absolute percentage deviation as $AAPD = 100|\hat{\lambda} - \lambda|/\lambda$. We present the AAPD results for the IDE ($\hat{\lambda}_{IDE}$) in Table 6.2. For various deployments with different densities, the AAPD results show that the estimation results are at an acceptable level; the AAPD values are generally less than 3. The IDE considers only path loss and non-distance related fading in signal measurements. Over channels that are prone to different types of fading, the deviations will be larger.

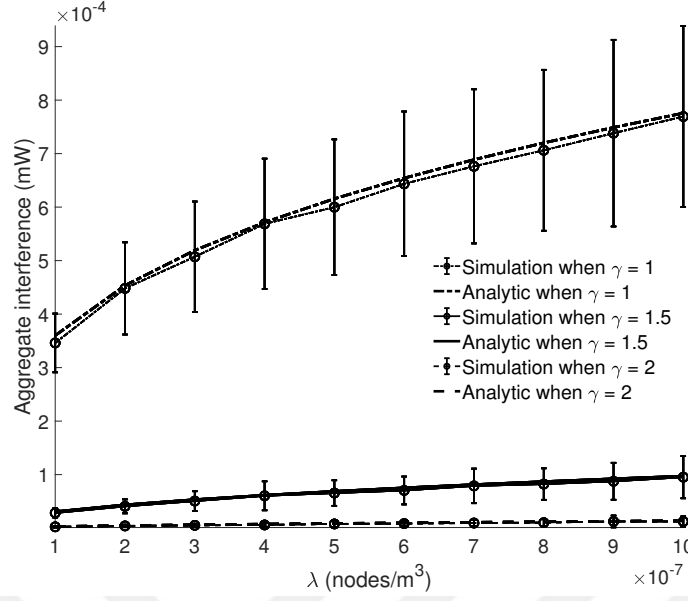


Figure 6.3: Mean aggregate interference power (mW) for various deployment densities when $\gamma = 1, 1.5$ and 2 , respectively, and $P_t = 100 \text{ mW}$.

Table 6.2: The AAPD and 99% confidence limits in the estimators for various deployments (λ) (**nodes/m³**) where $\gamma = 1.5$ and $N = 6$.

λ ($\times 10^{-6}$)	$\hat{\lambda}_{IDE}$ ($\times 10^{-6}$)	AAPD (%)	99% confidence limits of $\hat{\lambda}_{IDE} \times (10^{-8})$
0.2	0.21	3.08	± 0.24
0.4	0.41	2.30	± 0.46
0.6	0.60	0.66	± 0.59
0.8	0.81	1.29	± 0.78
1	0.99	0.61	± 0.84
1.2	1.22	2.06	± 1.31
1.4	1.42	1.24	± 1.38
1.6	1.64	2.23	± 2.33

6.1.2.3 Validation of the Multi-access Edge Cloud-based Network Density Estimator (CDE)

In the simulations for validating the Multi-access Edge Cloud-based Network Density Estimator (CDE), a set of user equipment and base stations are assumed to be uniform randomly deployed in a field of interest following 3-D Poisson process in Matlab. At each run of the simulator, the locations change randomly. UEs measure the RSS from their either first closest base stations by using the channel model described in Section 4.2.1 and these measurements are assumed to be collected at a mobile edge computing (MEC) entity. Therefore, $k_j = 1$ and $K = \sum_{j=1}^n k_j = n$, for $\hat{\lambda}_1$ where n is the number of samples collated at the MEC. Then, (4.9) is employed to compute the estimator in nodes/m³. The results are the averages of 10^4 runs. The values of the parameters employed in the simulations are shown in Table 6.1.

We present how accurate the CDE performs in Table 6.3 for various actual deployment densities λ . The first column of this table is the actual density and the second column is the result of the estimator $\hat{\lambda}$. The CDE works with acceptable accuracy and the AAPD is always less than 3%.

Table 6.3: The AAPD in the CDE for various actual deployment densities λ (nodes/m³) where $\gamma = 3$, and $\hat{\lambda}_{CDE_1}$ (nodes/m³).

λ ($\times 10^{-3}$)	$\hat{\lambda}_{CDE_1}$ ($\times 10^{-3}$)	AAPD (%)	99% confidence limits of $\hat{\lambda}_{CDE_1}$ ($\times 10^{-5}$)
1	0.98	2.50	± 0.80
2	1.96	2.09	± 1.54
3	2.92	2.66	± 2.37
4	3.91	2.16	± 3.18
5	4.93	1.44	± 4.06
6	5.93	1.16	± 4.73
7	6.85	2.11	± 5.66
8	7.91	1.12	± 6.49

The CDE results when $\lambda = 5 \times 10^{-4}$ nodes/m³ for different path-loss exponent γ

values are shown in Table 6.4. The AAPD values are considerably small for any channel model with various path-loss exponent values. The effect of the path-loss exponent on the accuracy of the CDE is not dramatic.

Table 6.4: The impact of the path-loss exponent (γ) on the CDE and the AAPD in the estimators where the actual deployment density is $\lambda = 5 \times 10^{-3}$ (nodes/m³), and $\hat{\lambda}_{CDE_1}$ (nodes/m³).

γ	$\hat{\lambda}_{CDE_1}$ ($\times 10^{-3}$)	AAPD (%)	99% confidence limits of $\hat{\lambda}_{CDE_1}$ $\times (10^{-5})$
2	4.91	1.71	± 3.54
2.5	4.90	1.94	± 3.46
3	4.93	1.32	± 3.55
3.5	4.91	1.87	± 3.54
4	4.92	1.52	± 3.54
4.5	4.94	1.29	± 3.57
5	4.90	1.98	± 3.54
5.5	4.91	1.75	± 3.44
6	4.93	1.45	± 3.50

Unfortunately, the CDE has some deficiencies. Firstly, similar to the IDE it only considers the path-loss and the non-distance related fading. Secondly, the time to compute the CDE can be long. UEs collect measurements and send them back to the base stations. Base stations convey these measurements to the mobile edge computing (MEC) entity in the network and the MEC estimates the density and informs the base stations about the result. As the third deficiency, we can partially say that the CDE may yield biased results when the measurements are collected from overlapping regions. Since we employ likelihood estimation, the CDE depends on the strict assumption of independence among measurements. When the measurements are collected from overlapping regions, there will be a large amount of correlation among measurement samples that will create a bias in the estimates.

Table 6.5: The accuracy of different estimation AAPD results of $\hat{\lambda}_{IDE}$ (**nodes/m³**), and $\hat{\lambda}_{CDE}$ (**nodes/m³**), respectively when $\gamma = 1.5$.

$\lambda (\times 10^{-3})$	$\hat{\lambda}_{IDE}$			$\hat{\lambda}_{CDE}$		
	$\hat{\lambda}_{IDE}, (\times 10^{-3})$	AAPD, %	99% confidence limits, ($\times 10^{-5}$)	$\hat{\lambda}_{CDE}, (\times 10^{-3})$	AAPD, %	99% confidence limits, ($\times 10^{-5}$)
1	0.95	4.92	± 0.23	0.94	6.45	± 0.20
2	1.92	4.16	± 0.46	1.90	5.13	± 0.39
3	2.88	3.95	± 0.69	2.86	4.57	± 0.57
4	3.85	3.66	± 0.94	3.83	4.17	± 0.74
5	4.83	3.35	± 1.13	4.81	3.89	± 0.94
6	5.80	3.28	± 1.42	5.78	3.62	± 1.15
7	6.79	2.99	± 1.59	6.76	3.38	± 1.29
8	7.75	3.17	± 1.87	7.73	3.34	± 1.45

6.1.2.4 Discussions About Density Estimators

With the help of the Monte Carlo simulations, two different approaches are performed by using both 3-D edge cloud-based density estimator and the newly proposed 3-D aggregate interference based density estimator. In these experiments, we assume that UEs are able to collect RSS measurements from their first six ($k = 1, 2, 3, 4, 5, 6$) and ($N = 6$) closest BSs. As it can be seen in Figure 6.4 and Table 6.5, aggregate interference method provides more accurate results in comparison to collaborative estimator. In these simulations at each run nodes positions are changed randomly.

When both of two estimators use the first k^{th} closest BS measurements, the results are really prone to the accuracy of the RSS measurements. In addition to the number of proximity indexes, the location of base stations and UEs that RSS values collected also affect the accuracy of the estimators. In interference-based density estimator, if the RSS measurements are collected from large distant base stations, the estimations provide more accurate results. Aggregate interference estimator can be performed by an individual node, however CDE requires the other nodes' contributions to provide more accuracy. MEC-based density estimator can be performed even when the channel conditions is very harsh such as when the path-loss exponent is greater than the value of three.

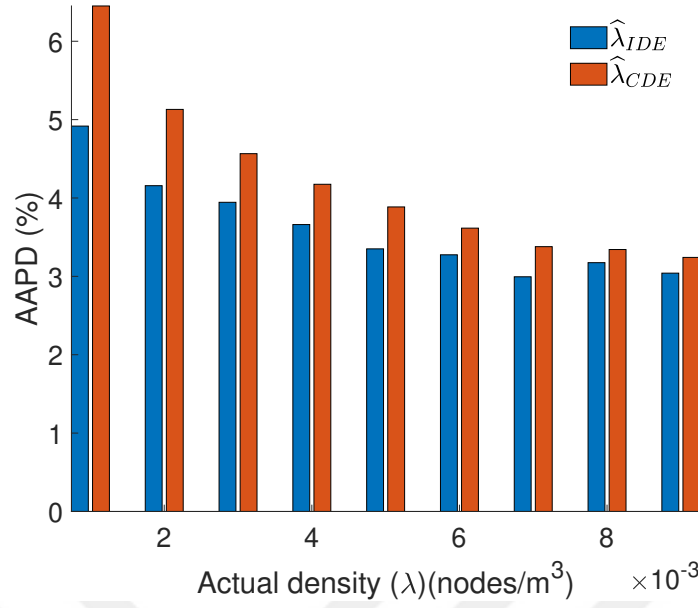


Figure 6.4: The accuracy of different estimation, average absolute percentage deviation (AAPD) results of $\hat{\lambda}_{IDE}$ and $\hat{\lambda}_{CDE}$, respectively (nodes/m³) when $\gamma = 1.5$.

6.1.2.5 Impact of Neighbor Proximity Indices

We simulate an environment which is a spherical volume as it can be seen in Figure 6.5. In this volume, we distribute the base stations and user equipment uniform randomly. In this case, as a different application scenario from Section 6.1.2.3, all of the user equipment is involved in the estimation process in a fixed topology. At each step, UEs collect RSS measurements from their first closest BS for computing $\hat{\lambda}_{CDE_1}$ in the first variant of the CDE. In the second variant of the CDE, UEs collect RSS measurements from the first six closest base stations for computing $\hat{\lambda}_{CDE_6}$. We assume that each UE sends these measurements to MEC over the associated BS. Then, MEC performs (4.9) by using these measurements. The results are presented in Table 6.6.

According to the results, the CDE has accurate outcomes. However, if we increase the number of closest neighbor BSs to get RSS measurements, it increases the sampling from overlapping regions, which results in less accurate outcomes than the estimation results including RSS measurements from the first closest BS. An increase in the number of the nodes near the network edge effects the results negatively since

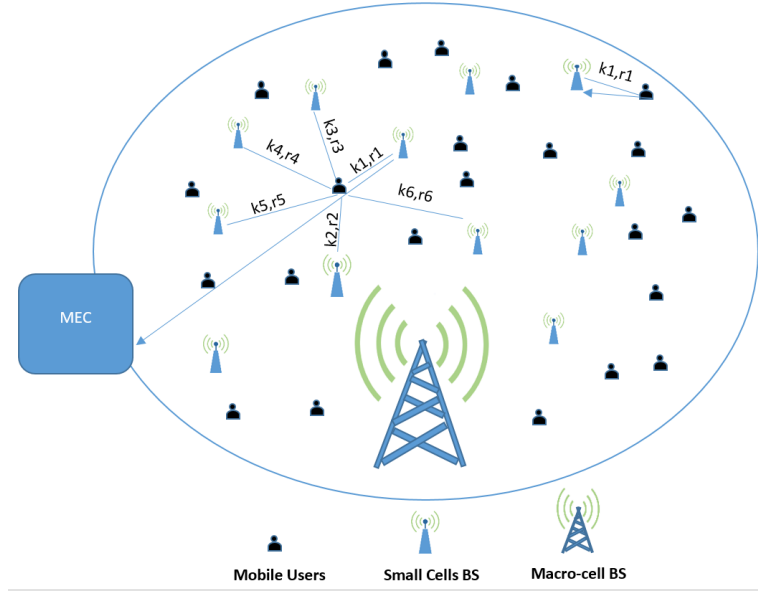


Figure 6.5: Collecting RSS measurements from the k^{th} nearest BS.

Table 6.6: The actual densities (λ) (nodes/m³) versus the estimated densities ($\hat{\lambda}$) (nodes/m³) for $\hat{\lambda}_{CDE_1}$ and $\hat{\lambda}_{CDE_6}$. The AAPD (%) results are also presented.

	$\hat{\lambda}_{CDE_1}$			$\hat{\lambda}_{CDE_6}$		
$\lambda (\times 10^{-3})$	$\hat{\lambda}_{CDE_1}, (\times 10^{-3})$	AAPD, %	99% confidence limits, ($\times 10^{-6}$)	$\hat{\lambda}_{CDE_6}, (\times 10^{-3})$	AAPD, %	99% confidence limits, ($\times 10^{-6}$)
1	0.94	6.43	± 1.84	0.91	9.18	± 0.89
2	1.89	5.28	± 2.73	1.85	7.41	± 1.33
3	2.86	4.59	± 3.16	2.81	6.48	± 1.69
4	3.83	4.21	± 3.76	3.76	5.88	± 1.82
5	4.80	3.96	± 4.31	4.72	5.51	± 2.12
6	5.78	3.59	± 4.67	5.69	5.15	± 2.32
7	6.76	3.46	± 5.09	6.66	4.91	± 2.40
8	7.73	3.34	± 5.44	7.62	4.73	± 2.59

measurements are exposed to the shadowing and the multi-path fading more than the nodes near the middle of the network. Moreover, Table 6.6 shows that when the number of closest neighbors increases the variance of the estimator results.

The neighbor proximity has also impact on the estimator IDE, which is presented in Figure 6.6. It can be seen that when the proximity index increases, the accuracy of the estimator increases, and the variance of the results decreases.

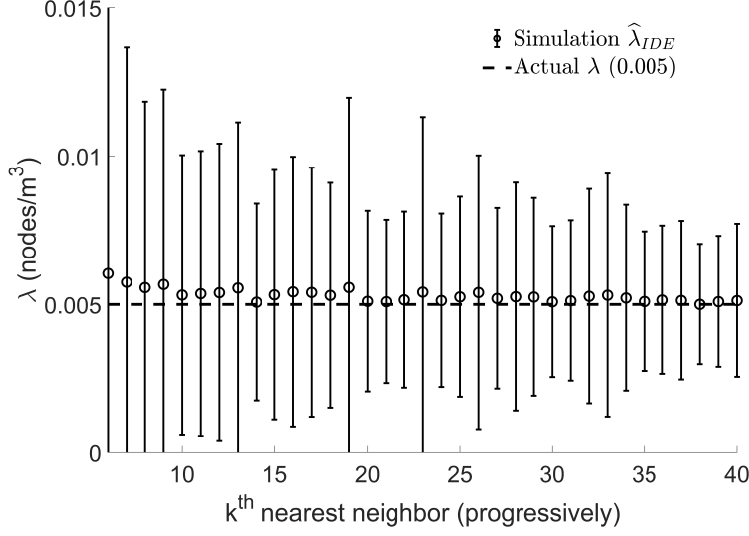


Figure 6.6: The estimator $\hat{\lambda}_{IDE}$ results along with different proximity indexes k where $\gamma = 3$, and $\lambda = 0.005$ (nodes/m³).

6.1.2.6 Impact of Log-normal Shadowing

In order to derive our proposed density estimators, we exploit the deterministic simple path-loss model as presented in Section 4.2.1. However, due to the obstructions such as buildings, walls, or trees received signal strength measurements are subject to a stochastic channel impediment which is called shadowing. These stochastic external factors give rise to log-normally distributed (or normally distributed in the dB scale) received signal strength results. Although two proposed estimators consider small-scale fading effects within the coefficient C as expressed in Section 4.2.1, shadowing is not incorporated in these models. For the very reason, a set of simulation is made by using (6.1) to analyze the shadowing effects:

$$P_k(r_k) = 10(\log_{10}(C) + \log_{10}(P_t) + \gamma \log_{10}(\frac{r_0}{r_k})) + \psi \sigma_\psi, \quad (6.1)$$

where ψ is based on zero-mean Gaussian distribution with a standard deviation of σ_ψ . We analyze the impact of log-normal shadowing characterized by the standard deviation of $2 \leq \sigma_\psi \leq 12$ dB on both proposed estimators [227]. From the light of the results, we observe that while the shadowing effect increases, the accuracy of the results significantly decreases. Thus, the proposed estimators can be enhanced by incorporating shadowing models. To remove shadowing, a different path-loss model

which is already presented in [228] is used as follows:

$$P_k(r_k) = CP_t \left(\frac{r_0}{r_k} \right)^\gamma e^{-\frac{\sigma^2}{2\left(\frac{10}{\log(10)}\right)^2 \gamma^2}}, \quad (6.2)$$

where σ represents the standard deviation of the log-normally distributed shadowing and can be computed by collecting multiple x_i values between the same pair of nodes. When the standard deviation is 2 dB, 3 dB, and 4 dB, AADP results of estimations obtained from IDE are 3.27%, 24.75%, and 62.26%, respectively. However, if we incorporate the shadowing model, and leverage (6.2) instead of simple path-loss model, AAPD results became 0.76% and 13.93%, and 38.07% respectively. Since the cooperative density estimator has cooperation among the nodes, the results of this estimator may be less prone to shadowing effects than the interference-based density estimator. By considering our observations and another analysis for RSS-based distance estimation under log-normal shadowing [229], it can be concluded that RSS-based estimators are highly susceptible to log-normal shadowing even when a shadowing model is applied. The main observation from the impact of shadowing analysis is that log-normal shadowing corrupts estimations and causes exponentially growing errors over the measurements.

6.1.2.7 Impact of Path-loss Model

Choosing a path-loss model in wireless networks is critical if an RSS-based method is using. For the sake of simplicity, the simple path-loss model which is considered as an isotropic model can be chosen while deriving the analytic models as we do in this thesis. However, we can enhance our models to overcome the line-of-sight and non-line-of-sight effects at the same time in a wireless network.

We leverage an anisotropic path-loss exponent which is already introduced in [78], and demonstrate the results by comparing these two different approaches. $\beta = -\frac{\log \frac{P_{min}}{P_t}}{\log(R_{max})}$ is the anisotropic path-loss coefficient [78], where R_{max} is the distance between a BS and the farthest position of the coverage area, P_{min} is minimum threshold power in this coverage boundary. Figures 6.7 and 6.8 presents the results form IDE and CDE when different coverage areas (R) are considered. Since CDE has

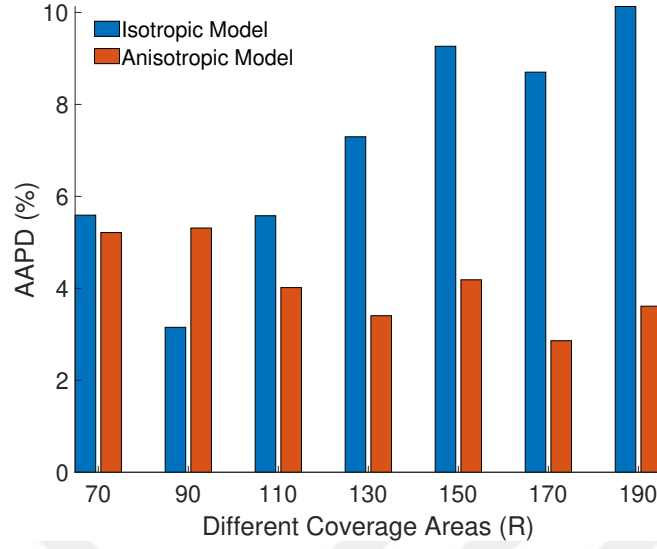


Figure 6.7: The comparison of isotropic and anisotropic path-loss model for different estimations, and average absolute percentage deviation (AAPD) results of $\hat{\lambda}_{IDE}$ when isotropic $\gamma = 2$.

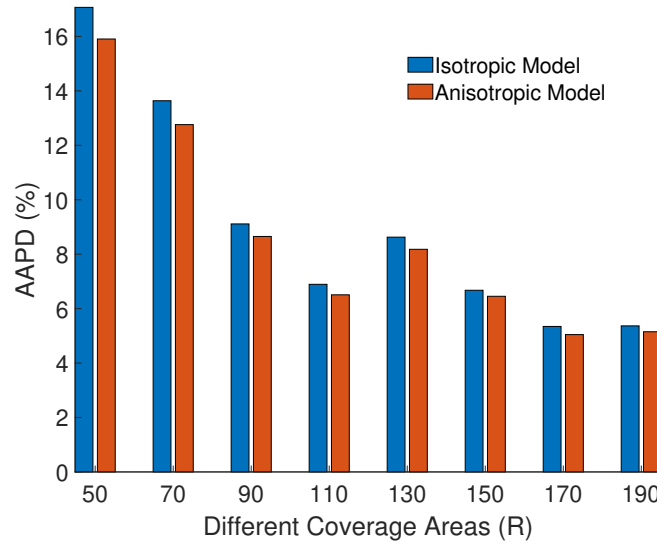


Figure 6.8: The comparison of isotropic and anisotropic path-loss model for different estimations, and average absolute percentage deviation (AAPD) results of $\hat{\lambda}_{CDE}$, respectively when isotropic $\gamma = 2$.

collaboration between the nodes, and take samples from different sides of the network, CDE has more accurate results than IDE. While the size of the network area is changing, the accuracy of the anisotropic model is more higher than the isotropic one. If we use the isotropic path-loss coefficient, since it is a constant value which we choose at the beginning, it does not change during the estimation process. However, anisotropic model can adapt itself to these changes at run-time, and provide more convenient values to the estimators.

6.1.2.8 Impact of Non-uniform Distributions

Since cellular networks have a stochastic nature in real-life, the distribution of base stations and users may be non-uniform. In this thesis, although we assume that distributions of BSs and UEs are uniform to propose a tractable and easily understandable analytic model, we also analyze some non-uniform deployments to show how this phenomenon affects our proposed estimators. To create non-uniform scenarios, we exploit Beta (B) distribution which is an asymmetrical two-parametric distribution close to the log-normal distribution [230]. (6.3) represents the PDF of Beta distribution [231]. Based on different shape tendencies provided by B distribution, we deploy BSs and UEs in a 3-D simulation environment. Table 6.7 roughly categorizes all these different deployments into six scenarios entitling different tendencies. In the first four scenarios, we deploy BSs and UEs based on B distribution by using the values of a and b for each of BS and UE distributions. In the last two remaining scenarios, firstly we uniformly deploy BSs, but we apply a and b values in Table 6.7 for the distribution of UE, which are following the three non-uniform tendencies. Secondly, we just use these two parameters for the BS distribution, but the deployment of UEs are selected uniformly. In Figure 6.9, all these tendencies employing different values of a and b are demonstrated. In Table 6.7, the first scenario is called *Uniform* since the parameters a and b of B distribution are equal to 1, where BSs and UEs are located uniformly in the environment. The second one is called *Central Tendency* providing a centralized distribution so that BSs and UEs are gathered at the center of the spherical network area as indicated in Figure 6.9. *Centrifugal Tendency* is the third scenario where the distributions of BSs and UEs are off-centered. This tendency locates BSs and UEs close to the boundaries of the network. The tendency of *Skewness*

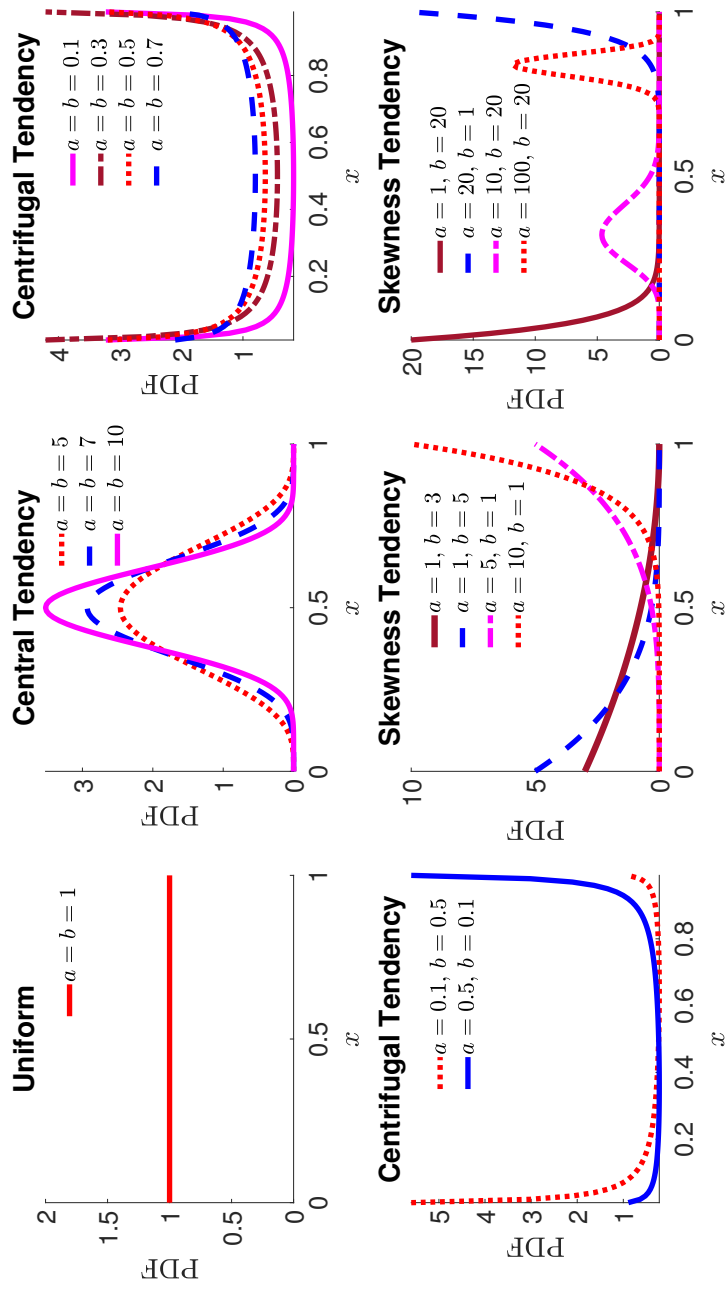


Figure 6.9: The Probability Density Function (PDF) of B Distribution vs. x parameter when different a and b parameters are used.

has a skewed shape, in which UEs and BSs are located at a particular region of the network. The last scenarios include *Non-uniform* distribution for UEs, and *Uniform* distribution for BSs, *Uniform* distribution for UEs, and *Non-uniform* distribution for BSs. The PDF of B distribution is

$$f(x|a, b) = \frac{1}{B(a, b)} x^{a-1} (1-x)^{b-1} I_{[0,1]}(x), \quad (6.3)$$

where $B()$ is the Beta function, a and b are two different shape parameters which change the shape of the distribution, and $I_{[0,1]}$ is to ensure that the values of the variable x is in the range of between 0 and 1.

Table 6.7: When λ equals to $1(\times 10^{-4})$ (λ) (nodes/m³), ($\hat{\lambda}$) (nodes/m³) of $\hat{\lambda}_{IDE}$ and $\hat{\lambda}_{CDE}$ for different distributions are presented. AAPD (%) results are presented with their 99% confidence interval ($CI_{99\%}$).

Distributions		Shape Parameters		$\hat{\lambda}_{IDE}$			$\hat{\lambda}_{CDE}$		
BS	UE	a	b	$\hat{\lambda}_{IDE}$ ($\times 10^{-4}$)	AAPD %	$CI_{99\%}$ ($\times 10^{-6}$)	$\hat{\lambda}_{CDE}$ ($\times 10^{-4}$)	AAPD %	$CI_{99\%}$ ($\times 10^{-6}$)
Uniform	Uniform	1	1	0.98	1.24	± 0.33	0.99	0.32	± 0.40
Central Tendency	Central Tendency	3	3	0.65	34.84	± 1.91	0.85	15.32	± 0.74
		5	5	0.85	14.86	± 3.65	1.13	13.03	± 1.43
		7	7	1.08	7.58	± 3.08	1.50	49.58	± 2.23
Centrifugal Tendency	Centrifugal Tendency	0.1	0.1	0.75	25.46	± 2.35	1.74	74.00	± 3.87
		0.5	0.5	0.56	44.46	± 2.24	0.63	37.30	± 0.57
		0.7	0.7	0.48	52.45	± 1.64	0.59	41.50	± 0.43
Skewness	Skewness	1	3	1.11	10.70	± 4.10	1.84	83.56	± 2.38
		4	1	0.77	22.78	± 2.80	0.79	21.13	± 1.09
Uniform	Non-uniform	10	10	0.71	29.01	± 5.84	0.72	27.85	± 0.26
		0.3	0.3	0.71	28.93	± 8.43	0.53	46.89	± 0.19
		0.5	0.5	0.73	26.86	± 7.55	0.61	39.44	± 0.22
		0.7	0.7	0.73	27.16	± 7.03	0.65	34.94	± 0.21
		1	4	0.94	6.26	± 6.10	0.60	40.43	± 0.32
		1	5	0.90	10.24	± 5.77	0.56	44.35	± 0.30
		4	1	0.51	48.77	± 6.91	0.49	50.97	± 0.21
		20	1	0.47	53.43	± 4.23	0.38	61.62	± 0.21
		20	10	0.61	38.90	± 5.49	0.58	42.45	± 0.26
		10	20	0.88	12.12	± 6.11	0.81	19.06	± 0.31
		100	20	0.55	45.40	± 6.21	0.45	55.13	± 0.23
Non-uniform	Uniform	1	20	0.52	47.86	± 1.60	0.29	70.73	± 0.28
		20	1	0.09	91.30	± 1.86	0.32	67.65	± 0.18

According to our observations, we can remark that the *Uniform Tendency* scenario

where both BSs and UEs are deployed uniformly, the accuracy of the estimators are the best in comparison to the other cases as expected since we create our models based on the 3-D Poisson Point Process with an assumption including a uniform deployment of BSs and UEs.

In *Central Tendency*, while the level of the centrality is soaring the estimator IDE provides resilient results. The reason for this case is that when nodes (UEs and BSs) are close to each other near to the center of the environment, the amount of the path-loss, shadowing, the nodes causing non-negative effects at the corner of the network decrease. However, since the estimator CDE take samples from different UEs collaboratively, the closest nodes at the center cause an increase of overlapping measurements, and some sparse nodes near to the boundary of the network may not provide good measurements that are why the estimator CDE gives worsening outcomes as the central tendency is rising.

In scenarios built upon *Centrifugal Tendency*, due to BSs and UEs close to the boundary of the coverage area, and the distances between the nodes are larger, the average interference will then be decreased progressively. Thus, the accuracy of the results provided by the estimator IDE becomes lower. However, while the centrifugal tendency is diminishing, the estimator CDE yields more accurate results because BSs and UEs close to the center become sparse nodes, which increases the error rate of the measurements.

When the deployment of BSs and UEs tend to *Skewness*, they gather around a particular area of the network where BSs and UEs are too close to each other. Symmetrically changing the parameters a and b may not provide the same shape variation. Thus, different observations are made for the values of these two shape parameters. For example, when we increase b , we observe that the accuracy of the results is declining further. However, the impact of changing the value of a causes smaller effects over the results. After the value of 10 for a or b , which means higher non-uniform deployments, outcomes of the estimators become less accurate. Especially, the distribution on BSs affects the accuracy of the results significantly in comparison to the distribution of UEs.

With these four deployment tendencies, we also analyze each of BSs and UEs indi-

vidually such that UEs have a non-uniform tendency, but the distribution of BSs are uniform. In this case, the deployment of UEs follows above three non-uniform tendencies. When UEs have a central tendency, the accuracy of the estimator results is close to each other. However, in the case of centrifugal tendency, estimators IDE and CDE have different accuracy for their outcomes depending on the positions of UEs and BSs in the middle or at the corner, and the inter distances between BSs and UEs. Eventually, when the deployment of BSs and UEs are uniform, if the samples are taken from UEs which are close to the center of the network, two estimators provide more and more accurate results. Furthermore, if the network pursuing a non-uniform distribution, then the number of the k^{th} nearest neighbor can be increased, and samples can be taken from UEs at anywhere of the environment randomly to get better outcomes. Moreover, we observe that in sparse networks, the performance of IDE is better than the estimator CDE because CDE which needs collaboration among the UEs in the network. However, in dense networks, the estimator CDE gives more accurate results if the samples are collected from UEs randomly for the non-uniform deployments. The average AAPD of the proposed estimators' results for non-uniform deployments is approximately 27% for IDE and 40% for CDE.

Since IDE and CDE follow Poisson Point Process and based on a uniform distribution assumption, which is not mostly applicable in practice that is consisting of non-uniform deployments. However, we can utilize these network density estimators by improving the accuracy of the results with the help of the following ways: For instance, we can divide the network into clusters and we can manage them easily. We can take the average of the multiple measurements with the help of multi-access edge computing. Moreover, the fusion of IDE and CDE can be leveraged. We can improve by adding multi-path fading models such as the Rayleigh fading model, and other channel impairment models such as shadowing to our RSS-based density estimators. Even if they are more complex while deriving analytic models, to create more realistic models, we can change the distribution of our model depending on a log-normal distribution or alpha-stable distribution as stated in [58].

All in all, in Section 6.1.2.4, we analyze our proposed estimators by taking into consideration of neighbor proximity, the channel impediments such as shadowing, the impact of the propagation model, and finally we examine the accuracy of the esti-

mators under different non-uniform deployments. We can conclude that RSS-based estimators can be derived by using simple models to ease tractability, but at the same time, we should consider all these factors which are because of the stochastic nature of received signal strength.

6.1.3 Validation of 3-D Density Estimator for FANETs

In this analysis, we present the impact of density estimation errors in addition to showing the paramount importance of the UAV density in dynamic channel access schemes, we examine the impact of the UAV density on the channel utilization and channel access probability.

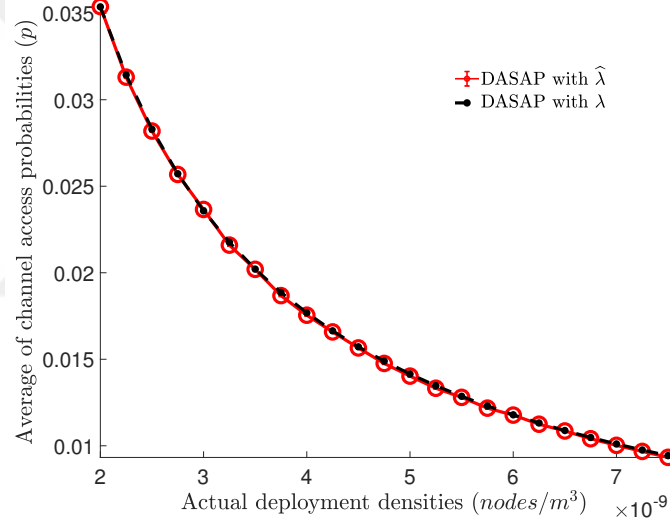


Figure 6.10: Averages of channel access probability results with using estimated density ($\hat{\lambda}$) and actual density (λ) when the network density is increasing. Actual density (λ) is between the range in 2×10^{-9} and 7.5×10^{-9} .

We construct a flying ad hoc network by deploying random UAVs in a spherical area. The simulation parameters are represented in Table 6.12. In this simulation, each time we give different deployment densities. We perform DASAP to update the channel access probabilities with using actual density and estimated density values, respectively. In Figure 6.10, when the density of UAVs increases, the channel access probability of that UAVs is getting less than its previous value. Figure 6.11 exhibits that DASAP

provides a maximum and stabilized channel utilization while density is changing. We also present the accuracy of the results with average absolute percentage deviation (AAPD) by considering the utilization rates with the estimated density ($\hat{\lambda}$) and the deployment density (λ). We define the average absolute percentage deviation as $AAPD = 100 \frac{|U(\hat{\lambda}) - U(\lambda)|}{U(\lambda)}$. Two outcomes are close to each other and the error rates between these two results are presented in Table 6.8. We demonstrate the cohesive relation between the density of UAVs and the dynamic channel access probability in Figure 6.10.

In DASAP, the edge UAVs may estimate the density low in comparison to the UAVs close to the center. Then their channel access probability is higher than the other UAVs. In other words, if a UAV has higher density then this UAV should talk less than the other. However, if a UAV has fewer neighbors then this UAV should talk more.

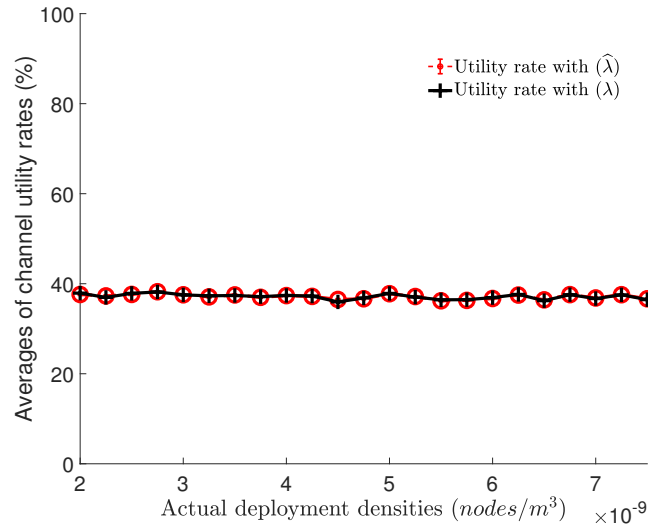


Figure 6.11: Different deployment density values vs. channel utilization rates (%) with estimated density ($\hat{\lambda}$) and actual density (λ). Actual density (λ) is between the range in 2×10^{-9} and 7.5×10^{-9} .

Table 6.8: The AAPD and 99% confidence limits in the estimators for various utilization rates (%) with estimated density ($\hat{\lambda}$) and actual density (λ). Actual density (λ) is between the range in 2×10^{-9} and 7.5×10^{-9} .

utilization rate (%, λ)	utilization rate (%, $\hat{\lambda}$)	AAPD (%)	99% confidence limits of utilization rates
37.61	37.91	0.80	± 0.04
37.29	36.96	0.89	± 0.03
37.62	37.86	0.63	± 0.03
38.22	38.17	0.12	± 0.03
37.54	37.52	0.05	± 0.03
37.08	37.31	0.63	± 0.03
37.51	37.39	0.32	± 0.04
36.98	37.13	0.41	± 0.05
37.36	37.40	0.10	± 0.03
37.18	37.26	0.21	± 0.05
36.66	36.46	0.55	± 0.04

6.2 Validation of Density-adaptive and -aware Applications

In this section, we present the simulation results in detail for both network outage and transmit power adaptation techniques based on the network density, which are operational for two-dimensional and three-dimensional wireless networks. In addition, we present the validation of density-aware channel utilization based on density-adaptive slotted ALOHA protocol for FANETs.

6.2.1 Validation of 2-D Density-aware Network Outage and Density-aware Transmit Power Adaptation (DTPA) for Wireless Networks

We simulate a circular area with a radius of 100 m consisting of uniform randomly distributed nodes with an actual deployment density of λ nodes/m². At each simulator run, we select a random point to be used as the reference node. We calculate the

RSS based on the simple path-loss model explained in Section 5.1 from the closest neighbor of the reference node where T is 5×10^{-13} mW, K is 10^{-5} , and γ is 3. If the computed RSS is lower than the threshold value T , this run is classified as outage, otherwise, it is within the coverage of the clustered network and evaluated as successful.

Table 6.9: The validation of the transmit power adaptation technique in (5.3) for various outage probability requirements P_O^* where $\lambda = 0.05$ nodes/m².

Required P_O^*	Achieved P_O	Standard deviation
0.0100	0.0099	0.0018
0.0126	0.0137	0.0030
0.0178	0.0189	0.0048
0.0204	0.0194	0.0044
0.0256	0.0261	0.0036
0.0282	0.0284	0.0046
0.0308	0.0320	0.0032
0.0360	0.0354	0.0067
0.0412	0.0449	0.0080
0.0438	0.0433	0.0066
0.0490	0.0488	0.0054

We run the simulations 10^4 times and the ratio of the number of outages to the total number of simulation runs is determined as outage ratio that is represented as achieved P_O in Table 6.9. The outage model (5.1) and the transmit power adaptation technique in (5.3) provide us accurate results as can be seen in Table 6.9. The achieved outage closely matches the required outage that indicates that the proposed transmit power adaptation technique is successful.

Impact of Density on Outage Probability

Nodes in dense ad hoc networks will be more closer to each other and the attenuation of signals measured by neighbors will be smaller (i.e., RSS of signals will be larger) in comparison to sparse networks. As demonstrated in Figure 6.12, the densification

of a network will make the probability of outage smaller if the other parameters such as P_t and T are kept constant.

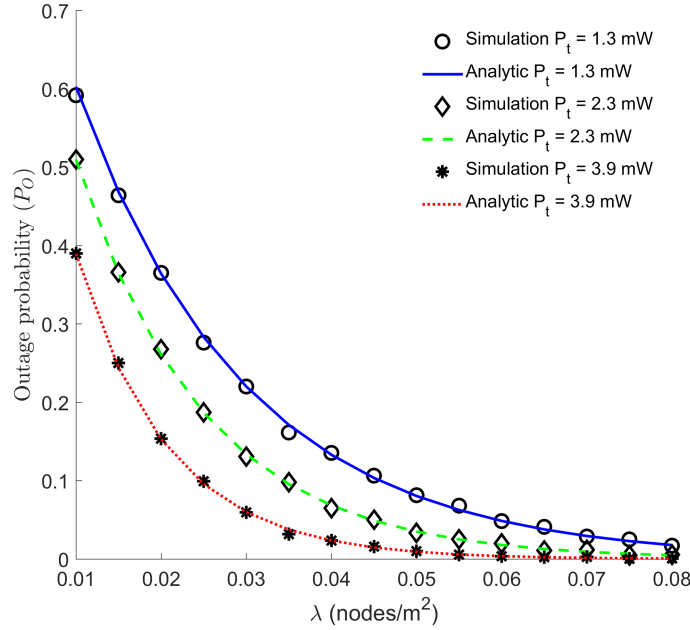


Figure 6.12: The impact of density on outage probability.

In Figure 6.12, we consider $\hat{\lambda}$ computed by using our proposed estimator. At each run of the simulator, the network density is estimated and the network outage is calculated by using (5.1) for various P_t values. Figure 6.12 shows that the network density affects the quality of service and coverage of the network. In dense networks, the outage probability will lessen and the transmit power will be smaller in contrast to sparse networks.

Impact of Density on Transmit Power Adaptation

In the validation of the proposed transmit power adaptation technique in (5.3) for ad hoc networks, we use a similar experimentation setting to the aforementioned outage simulator. In a simulation run, if the computed outage does not match the required outage probability (P_O^*), we change the transmit power by performing binary search: if the calculated outage is smaller than the given P_O^* , the transmit power is decreased, otherwise it is increased. The adapted transmit power (P_t) values can be seen in

Figure 6.13. In this figure, we show the simulation results by employing actual (λ) and estimated ($\hat{\lambda}$) densities as input to (5.3) for various outage requirements.

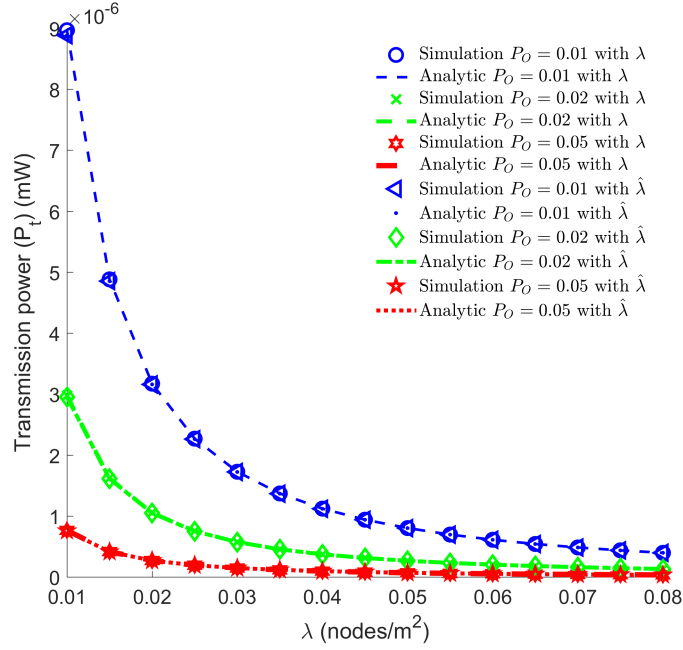


Figure 6.13: Transmit power adaptation based on estimated density ($\hat{\lambda}$).

When a network designer becomes more tolerant to degraded quality of experience by nodes due to outage, the amount of energy conservation can be increased since smaller transmit power levels can be employed. However, nodes' satisfaction in terms of connectivity is significantly related to the outage probability. As the network density becomes denser, it will be required to decrease the transmit power in a density-aware fashion to preserve coverage, to keep the outage probability under control and to conserve energy. The main advantage of the proposed technique is that it requires minimal communication overhead, fast and simple to implement.

6.2.2 Validation of 3-D Density-aware Network Outage and Density-aware Transmit Power Adaptation (DTPA) for Wireless Networks

This section explains the detailed simulation results for both density-aware network outage and density-adaptive transmit power adaptation techniques, which can be applied in three-dimensional networks.

6.2.2.1 Density-aware Outage Analysis

In this section, we demonstrate the impact of density, transmit power and path-loss exponent on network outage [20].

Simulator Model

We uniform randomly determine locations of base stations in a field with an actual deployment density of λ nodes/m³. A uniform randomly selected point is considered to be the location of the reference user equipment. Using the simple path-loss model described above, we compute the received signal strength from the closest base station. If the signal strength is larger than the threshold value (receiver sensitivity) the run is assumed to be successful; otherwise, an outage occurs. The ratio of outages out of 10^4 runs of the simulations is recorded as the outage probability. We simulated a $500 \times 500 \times 500$ m³ area, with a transmit power of 100 mW, by considering different deployment densities such as sparse, dense and ultra-dense, and the path-loss exponent is three; i.e., $\gamma = 3$. The values of the parameters employed in the simulations are shown in Table 6.1. In the figures we present in this section, we show the results of the simulations together with the results of the analytic model in (5.2).

Impact of Network Density on Outage

As density increases, there will be a larger number of base stations deployed in the field. Consider a randomly selected user equipment in the field. The distance of it to the closest BS will be smaller. Consequently, the path-loss will be smaller in dense networks. As shown in Figures 6.14- 6.16, the outage probability in dense networks will be smaller assuming that all other parameters are kept constant. The density of BSs impacts the quality of service as shown in these figures. The transmit power has a positive impact on the received signal strength. The more transmit power means more receive signal strength as it can be understood from the propagation model and is presented in Figure 6.14. When the network is dense, the outage probability will decrease obviously.

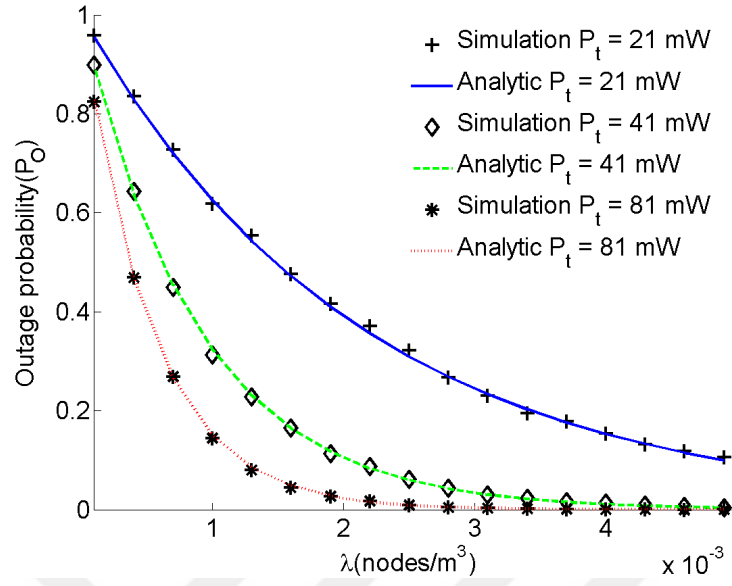


Figure 6.14: Impact of density on outage probability for different transmit powers.

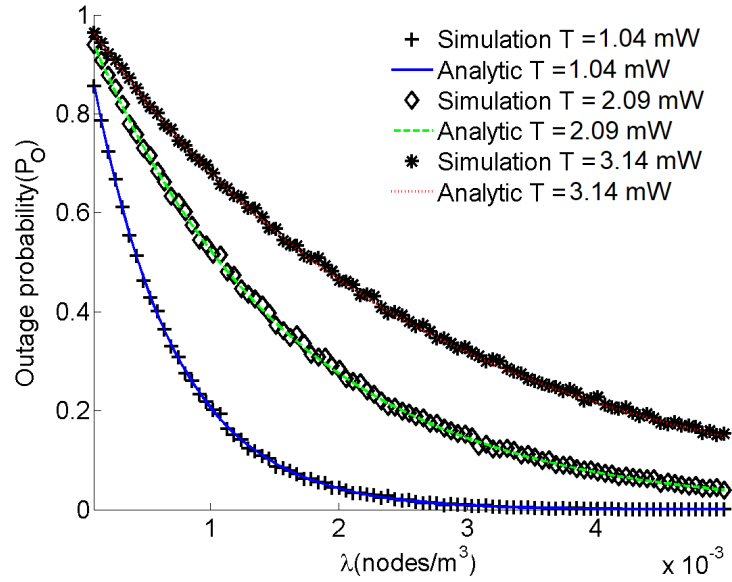


Figure 6.15: Impact of density on outage probability for various thresholds.

For the same distance and level of noise, the crucial factor affecting the quality of communication is the threshold level of sense; i.e., receiver sensitivity. In other words, it is easier to communicate with a UE that has a higher level of sensitivity as demonstrated in Figure 6.15. By increasing the complexity of receivers, the threshold can be decreased. Complexity and cost of receivers introduce a trade-off with coverage.

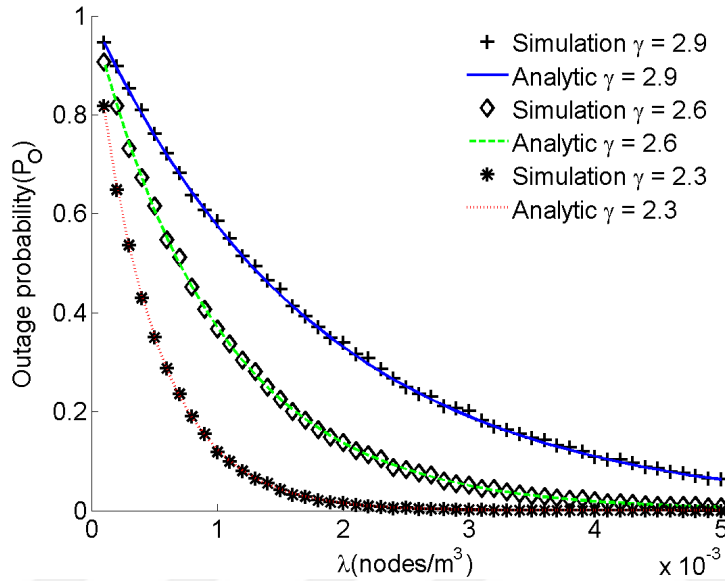


Figure 6.16: Impact of density on outage probability for different network conditions.

Figure 6.16 demonstrates the relation between outage P_O , λ and γ . The path loss exponent (γ) negatively affects the received signal strength. When the channel is prone to high loss, i.e., when the environment is harsh, it is more probable for the randomly selected reference node to be out of coverage.

Impact of Transmit Power on Outage

A large amount of transmit power is beneficial for the quality of service in a network albeit bad for the environment. The more transmit power implies the more coverage area when the other variables are constant. Furthermore, it implies a larger amount of interference. However, in this thesis, we assume a robust interference management scheme that may overcome the negative impact of interference on capacity. If the

threshold decreases, then the outage approaches to zero as in Figure 6.17. If the density of the network increases, e.g., additional (mobile) base stations are deployed or redundant base stations are turned on, the outage probability approaches to zero as shown in Figure 6.18. The threshold has the same impact on a network similar to that of the density.

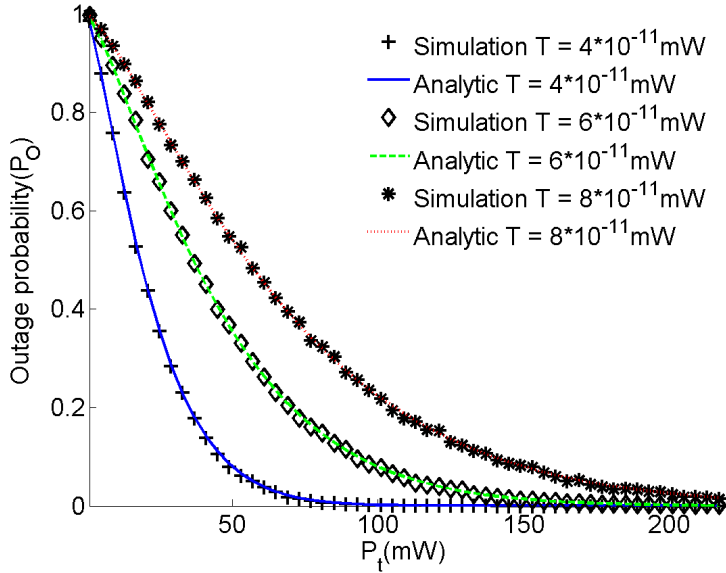


Figure 6.17: Impact of transmit power on outage probability for particular thresholds.

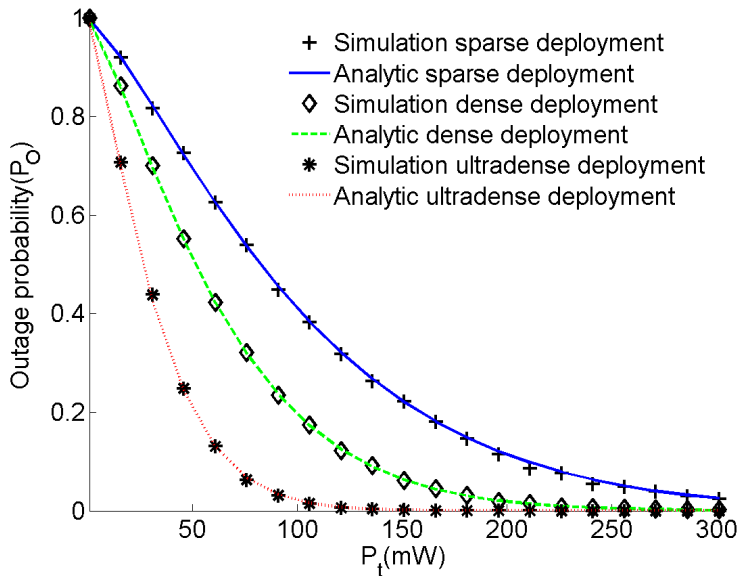


Figure 6.18: Impact of transmit power on outage probability for various deployments.

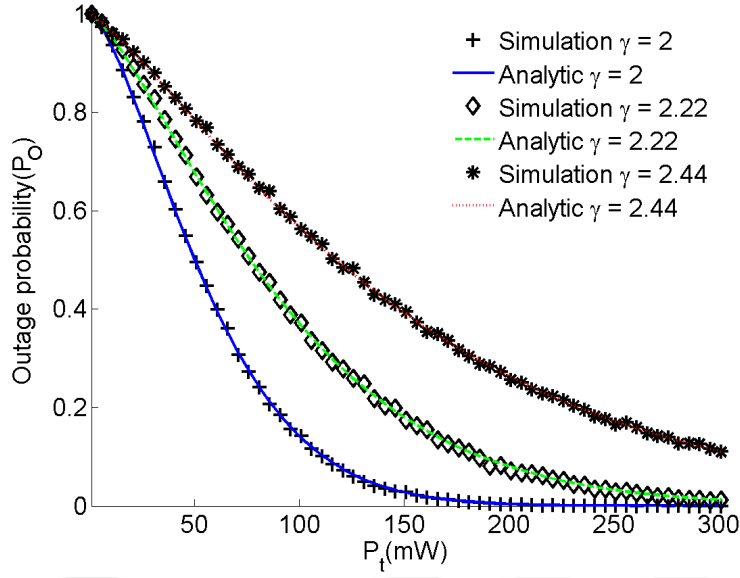


Figure 6.19: Impact of transmit power on outage probability different network conditions.

Impact of Path-loss Exponent on Outage

The path loss exponent is a significant factor that characterizes the wireless channel. When γ is extremely high, then it is more probable to be out of coverage as it can be observed in Figure 6.19 and 6.20. Let's consider the same transmit power, it can be clearly seen that when the path-loss exponent is high then the network coverage will decrease. Thus, it is more important that an estimator should determine the channel conditions like the path-loss exponent.

Impact of Receiver Sensitivity on Outage

We consider the receiver sensitivity as a threshold value that is the minimum requirement to be able to decode signals. If the threshold value increases, the outage probability will increase as it is shown in Figure 6.21. Increasing the transmit power leads to a declining outage ratio. As it can be seen in Figure 6.22, both the threshold and the path-loss exponent considerably affect the network outage.

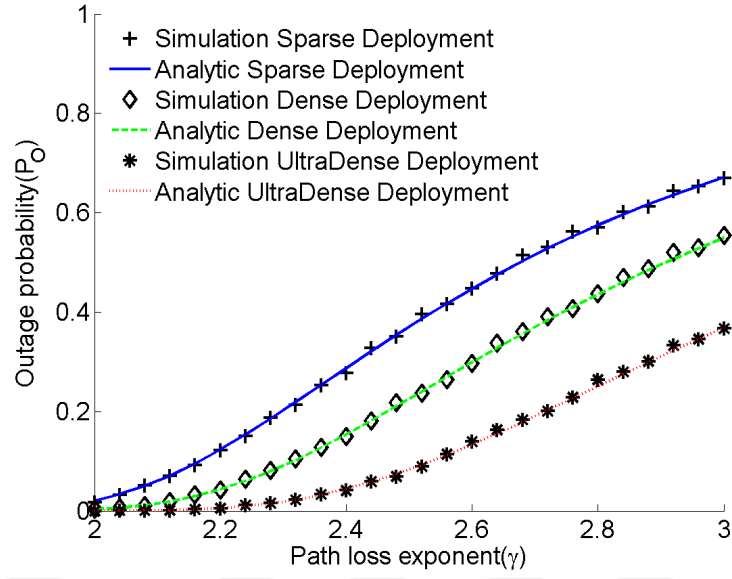


Figure 6.20: Impact of path-loss exponent (γ) and threshold (T) on outage probability for various deployments.

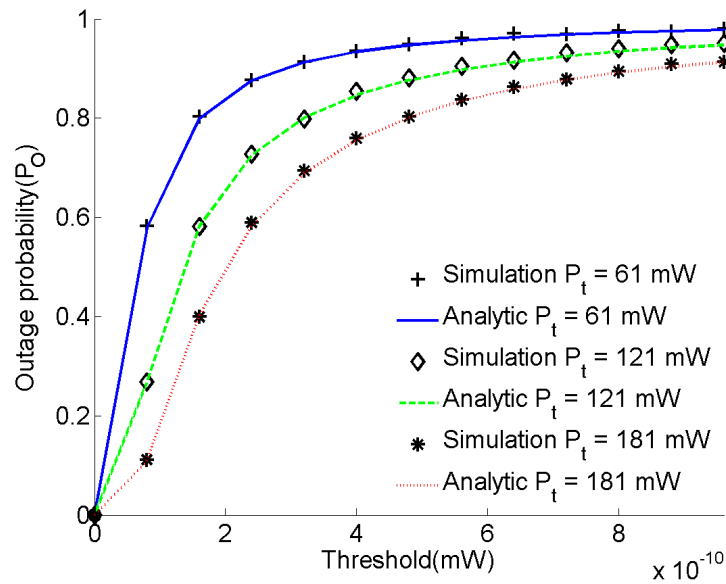


Figure 6.21: Impact of path-loss exponent (γ) and threshold (T) on outage probability for particular transmit powers.

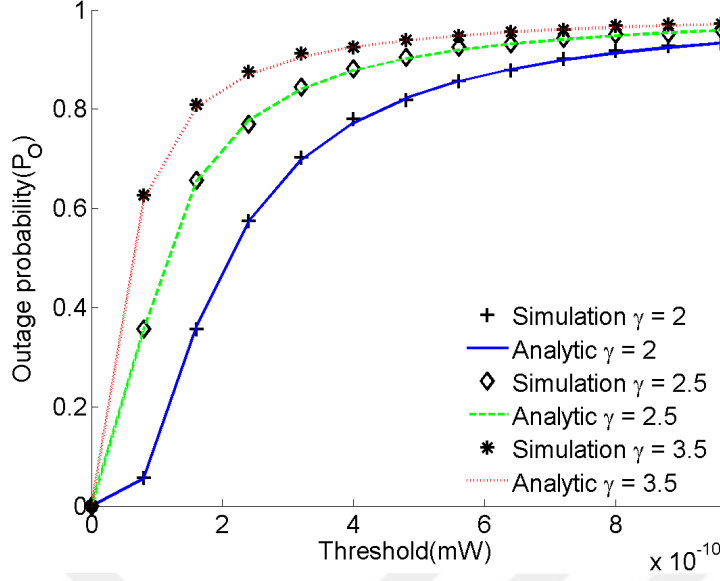


Figure 6.22: Impact of path-loss exponent (γ) and threshold (T) on outage probability for different channel conditions.

6.2.2.2 Validation of Density-aware Outage Probability

In the light of the results presented in Section 6.2.2.1, we claim that in a cellular network, base stations have to change their transmit power according to the network density. The base stations have to be able to estimate the network density by means of equipped with tools and techniques. Pre-configured decisions will not be sufficient since especially when mobile base stations are considered, future cellular networks will be highly dynamic. Steady configured parameters will decrease the quality of service, and result in many coverage control problems.

In this work, we present a run-time adaptable density-aware and -adaptive three-dimensional cell zooming technique using (5.2), and validate it by using Algorithm 2. For one deployment density (λ) and one transmit power (P_t) settings the time complexity of Algorithm 2 is $O(S)$, where S is the number of simulation runs. This adaptation is also important for energy conservation. After determining the minimum transmit power budget of a base station using this technique, the power can be allocated to individual users or resource blocks [232] as a sequel that is out of the scope of this work.

Algorithm 2 Validation of Density-aware Outage Probability Model

```
1: Input:  $\lambda, \gamma, P_t, k, T, Cntr = 0$ 
2: Output: (Analytic)  $P_{O_A}$  and (Simulated)  $P_O$ 
3: for  $S=0; S<10000; S++$  do
4:   Select a set of UE and BSs;
5:   Find  $(\hat{\lambda})$  by using CDE (4.9) or IDE (4.6);
6:   Select a UE as reference (node);
7:   Find  $r_k$  using Euclidean distances between UE and BSs, where  $k = 1$ ;
8:   Calculate  $x_k \leftarrow CP_t \left( \frac{r_0}{r_k} \right)^\gamma$ ;
9:   if  $x_k < T$  then
10:      $Cntr++$ ; //This UE is in outage
11:   else
12:     Do nothing; //This UE is in the coverage area
13:   end if
14: end for
15: Find  $P_{O_A}$  by using (5.2) with  $\hat{\lambda}$ 
16:  $P_O \leftarrow Cntr/S$ ;
17: return  $(P_{O_A}, P_O)$ ;
```

In Algorithm 2, a set of uniform randomly distributed base stations and user equipment with a density of λ (nodes/m³) is simulated using MATLAB. In a 3-dimensional field, after selecting a set of base station and user equipment positions, the estimated density ($\hat{\lambda}$) is calculated. Then, a random point is picked as the position of the reference user equipment (UE). The distance between the UE and the closest base station is found, using the channel model presented in Section 4.2.1, and we calculate the received signal strength. If the received signal strength is less than the given threshold (T), this simulation run is recorded as an outage. For the same simulation environment, the simulations are repeated 10^4 times and the ratio of outages is computed. According to the results, we compare the analytic outage probability (P_{O_A}) by considering (5.2) and the simulated outage ratio (P_O). In Figure 6.23a and 6.23b, we show the adapted outage probability for various transmit powers as the density of the network changes. These simulation results validate the analytic model for cell zooming presented in (5.2) and in (4.8). The results indicate that if the transmit power of

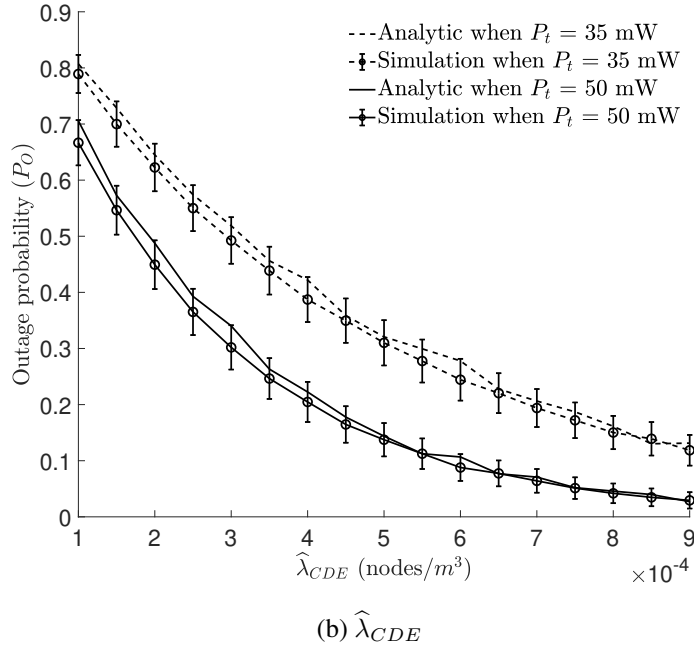
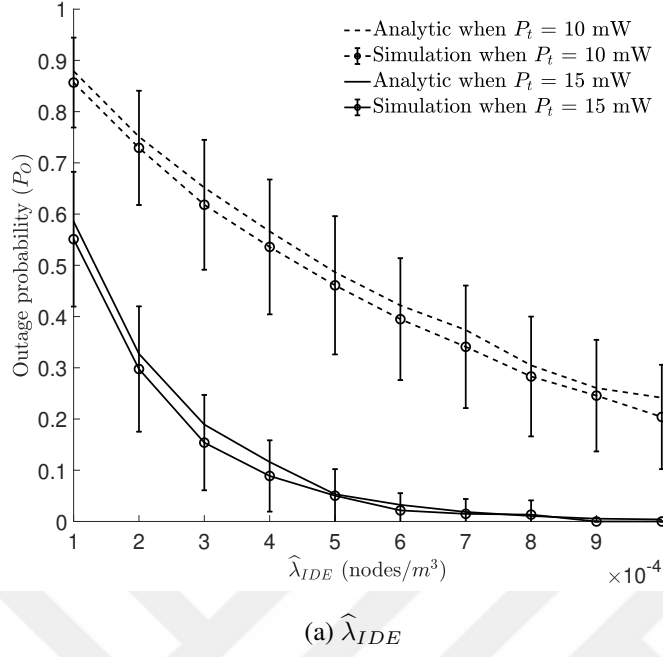


Figure 6.23: Analytic outage values based on the estimated network density $\hat{\lambda}_{IDE}$ and $\hat{\lambda}_{CDE}$ for different transmit powers (P_t) when the network density is changing.

BSs (P_t) does not change, the outage probability (P_O) of a UE decreases when the network is getting denser. However, in sparse networks, the outage probability increases if the same P_t is used. This results also claims that there is a direct relation between the base station density and network outage. By considering the impact of the estimators, it can be said that since CDE is based on collaboration between the nodes, and if the k^{th} nearest neighbor increases, the variance of the results will be smaller than the estimator IDE. Depending on the positions of selected UEs and BSs, the accuracy of the results is changing. For instance, UEs and BSs located close to the center of the network increase the accuracy of results, on the other hand, UEs and BSs near to the border of the coverage area decreases the results. When a network operator becomes more tolerant to degraded quality of experience by users due to the outage, the amount of energy conservation can be increased. However, customer satisfaction is significantly related to the outage probability. As the network density increases, it will be required to decrease the transmit power in a density-aware fashion to preserve coverage, to keep the outage probability under control and to conserve energy. The main advantage of the proposed cell zooming technique is that it requires minimal communication overhead, fast and simple to implement. However, the deficiencies of the estimator have to be enhanced. A much faster density estimator that is tolerant to correlated samples is required.

6.2.2.3 Validation of the Density-aware Transmit Power Adaptation

In this section, we validate (5.4) by using two different schemes: one of them is based on the global density of BSs that we used in Section 6.2.2.2, where all measurements are collected with the help of edge computing. As the second approach, each of BSs determines its own density result without using edge computing, in other words, we use local densities belongs to each of BSs.

6.2.2.4 Validation of Density-aware Power Adaption Technique with Edge Computing

A density-aware MEC based transmit power adaptation scheme is presented.

To validate (5.4), we follow Algorithm 3. The algorithm has $O(S)$ time complexity, where (S) is the simulation count for one deployment density (λ) and one required outage (P_O^*) . We simulate a spherical volume consisting of uniform randomly distributed BSs and UEs with different actual deployment densities of λ (nodes/m³). At each simulator run, we estimate the effective density for the whole network, then we select a random point to be used as the reference UE. We update the transmit power of each BS by considering the model in (5.4). Then, we calculate the RSS based on the simple path-loss model explained in Section 5.1 from the closest BS of the reference UE where γ is 2. If the computed RSS is lower than the given threshold value T , the result of this run is classified as an outage, otherwise, it is evaluated as successful since it is within the coverage of the clustered network. We run the simulations 10^4 times and the ratio of the number of outages to the total number of simulation runs is determined as outage ratio that is represented as achieved P_O in Table 6.10 with using $\hat{\lambda}_{IDE}$, and $\hat{\lambda}_{CDE}$.

Algorithm 3 Validation of Density-aware Power Adaptation Technique

```

1: Input:  $\lambda, \gamma, P_t, k, T, P_O^*, Cntr = 0$ 
2: Output: (Simulated)  $P_O$ 
3: for  $S=0; S<10000; S++$  do
4:   Select a set of UE and BSs;
5:   Find  $(\hat{\lambda})$  by using CDE (4.9) or IDE (4.6);
6:   Set  $P_t^*$  for all BSs using (5.4) with  $\hat{\lambda}$  and  $P_O^*$ 
7:   Select a UE as reference (node);
8:   Find  $r_k$  using Euclidean distances between UE and BSs , where  $k = 1$ ;
9:   Calculate  $x_k \leftarrow CP_t \left( \frac{r_0}{r_k} \right)^\gamma$ ;
10:  if  $x_k < T$  then
11:     $Cntr++$ ; //This UE is in outage
12:  else
13:    Do nothing; //This UE is in the coverage area
14:  end if
15: end for
16:  $P_O \leftarrow Cntr/S$ ;
17: return  $(P_O)$ ;
```

Table 6.10: Required outage probability (P_O^*) vs calculated outage probability (P_O) by using the $\hat{\lambda}_{IDE}$, $\hat{\lambda}_{CDE}$, which are the global density of base stations, and AAPD (%) results.

P_O^*	$\hat{\lambda}_{IDE}$			$\hat{\lambda}_{CDE}$		
	P_O	AAPD, %	99% confidence limits, ($\times 10^{-5}$)	P_O	AAPD, %	99% confidence limits, ($\times 10^{-5}$)
0.02	0.022	11.31	± 1.12	0.022	8.81	± 0.28
0.025	0.027	6.93	± 1.13	0.027	7.29	± 0.36
0.03	0.031	4.37	± 1.35	0.031	4.71	± 0.33
0.035	0.036	2.92	± 0.96	0.036	4.06	± 0.36
0.04	0.040	1.14	± 1.38	0.041	3.60	± 0.27
0.045	0.045	0.54	± 1.23	0.046	2.35	± 0.19

The outage model (5.2) and the transmit power adaptation technique in (5.4) provide us accurate results as it can be seen in Table 6.10. For each required outage value, we use different actual density (λ) values which are between 1×10^{-4} (nodes/m³) and 9×10^{-4} (nodes/m³). Then the average outage results for different densities are presented. The achieved outage closely matches the required outage which means that the proposed transmit power adaptation technique based on the provided outage probability is successful. Each of the estimators can be used in order to make the network coverage dynamic. The main conclusion to be drawn is that the relation between the density of base stations and network outage require the adaption of the transmit power by considering this relation.

6.2.2.5 Validation of Density Estimator and Power Adaption Technique without Edge Computing

A new approach as utilizing both of these estimators without using the edge computing can be applied locally in the network, and the power adaption technique can be employed with these local estimation measurements. In other words, instead of the global density of the network, each of the base stations can use its own effective density result.

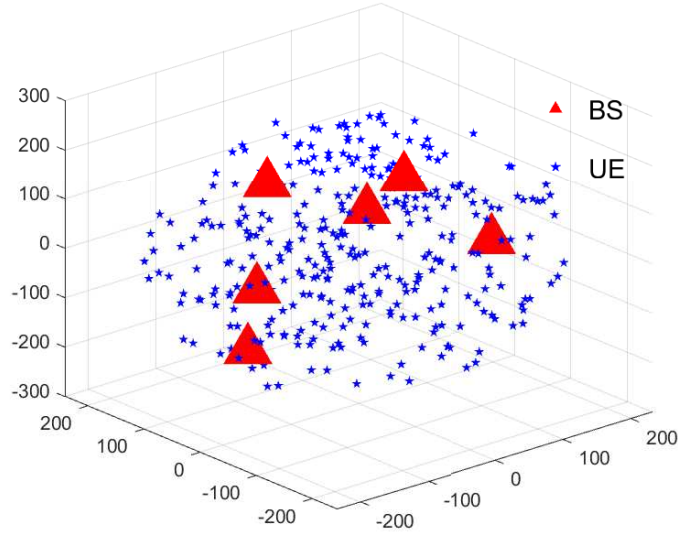


Figure 6.24: Collecting $\hat{\lambda}$ measurements (nodes/m³) from the first k nearest UEs.

In these simulations, as it can be seen in Figure 6.24 each base station uses its calculated density measurement by using density estimations of its connected closest UEs. Each user equipment receives a number of RSS measurements from their first k closest base stations and estimates the density by employing IDE or CDE methods. Each base station collects the estimation results from their closest user equipment, and the average of these estimations are calculated as local base station density. After each base station determines the density result itself, (5.4) is used for adapting the transmit power based on the required outage probability. In the simulations, the same approach like in Section 6.2.2.3 is exploited so that every time each BS changes its transmit power based on the estimated density and the outage probability.

Table 6.11 presents the AAPD results between the required outage and the analytic outage values. The average outage results for different densities are presented. In these simulations, at each run of the simulation, each BS calculates its own density instead of using the global density, then they change their transmit powers using the model in (5.4). For the rest of the steps, the same approach in Section 6.2.2.2 is used for calculating the required outage and analytic outage. The results in Table 6.10 and Table 6.11 indicate that the IDE has more accurate results so that we may employ the IDE as a density estimator based on the measurements of its associated UEs.

Table 6.11: Required outage probability (P_O^*) vs calculated outage probability (P_O) by using the $\hat{\lambda}_{IDE}$ (nodes/m³), $\hat{\lambda}_{CDE}$ (nodes/m³), which are the local density results belong to each of BSs, and AAPD (%) results.

P_O^*	$\hat{\lambda}_{IDE}$			$\hat{\lambda}_{CDE}$		
	P_O	AAPD, %	99% confidence limits, ($\times 10^{-5}$)	P_O	AAPD, %	99% confidence limits, ($\times 10^{-5}$)
0.02	0.022	8.46	± 0.98	0.023	17.60	± 0.52
0.025	0.027	7.26	± 2.35	0.029	15.00	± 1.68
0.03	0.031	4.69	± 2.07	0.034	12.84	± 1.10
0.035	0.036	2.72	± 1.45	0.039	12.17	± 0.95
0.04	0.041	1.38	± 2.48	0.044	7.61	± 1.13
0.045	0.045	0.84	± 2.74	0.049	7.28	± 2.93

Since the CDE needs more measurements than IDE, it provides less accurate results in comparison to the outcomes of the IDE. In these simulations, more accurate results are obtained while the large number of UE is considered and the network is getting denser.

6.2.3 Validation of Density-aware Slotted ALOHA Potocol (DASAP) for FANET

In this section we explain the simulation details for DASAP, and make various analysis to validate our approach by using Monte Carlo simulations implemented in MATLAB. In our analyses, we compare our proposal DASAP with its opponents, analyze the impact of parameters such as number of time slots, moving average smoothing factors, and initial channel access probabilities. We also investigate the performance of DASAP under different non-uniform deployments and a mobility model. All of the simulation parameters are presented in Table 6.12.

Simulator Model

Implementation of DASAP simulation is presented in Algorithm 4. In simulations, a number of UAVs is uniform randomly deployed with a density of λ (nodes/m³) in a

Table 6.12: The symbols, notations, values and units of the 3-D simulation parameters for DASAP.

Parameter	Default Value	Units	Ref
Actual density, λ	$\frac{N}{4/3\pi r^3}$	nodes/ m^3	[36]
Estimated (effective) density, $\hat{\lambda}$	(4.6)	nodes/ m^3	
Channel access probability, p	[0,1]		[46]
UAV selection probability, p_s	[0,1]		
Contention probability, p_c	[0,1]		
Number of UAVs, N	[10,110]		[35]
Speed of UAVs, V	[10,100]	m/s	[44]
Sparse deployment, λ_S	$\frac{10}{4/3\pi r^3}$	nodes/ m^3	[36]
Dense deployment, λ_D	$\frac{50}{4/3\pi r^3}$	nodes/ m^3	[36]
Ultra-dense deployment, λ_U	$\frac{104}{4/3\pi r^3}$	nodes/ m^3	[36]
Path-loss exp. γ	2		[223]
Reference distance, r_0 ,	1	m	[223]
Transmit power, P_t	100	mW	[35]
Number of time slots, $nofSlots$	[50, 1000]	mW	[33]
Nearest neighbor index, k	$[1, \infty)$		[42]
K	10^{-5}		[44]
Radius, r	1500	m	[36]
Max. communication range, r_c ,	$(\frac{T}{CP_t})^{1/\gamma}$	m	[42]

three dimensional spherical environment, where the radius, r is set as 1.5 km , which is implemented with the code segment between line 1 and line 7. We divide time into a number of slots. The number of slots are designated as S . We simulate the communication protocol between UAVs by taking advantage of the slotted ALOHA protocol just with a dynamic probability scheme. We initially set the probability of channel access (p) as randomly in line 4, where N is the number of UAVs, and V is the volume in this FANET. We consider two states for a time slot as we already defined in Section 5.3. Each of estimating UAVs can measure the power on the channel, and measure the aggregate interference by using the summation of the received signal strength from its neighbors using the method as presented in the line 8 and in

Algorithm 4 Density-adaptive Slotted ALOHA Protocol (DASAP)

```
1: Input:  $\lambda, \gamma, P_t, k, K, p, \text{alpha} = [0, 1], u = 0, c = 0, w = 0, S, r = 1500$ .
2: Output:  $[U], [W], [C]$ 
3: Calculate  $V \leftarrow 4/3\pi r^3$ ;
4: Initialize  $p \leftarrow \text{rand}(N, 1)$ ;
5: Calculate  $N \leftarrow \lambda V$ ;
6: for  $t=0; t < S; t++$  do
7:   positions  $\leftarrow$  Generate 3-D positions
8:   Calculate  $x_k \leftarrow K P_t \left( \frac{r_0}{r_k} \right)^\gamma$ ;
9:    $b \leftarrow 0$ ;
10:   $p_s \leftarrow \text{rand}(N, 1)$ ;
11:  for  $j=0; j < N; j++$  do
12:    Find  $(\hat{\lambda})$  (4.6);
13:    Calculate  $\lambda_c = \hat{\lambda}/p_s$ ;
14:     $p(j) = \alpha \left( \frac{1}{(\hat{\lambda} 4/3\pi r_c^3)} \right) + (1 - \alpha)p(j)$ ;
15:  end for
16:  for  $j=0; j < N; j++$  do
17:     $p_c \leftarrow \text{rand}(N, 1)$ ;
18:    if  $p \geq p_c$  then
19:       $b++$ ;
20:    end if
21:  end for
22:  if  $b == 1$  then
23:     $u++$ ;
24:  else
25:    if  $b == 0$  then
26:       $w++$ ;
27:    else
28:       $c++$ ;
29:    end if
30:  end if
31:   $U \leftarrow (u/t)100$ ;
32:   $W \leftarrow (w/t)100$ ;
33:   $C \leftarrow (c/t)100$ ;
34: end for
35: return  $U, W, C$ ;
```

line 12 of the Algorithm 4 and as explained in Section 5.3, where we find r_k using Euclidean distances between each of UAVs by considering $k = 1$. In line 9, b represents the number of UAVs which can send a packet. We have already proved that this summation have an apparent cohesion between (μ_I) and the aggregate received signal strengths in [42]. Then, we randomly select a set of UAVs with a probability p_s in order to determine some of them as estimating UAVs and some of them as transmitter UAVs so that they can generate random signals in Estimating slots, and the remaining UAVs can measure the total signal power by aggregating the received signal strengths from their nearest neighbors by using the summation of x_k values. The estimating UAVs employ (4.6) to estimate the effective density of UAVs in line 13. The obtained estimation value should be divided by the selection probability (p_s) to determine the actual density as we do in line 14. Now, we have the current UAV density of the whole network ($\hat{\lambda}$). The UAV can now update its channel access probability based on (5.5) as explained in Section 5.3 which is formulated in line 15, where we set the value of α as 0.5, meaning that we give the same chance for the effective channel access probability and the previous channel access probability value. After all estimating UAVs completed the estimation slot process, in other words, after all estimating UAVs update their channel access probability values, in the successive step, we simulate the second mini-slot of the time slot where each of UAVs in the network can send a packet depending on their channel access probability afterwards line 17. We consider the updated UAVs' access probability value of p for the successive mini-slots. There may be the following scenarios for each channel slot; one UAV, or more than one UAV or none UAVs may send a packet to the network by obeying a channel access probability p and contention probability (p_c). The contention probability p_c provides simulating a random packet transmission behaviour in this regard. At the beginning of a time slot, if only one UAV sends packet, then this step is recorded as successful step, u , as illustrated in the Algorithm 4 in line 24, or if more than one UAV try to send their packets this time slot is counted as collision, c in line 29, otherwise, the time slot is considered as wasted slot, w in line 27. The rates for utilization U in line 32, collision C in line 34, and wasted slots W in line 33 can be obtained via dividing the values of u , c and w by the number of time slots at each time. In this regard, we define the channel utilization rate as the number of successful transmission per the number of reserved time slots. The number of collided slots per the number of time slots defines

the collision rate, and waste rate is equal to the idle slots per the number of time slots as denoted in Algorithm 4.

Comparison between the Simple Slotted ALOHA Protocol, Stabilized Slotted ALOHA Protocol and DASAP

In this section, we compare our proposed technique DASAP with two opponent techniques. The first one is the theoretic slotted ALOHA protocol (SAP), and the other one is the stabilized slotted ALOHA protocol utilizing a binary exponential back-off scheme with upper and lower bounds of the channel access probability p .

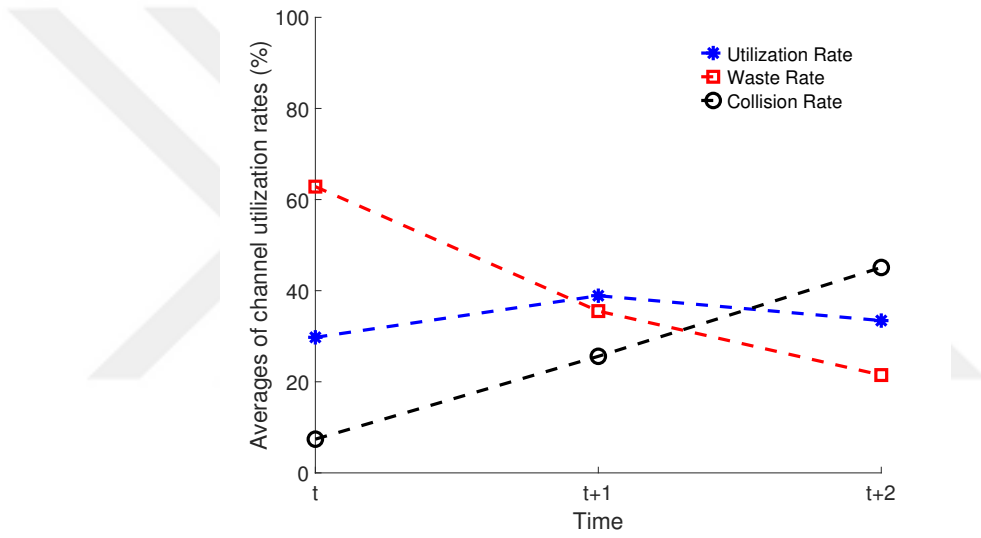


Figure 6.25: Time for different deployment densities vs. averages of channel utilization, waste and collision rates when $\lambda_{t+2} > \lambda_t > \lambda_{t+1}$, where $\lambda_{t+2} = 7 \times 10^{-9}$, $\lambda_t = 4.5 \times 10^{-9}$, and $\lambda_{t+1} = 2 \times 10^{-9}$, and channel access probability (p) is fixed and optimal for λ_t , $p = 1/63$, and the number of slots are equal to 1000.

Slotted ALOHA Protocol (SAP) and Stabilized Slotted ALOHA Protocol (STSAP)

In the simulations, SAP and STSAP are almost the same implementation as we discussed in Section 5.3.4. However, in STSAP, we should change the channel access probability, if the transmission is successful or unsuccessful. In Figure 6.25 it can

be seen that if we have a fixed probability and different deployments, the utilization is only maximized when the proper channel access probability is in case for the deployment density value. As implemented in Algorithm 5 in [224, 225, 226], the stabilized slotted ALOHA protocol increases the channel access probability by setting $p = \min(2p, 1)$ in line 13 if the current time slot is successful. If the transmission is not successful due to a collision, the STSAP decreases p by setting $p = (p_{min}, p/2)$ in line 19, where p_{min} is the minimum channel access probability to avoid very low values of channel access probability. The other variables are presented in Table 6.12 and Section 6.2.3.

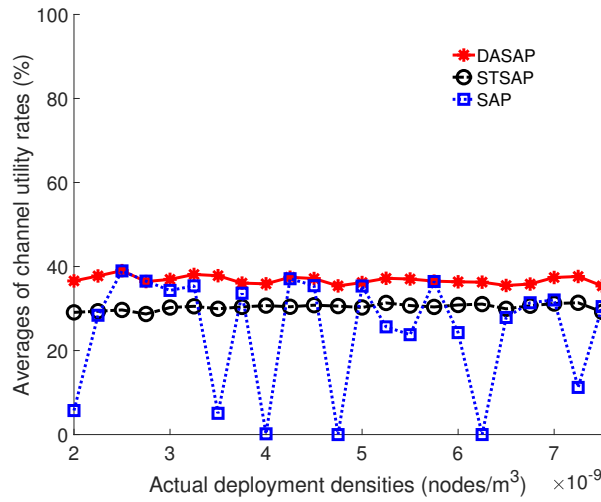


Figure 6.26: Averages of channel utilization rates from the comparison results of DASAP with other opponents which are slotted ALOHA protocol and stabilized slotted ALOHA protocol while the network density is soaring, when the number of time slot is selected as 10000, and $\alpha = 0.9$.

Analysis of The Comparison Results

In our comparison simulations, we set $\alpha = 0.9$, $S = 10000$, and the initial channel access probability is randomly chosen. Figure 6.26 shows the comparison results. Our proposal has better utilization performance in comparison to other opponents as depicted in Figure 6.26. We can see huge fluctuations in the utilization rate and the channel access probability in Figure 6.26 and Figure 6.27 for SAP. However, the scheme STSAP and our proposal have more and more stabilized results. In random

Algorithm 5 Stabilized Slotted Aloha Protocol (STSAP)

```
1: Input:  $p, p_{min} = 0.009, u = 0, c = 0, w = 0$ 
2: Output:  $[U], [W], [C]$ 
3: Initialize  $p \leftarrow 1/\text{rand}(N, 1)$ ;
4: for  $t=0; t < S; t++$  do
5:   for  $j=0; j < N; j++$  do
6:      $p_c \leftarrow \text{rand}(N, 1)$ ;
7:     if  $p \geq p_c$  then
8:        $b++$ ;
9:     end if
10:  end for
11:  if  $b == 1$  then
12:     $u++$ ;
13:     $p = \min(2p, 1)$ ;
14:  else
15:    if  $b == 0$  then
16:       $w++$ ;
17:    else
18:       $c++$ ;
19:       $p = \max(p_{min}, p/2)$ ;
20:    end if
21:  end if
22:   $U \leftarrow (u/t)100$ ;
23:   $W \leftarrow (w/t)100$ ;
24:   $C \leftarrow (c/t)100$ ;
25: end for
26: return  $U, W, C$ ;
```

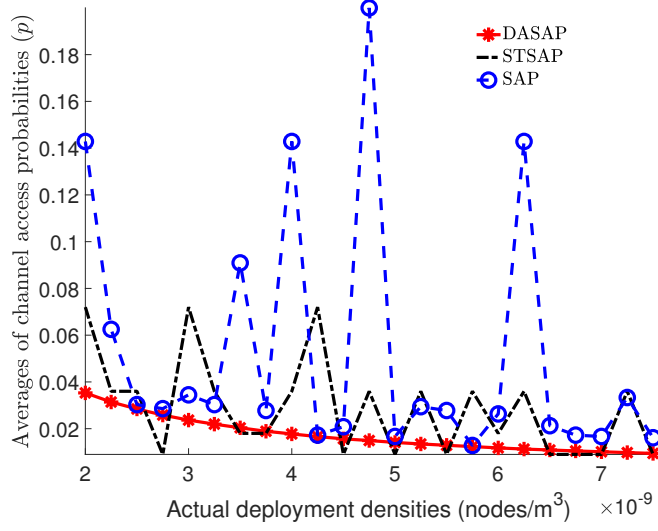


Figure 6.27: Averages of channel access probability rates from the comparison results of DASAP with slotted ALOHA protocol and stabilized slotted ALOHA protocol while the network density is soaring, when the number of time slot is selected as 10000, and $\alpha = 0.9$.

access schemes with dynamic probability, the optimization of the results should be made by considering the stabilization and the maximization of the system like doing so in our proposal DASAP.

Convergence Analysis

Since this study is based on dividing time into a number of mini slots, we investigate the impact of the number of time slots on the channel performance characteristics such as the rate of collided slots, the number of wasted slots, the percentage of utilization rate, and the channel access probability. We make three different simulations by using different number of time slots and different deployment scenarios. The first one includes the simulation where we divide the time into different number of time slots which are in the range of between 50 and 2000, at each step we perform DASAP for these different number of time slots. The averages of the related results are presented in Figure 6.28. Secondly, we make a simulation regarding with how channel utilization rates change during subsequent time slots to observe the conver-

gence of channel utilization rate in time. In the second simulation we divide time into 1000 slots, and we examine the variations in the results of channel utilization rates in time. Figure 6.29 and Figure 6.30 are the corresponding results from the second simulation. In the third simulation, we simulate a scenario to clearly analyze the relationship between different deployment densities and channel utilization rates in addition to access probabilities if we divide the time into various number of time-slots. Figure 6.31, 6.32, and 6.33 are obtained from the last simulation scenario.

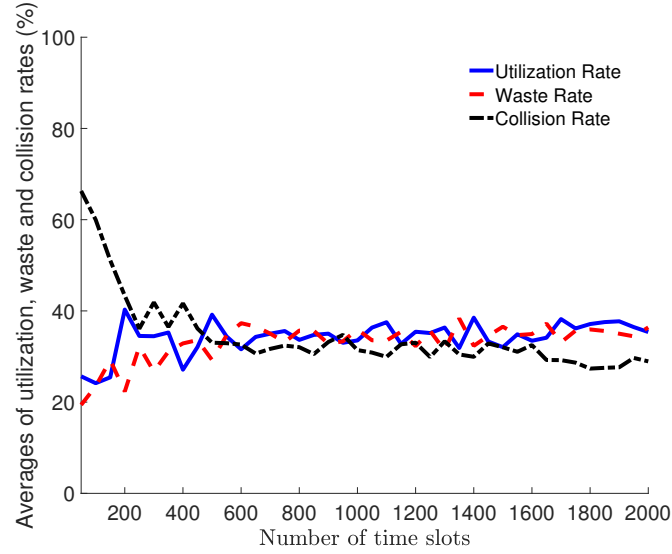


Figure 6.28: Averages of channel utilization, waste and collision measurements when different number of time slots are selected.

Figure 6.28 demonstrates the relationship between the different number of time slots versus channel utilization. In this simulation we deploy 104 UAVs, α is selected 0.5, and the initial access probabilities are chosen randomly between 0 and 1. According to our observations, when we use a higher value of the number of time slots we obtain higher channel utilization rates. While the number of time slots are getting larger, then the increase in the channel utilization rates is getting lower and converge at a channel utilization rate. As a matter of fact, we get more stabilized channel access probability values in this case. Moreover, While the number of the time slots are increasing, the collision rates are decreasing significantly, on the other hand, the wasted slots increase slightly.

In Figure 6.29, the instantly changed channel utilization results based on the sub-

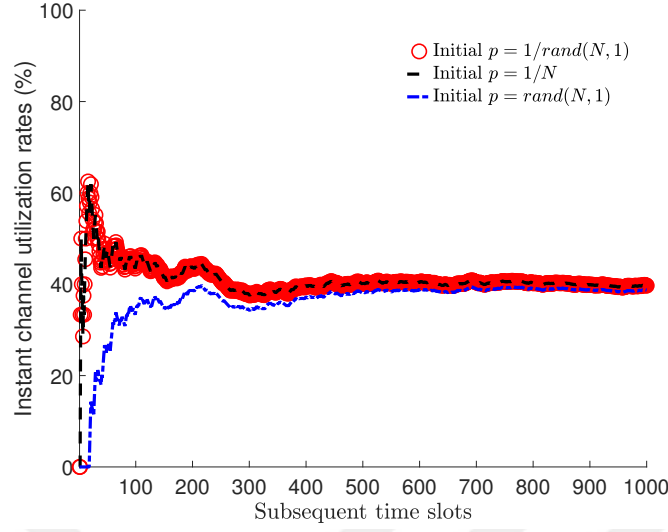


Figure 6.29: Instant channel utilization measurements' averages of different subsequent time slots are utilized when different number of initial probabilities are considered, and α is selected as 0.5. The time is divided into 1000 time-slots.

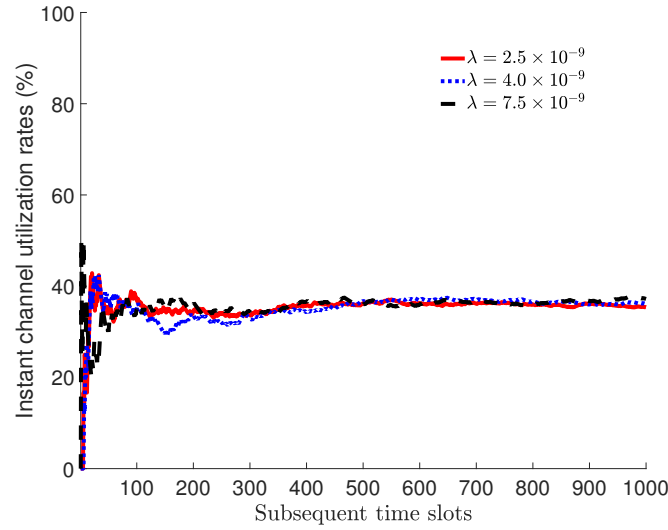


Figure 6.30: Averages of instant channel utilization rates of different subsequent time slots are utilized when different number of UAVs (N) are considered, and $\alpha = 0.5$. The time is divided into 1000 time-slots.

sequent number time slots when different initial probabilities are considered. This figure illustrates the initial probabilities impact on the channel utilization changes in time. Figure 6.30 shows the instant channel utilization results depending on the subsequent number time slots when different deployment densities are considered. According to the results, we can say that after approximately 300 time slots, channel utilization results provided by DASAP converge a rate of utilization value.

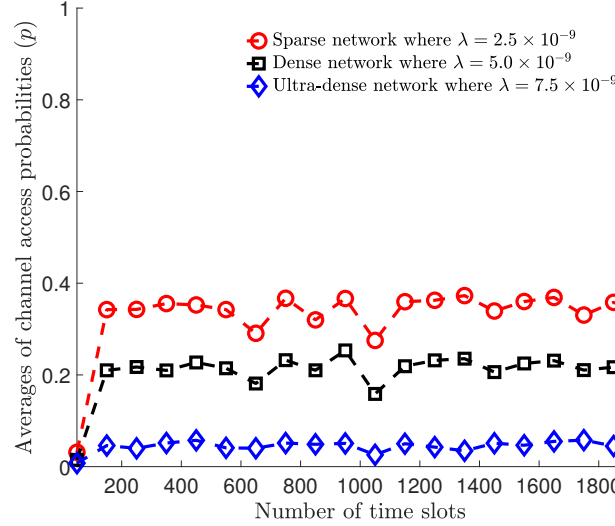


Figure 6.31: How channel access probabilities change in different number of time slots. The averages of measurements are presented when different network scenarios, namely, different number of UAVs are considered.

We also analyze the impact of the number of time slots for different deployments. Figure 6.31 illustrates the impact of the time slots on channel access probabilities when different deployments are in question. In Figure 6.31, for the same density, when the number of time slots are increasing, the probability of the channel access is stabilized during the simulation. For a different perspective, when the channel access probability is smaller when the network is getting denser in case of the same number of time slots. In the simulation for Figure 6.31, and Figure 6.32, 26, 62, and 104 UAVs are deployed for sparse network, dense network, and ultra-dense network, respectively. As can be seen in Figure 6.32 that while the number of time slots are increasing, the sparse networks have higher utilization rates in comparison to the dense and ultra-dense networks due to an increase in the collided slots.

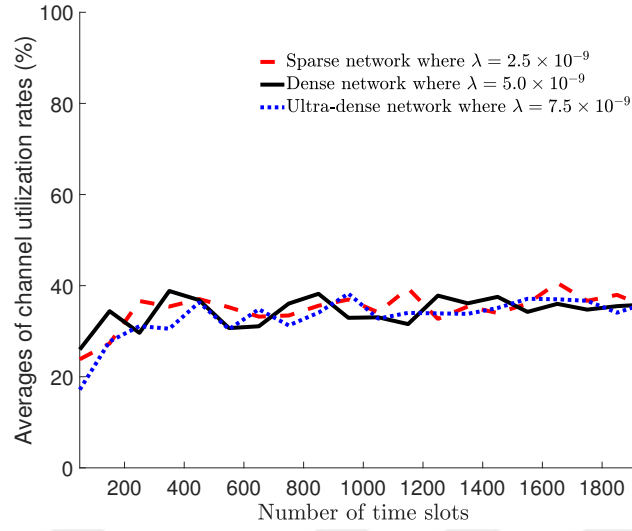


Figure 6.32: Averages of channel utilization rates for different number of time slots when different network scenarios are considered.

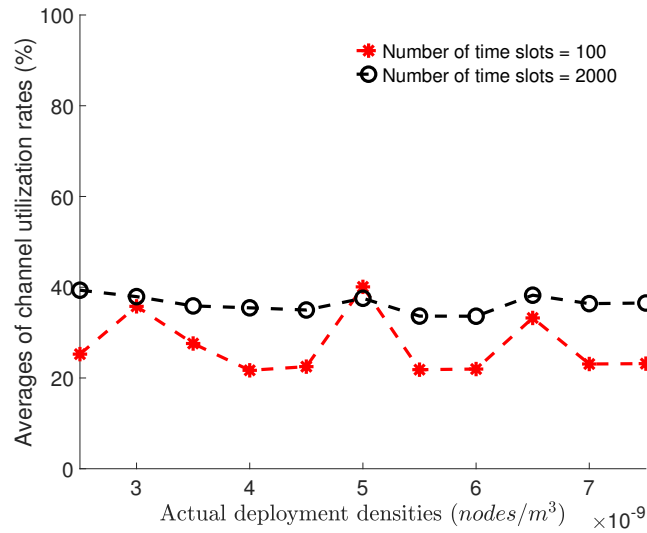


Figure 6.33: Averages of channel utilization rates by considering different actual deployment densities when different number of time slots are utilized.

Figure 6.33 demonstrates the impact of the density on channel utilization when different number of time slots are considered. We observe that the channel utilization results have a slight fluctuation if the number of time slots are sufficiently large. However, if the number of time slots are small than the fluctuations of the utilization results increases.

Impact of the Initial Access Probability

In dynamic random access schemes, one of the fluctuated parameters is the channel access probability which effect the channel utilization rates as illustrated in Figure 6.25. One of the design issues in this regard is that what is the correct and practical value to initialize the channel access probability? Since we need to stabilize and maximize the channel utilization, we need to make a fast update on the channel access probability for each of UAVs.

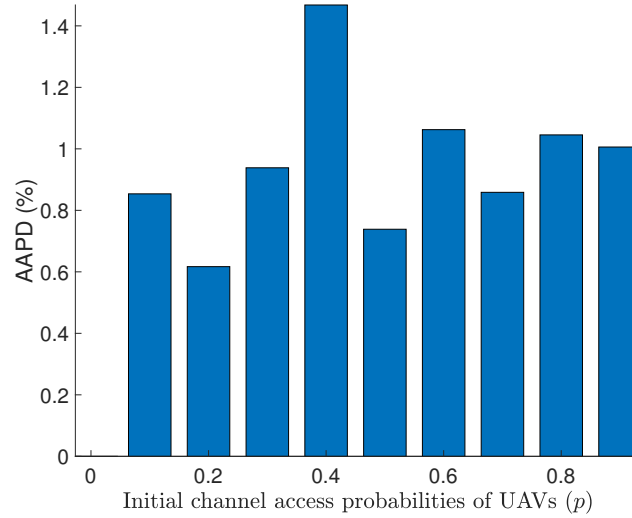


Figure 6.34: Initial channel access probabilities versus channel utilization error rates when p is increasing by 0.1 from 0.1 to 0.9, also a different p is changed depending on $(1/N)$ with different values of α . The number of time slots is 1000.

From the light of the results, we observe that if the channel access probability is initialized as $1/N$, we get the highest results for the channel utilization as illustrated in Figure 6.35. However, when the initial access probability is increasingly selected

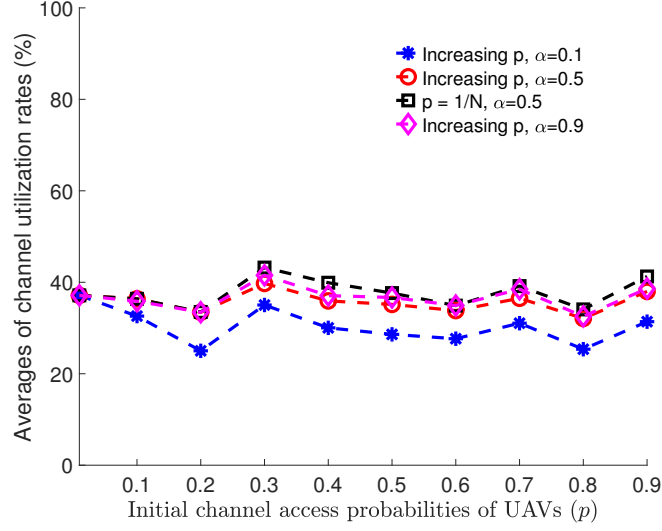


Figure 6.35: Averages for channel utilization rates for different values of moving average smoothing factor when $\lambda = 7.5 \times 10^{-9}$ and number of time slot is selected as 1000.

from the range of 0.1 and 0.9 as depicted in Figure 6.34 and Figure 6.35, the difference between two results is too smaller, in which it is at most 1.5%. Yet, there is still the initial probability selection is important in terms of practice, since we may not know the number of nodes (N) at the beginning or before any estimation process. Hence, it is applicable to randomly select the channel access probability. In Figure 6.35, by considering the update process (5.5) for channel access probability, the moving average smoothing factor (α) is another parameter which can effect the utilization results with the determination of the initial access probability. While α values are getting larger, we get the highest results for the utilization.

Impact of Moving Average Smoothing Factor

We denote α as the moving average smoothing factor in Algorithm 4. One of the research questions in this problem is that what is the impact of the smoothing factor on channel utilization? Figure 6.36 demonstrates the outcomes for different smoothing factors. In this simulation, we deploy 104 UAVs, we divide the time into 1000 equal time slots, and we randomly select the initial access probabilities. We also compare

two results: the first one is the outcomes for constant α , and the second one is for the changing α within a range of between 0.1 and 0.9.

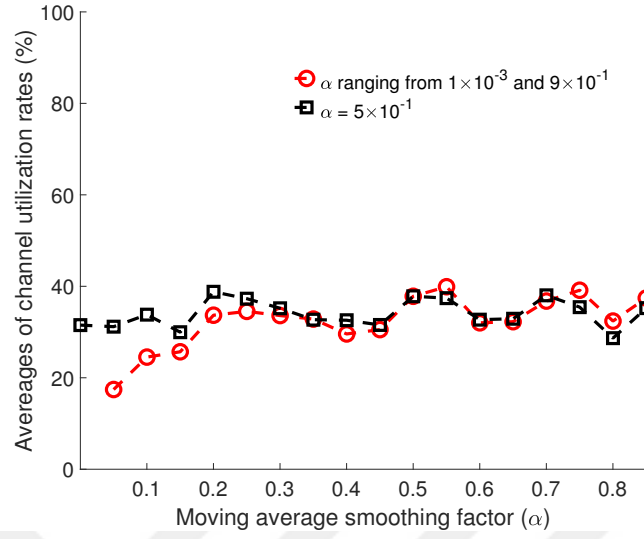


Figure 6.36: Averages fo channel utilization rates for different values of moving average smoothing factor when $\lambda = 7.5 \times 10^{-9}$ and number of time slot is selected as 1000.

We can see that the moving average smoothing factor gives different results between 0.1 and 0.5. When the value of α is reached to 0.5, after that the results are getting closer to each other, but the channel utilization rates significantly increase when the α increases until it reaches to 0.5. Moreover, the collision rates decrease rapidly, on the other hand, there is an increase in the wasted number of time slots up to the critical point of α .

Non-uniform Topologies

In this thesis, an understandable and easily tractable model is used while proposing and analyzing a communication protocol in addition to an estimator by assuming a uniform deployment. However, in real life, the distribution of UAVs in FANETs may be non-uniform because of their stochastic nature. To investigate the non-uniform deployments, we utilize Beta (B) distribution, a two-parameter asymmetrical distribution, which is similar to log normal distribution [42]. Thanks to Beta distribution

which provides different shape tendencies, we create a 3-D network simulation environment by deploying UAVs according to Beta distribution. Various shape tendencies have already explained in Section 6.1.2.8, proposed in [42]. The shape tendencies are categorized into four groups which are *Uniform Tendency*, *Central Tendency*, *Centrifugal Tendency*, and *Skewness Tendency*. *Uniform Tendency* defines a uniform deployment of UAVs. In *Central Tendency*, the distribution of UAVs is close to the center of the network. *Centrifugal Tendency* refers a deployment where each of UAVs is near to edge of the topology, and *Skewness Tendency* defines that UAVs in the network come together at a random position of the network. We use the values of a and b parameters which are presented in Table 6.13 to create our scenarios. In Table 6.13, *Uniform* is the first scenario in which the parameters a and b of B distribution are set as 1 such that UAVs are located uniformly in the simulation area. *Central Tendency* is the second scenario allowing a centralized distribution so that the positions of UAVs are close to the center of the spherical network environment. The third scenario is *Centrifugal Tendency* where the positions of UAVs are off-centered. UAVs are located at close to the boundaries of the network with this tendency. *Skewness* is the last case which has a skewed shape locating UAVs at a particular region of the simulation environment.

Observations from the results in Table 6.13 show that especially in highly non-uniform deployments, since DASAP uses the receive signal strength for the estimation process, it is negatively effected by the positions of the UAVs. However, as stated in the literature [58], to propose easily tractable models is commonly used. Hence, although we make an assumption that UAVs' distribution is based on a uniform Poisson point process, we need to analyze the proposed model performance in non-uniform deployments. In *Uniform Tendency* scenarios where UAVs are uniformly deployed, the approximation of the results in two methods is the best in comparison to the other deployments. In *Central Tendency*, while the centrality level is increasing the probabilistic estimator IDE gives less accurate results. The reason for this case is that when nodes are too close to each other so that an increase in overlapping measurements, and the nodes causing non-negative effects at the corner of the network topology decreases the accuracy. UAVs in *Centrifugal Tendency* are close to the boundary of the coverage area, and the distances between the nodes are larger. While this tendency

Table 6.13: When the actual density value equals to $1(\times 10^{-4})$ (λ) (nodes/m³), utility results (λ) (nodes/m³) and $\hat{\lambda}$ (nodes/m³) for different uniform and non-uniform distributions are presented. All AAPD (%) results are also presented with their 99% confidence interval ($CI_{99\%}$).

Distributions	Shape parameters		Utility rate, %	
UAV	a	b	with $\hat{\lambda}$	$CI_{99\%}$
Uniform	1	1	37.25	± 0.23
Central Tendency	3	3	39.37	± 0.24
	5	5	29.53	± 0.25
	7	7	26.32	± 0.23
Centrifugal Tendency	0.1	0.1	22.60	± 0.20
	0.5	0.5	37.62	± 0.18
	0.7	0.7	33.15	± 0.23
Skewness	1	3	25.36	± 0.31
	4	1	32.20	± 0.15
Various Non-uniform Deployments	10	10	18.90	± 0.37
	0.3	0.3	35.66	± 0.33
	1	4	13.24	± 0.12
	1	5	12.86	± 0.40
	1	20	3.22	± 0.36
	20	1	2.28	± 0.18
	20	10	14.17	± 0.27
	100	10	1.78	± 0.15
	100	20	2.83	± 0.31
	20	100	1.60	± 0.24
	10	100	1.49	± 0.24

is lessening, the results are getting more accurate. When the deployment of UAVs has *Skewness* tendency, they gather around a particular area of the network where UAVs are too close to each other. The same shape variation may not be provided by symmetrically changing the parameters a and b . Thus, various observations are obtained from the values of these two shape parameters. We observe that the affect of

the non-uniform deployments on probabilistic IDE is different from IDE presented in [42]. This is because of our probabilistic IDE works different from IDE. In the probabilistic IDE, each of UAVs receives locally and estimates its own density. All in all, we assume a uniform tractable model in this thesis, where non-uniform deployments have a negative impact on the accuracy of the results.

Mobility

In this thesis, as a common mobility model in simulation-based studies called random way point (RWP) is selected in order to analyze the impact of mobility on channel utilization when a density-aware dynamic channel access scheme is employed [233, 234]. The RWP model is a simple and mostly available for simulation studies [223]. The simulation parameters can be seen in Table 6.12. As explained in Section 5.3, we take a screen shot of the network during the estimation process requiring a short time-period, and we assume that UAVs are stationary. We simulate a FANET where the speed of UAVs are changing in the range of between 10 m/s and 100 m/s . For this experiment, at the beginning of each time slot, we obtain the screen shot of the network to re-optimize the channel access probabilities while UAVs are moving according to the RWP model [223].

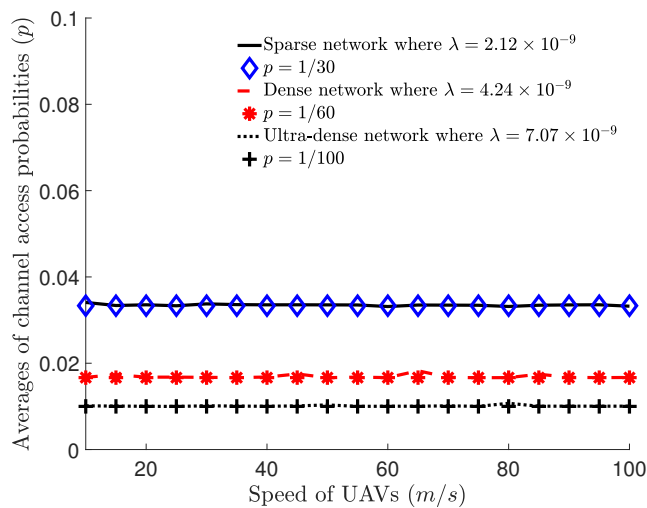


Figure 6.37: Different speeds of UAVs vs. channel access probabilities when different deployments are considered, and number of time slot is selected as 1000.

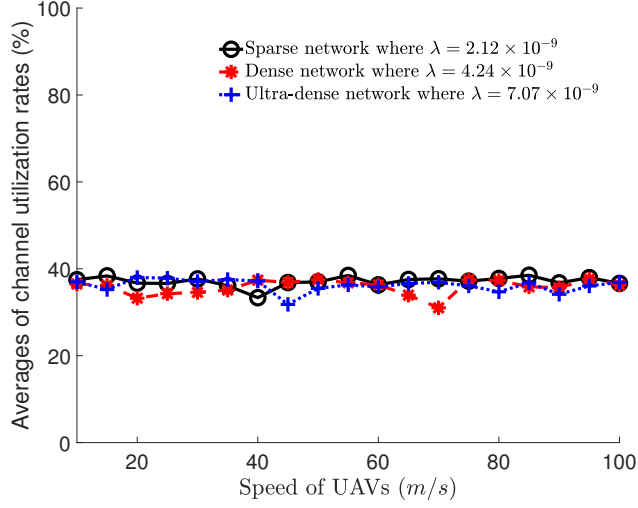


Figure 6.38: Different speeds of UAVs vs. channel utilization rates when different deployments are considered, and number of time slot is selected as 1000.

We perform this analysis by using two parameters which are UAV speed and the re-organizing interval for different network scenarios where we interpolate the UAVs' positions, namely, the screen shot of the network topology. As can be seen in Figure 6.37, while speed of UAVs are increasing, the channel access probability does not change significantly as expected since our proposed approach provide an optimal channel access probability. Figure 6.38 illustrates that an increase in speed of UAVs will not dramatically cause a change in channel utilization optimized by DASAP. Although increasing the speed will result in a higher change in FANET topology, we change the access probability based on the effective density which results in steady outcomes in terms of channel utilization.

If we consider a mobility model, we need to answer an important design questions which is in which frequency the network re-organization should be performed. Figures 6.39 and 6.40 demonstrate the relation between the network performance parameters and network reorganizing frequency that means how often we get the screen shot of the topology. For instance, we get the screen shot of the network as one in every two time slot. However, we estimate the network density at the beginning of each time slot. From the light of the results channel access probabilities are not dramatically changes as we can see when the network is re-organized with in different

reorganizing interval. Although there are some small variations in channel access probability, DASAP provides an optimum channel access probability close to the maximum probability value $1/N$ by maximizing the channel utilization.

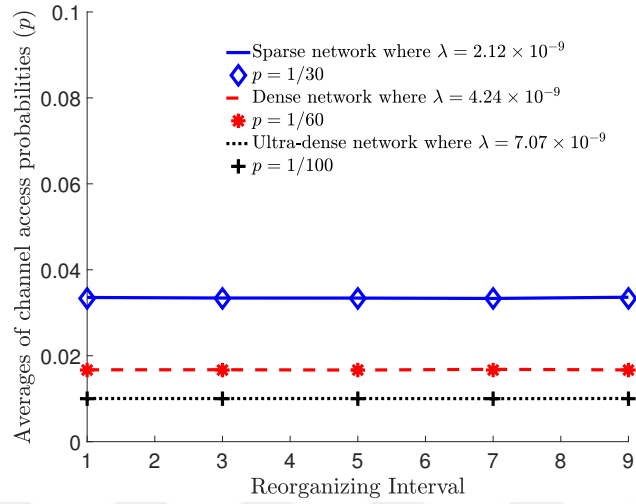


Figure 6.39: Different network optimization time intervals vs. channel access probabilities when different deployments are considered, and number of time slot is selected as 1000.

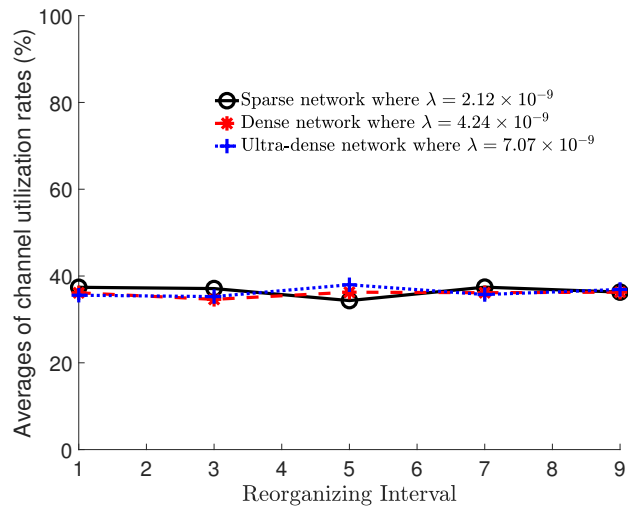


Figure 6.40: Different network optimization time intervals vs. channel utilization rates when different deployments are considered, and number of time slot is selected as 1000.

CHAPTER 7

CONCLUSION AND FUTURE WORK

With the invention of mobile devices, applications, and new network paradigms such as ultra-dense networks, mobile cells, and ever-changing topologies, the need for self-organized networking becomes more pronounced to increase the capacity, coverage, and performance. Dense networks provide redundant coverage, whereas connectivity is disrupted in sparse networks. Resource sharing such as channel utilization may become inefficient. We manifest and prove that future wireless networks have to be density-aware and -adaptive. We present a comprehensive analysis showing that recent technologies and developments accompany some opportunities and challenges in dynamic networks. These networks have to consider effective network density as an optimization parameter to adapt the network functions to this dynamism in the network topology. Therefore, we need robust and fast network density estimators. This thesis proposes novel density estimators: the distance matrix-based density estimator applied in ad hoc networks, the multi-access edge cloud-based density estimator performed in cellular networks, and the interference-based density estimator implemented in both cellular and flying ad hoc networks. We assert that density changes have to be estimated at run time, and the protocols have to be density-aware and -adaptive since static configurations of protocols and parameters will not be adequate in dynamic ad hoc networks. Therefore, we suggest density-aware network outage, density-aware transmit power adaptation techniques, which are operational for both two-dimensional and three-dimensional wireless networks as a run-time solution. Besides, we propose a density-aware channel utilization technique for flying ad hoc networks.

We propose the system design for density estimation in mobile networks and validate

these proposed estimators using Monte-Carlo simulations implemented in MATLAB. The distance matrix-based density estimator utilizes distances in clustered ad hoc networks. The proposal is validated by Monte-Carlo simulations and compared with other distance-based density estimators. The proposed estimator performs well with high accuracy even under substantial errors in distance measurements. The simulation results that we present for clustered ad hoc networks in this thesis indicate the necessity of the density-aware solutions for making network performance better from capacity, coverage, and energy conservation viewpoints. We also introduce received signal strength-based network density estimators. One of them uses the aggregate measurements, which is the interference-based density estimator, and the other one exploits the collaboratively collected measurements, which is named as multi-access edge cloud based density estimator. We also improve the interference-based density estimator for flying ad hoc networks requiring three-dimensional solutions in a dynamic probabilistic manner. In case of uniform deployments, the error rate of the estimators are less than 5%. However, if the topology of the network has a non-uniform deployment, then the accuracy of the estimators decreases.

We presented three density-aware and -adaptive networking applications. These applications are also validated by using Monte-Carlo simulations. Firstly, a simple, outage probability model is proposed and validated. Secondly, we propose a density-aware transmit power adaptation technique in a dynamic and self-configurable fashion to conserve energy and enhance service quality. From a theoretic perspective, the model considers only large-scale fading and is applicable in environments where the impact of multi-path fading is small. Transmit power of base stations must be density-aware to increase the capacity. We analyzed the impact of transmit power, channel model, and density on outage probability. As expected, transmit power and network density are quality of service-friendly parameters, unlike the rest. However, they are not cost- or environment-friendly. We also introduce a dynamic channel utilization technique based on a density-aware slotted ALOHA protocol. This protocol finds an optimal channel access probability close to the maximum value $1/N$ and maximizes the channel utilization. The system model with the estimator interference-based density estimator is very simple, fast, and easy to be implemented at the link layer of any ad hoc network.

As future work, this research can be extended by implementing the proposed protocols and estimators with using discreet event simulators such as OMNET or NS3 in order to validate the results by making experiments close to the real-life network conditions. We will also implement the estimator in outdoor and indoor test-beds and validate the results in practice. In addition, we will incorporate shadowing in the estimators. The fusion of various estimators or averaging estimators over time can also be considered in future work. For unmanned aerial vehicle assisted networks and flying ad hoc networks which may be deployed over large volumes instead of Euclidean distances, we may use geodesic distances in the future.





REFERENCES

- [1] S. Shakkottai, T. S. Rappaport, and P. C. Karlsson, “Cross-layer design for wireless networks,” *IEEE Communications Magazine*, vol. 41, no. 10, pp. 74–80, 2003.
- [2] S. Merkel, S. Mostaghim, and H. Schmeck, *Distributed Geometric Distance Estimation in Ad Hoc Networks*, pp. 28–41. Berlin, Heidelberg: Springer Berlin Heidelberg, 2012.
- [3] K. Lee, J. Lee, H. Lee, and Y. Shin, “A density and distance based cluster head selection algorithm in sensor networks,” in *Proc. of the ICACT*, vol. 1, (Phoenix Park, South Korea), pp. 162–165, Feb 2010.
- [4] R. K. Ganti and M. Haenggi, “Interference and outage in clustered wireless ad hoc networks,” *IEEE Transactions on Information Theory*, vol. 55, pp. 4067–4086, Sept 2009.
- [5] G. V. Rossi, Z. Fan, W. H. Chin, and K. K. Leung, “Stable Clustering for Ad-Hoc Vehicle Networking,” in *Proc. of the WCNC*, (San Francisco, California), pp. 1–6, March 2017.
- [6] H. Yang, H. Luo, F. Ye, S. Lu, and L. Zhang, “Security in mobile ad hoc networks: challenges and solutions,” *IEEE Wireless Communications*, vol. 11, pp. 38–47, Feb 2004.
- [7] J. Y. Yu and P. H. J. Chong, “A survey of clustering schemes for mobile ad hoc networks,” *IEEE Communications Surveys Tutorials*, vol. 7, pp. 32–48, First 2005.
- [8] C. Intanagonwivat, D. Estrin, R. Govindan, and J. Heidemann, “Impact of network density on data aggregation in wireless sensor networks,” in *Proceedings 22nd International Conference on Distributed Computing Systems*, (Vienna, Austria), pp. 457–458, July 2002.

- [9] I. Bor-Yaliniz and H. Yanikomeroglu, “The new frontier in RAN heterogeneity: Multi-tier drone-cells,” *IEEE Communications Magazine*, vol. 54, pp. 48–55, November 2016.
- [10] M. Kamel, W. Hamouda, and A. Youssef, “Ultra-dense networks: A survey,” *IEEE Communications Surveys Tutorials*, vol. 18, pp. 2522–2545, Fourthquarter 2016.
- [11] C. Galiotto, N. K. Pratas, L. Doyle, and N. Marchetti, “Effect of LOS/N-LOS propagation on 5G ultra-dense networks,” *Computer Networks*, vol. 120, pp. 126 – 140, 2017.
- [12] S. Sharafeddine and R. Islambouli, “On-demand deployment of multiple aerial base stations for traffic offloading and network recovery,” *Computer Networks*, vol. 156, pp. 52 – 61, 2019.
- [13] Q.-T. Thieu and H.-Y. Hsieh, “Outage protection for cellular-mode users in device-to-device communications through stochastic optimization,” *Computer Networks*, vol. 132, pp. 145 – 160, 2018.
- [14] H. Wang, G. Ren, J. Chen, G. Ding, and Y. Yang, “Unmanned aerial vehicle-aided communications: Joint transmit power and trajectory optimization,” *IEEE Wireless Communications Letters*, vol. 7, pp. 522–525, Aug 2018.
- [15] T. Zahir, K. Arshad, A. Nakata, and K. Moessner, “Interference management in femtocells,” *IEEE Communications Surveys & Tutorials*, vol. 15, no. 1, pp. 293–311, 2013.
- [16] B. Rengarajan, G. Rizzo, and M. A. Marsan, “Energy-optimal base station density in cellular access networks with sleep modes,” *Computer Networks*, vol. 78, pp. 152 – 163, 2015. Special Issue: Green Communications.
- [17] L. Suárez, L. Nuaymi, and J.-M. Bonnin, “Energy-efficient BS switching-off and cell topology management for macro/femto environments,” *Computer Networks*, vol. 78, pp. 182 – 201, 2015. Special Issue: Green Communications.
- [18] Y.-C. Wang and C.-A. Chuang, “Efficient eNB deployment strategy for heterogeneous cells in 4G LTE systems,” *Computer Networks*, vol. 79, pp. 297 – 312, 2015.

- [19] D. Han, H. Minn, U. Tefek, and T. J. Lim, "Network dimensioning, QoE maximization, and power control for multi-tier machine-type communications," *IEEE Transactions on Communications*, vol. 67, pp. 859–872, Jan 2019.
- [20] O. Yaman, A. Eroglu, and E. Onur, "Density-aware cell zooming," in *2018 21st Conference on Innovation in Clouds, Internet and Networks and Workshops (ICIN)*, (Paris, France), pp. 1–8, Feb 2018.
- [21] S. Jagadeesan, J. Riihijärvi, and M. Petrova, "Impact of three-dimensionality of femtocell deployments on aggregate interference estimation," in *2015 IEEE 26th Annual International Symposium on Personal, Indoor, and Mobile Radio Communications (PIMRC)*, (Hong Kong, China), pp. 737–742, Aug 2015.
- [22] Z. Niu, Y. Wu, J. Gong, and Z. Yang, "Cell zooming for cost-efficient green cellular networks," *IEEE Communications Magazine*, vol. 48, pp. 74–79, November 2010.
- [23] H. Chen, Q. Zhang, and F. Zhao, "Energy-efficient joint BS and RS sleep scheduling in relay-assisted cellular networks," *Computer Networks*, vol. 100, pp. 45 – 54, 2016.
- [24] R. Balasubramaniam, S. Nagaraj, M. Sarkar, C. Paolini, and P. Khaitan, "Cell zooming for power efficient base station operation," in *Proc. of the 9th IWCNC*, (Sardinia, Italy), pp. 556–560, July 2013.
- [25] S. Manegene, S. Musyoki, and P. Langat, "Application of cell zooming in outage compensation," *Journal of Electronics and Communication Engineering*, vol. 10, no. 4, pp. 60–69, 2015.
- [26] İlker Bekmezci, O. K. Sahingoz, and Şamil Temel, "Flying ad-hoc networks (FANETs): A survey," *Ad Hoc Networks*, vol. 11, no. 3, pp. 1254 – 1270, 2013.
- [27] A. Guillen-Perez and M.-D. Cano, "Flying ad hoc networks: A new domain for network communications," *Sensors*, vol. 18, no. 10, 2018.
- [28] A. Chriki, H. Touati, H. Snoussi, and F. Kamoun, "FANET: Communication, mobility models and security issues," *Computer Networks*, vol. 163, p. 106877, 2019.

- [29] C. D. Francesco, L. D. Giovanni, and C. E. Palazzi, “The interference-aware drone ad-hoc relay network configuration problem,” *Electronic Notes in Discrete Mathematics*, vol. 69, pp. 317 – 324, 2018.
- [30] O. K. Sahingoz, “Networking models in flying ad-hoc networks (FANETs): Concepts and challenges,” *Journal of Intelligent & Robotic Systems*, vol. 74, no. 1-2, pp. 513–527, 2014.
- [31] W. Zafar and B. M. Khan, “A reliable, delay bounded and less complex communication protocol for multicluster FANETs,” *Digital Communications and Networks*, vol. 3, no. 1, pp. 30 – 38, 2017.
- [32] M. A. Khan, A. Safi, I. M. Qureshi, and I. U. Khan, “Flying ad-hoc networks (FANETs): A review of communication architectures, and routing protocols,” in *2017 First International Conference on Latest trends in Electrical Engineering and Computing Technologies (INTELLECT)*, (Karachi, Pakistan), pp. 1–9, Nov 2017.
- [33] M. Seddik, V. Toldov, L. Clavier, and N. Mitton, “From outage probability to ALOHA MAC layer performance analysis in distributed WSNs,” in *2018 IEEE Wireless Communications and Networking Conference (WCNC)*, (Barcelona, Spain), pp. 1–6, April 2018.
- [34] I. Bekmezci, I. Sen, and E. Erkalkan, “Flying ad hoc networks (FANET) test bed implementation,” in *2015 7th International Conference on Recent Advances in Space Technologies (RAST)*, (Istanbul, Turkey), pp. 665–668, June 2015.
- [35] E. A. Marconato, M. Rodrigues, R. de Melo Pires, D. F. Pigatto, L. C. Q. Filho, A. R. Pinto, and K. R. L. J. C. Branco, “AVENS - a novel flying ad hoc network simulator with automatic code generation for unmanned aircraft system,” in *HICSS*, (Waikoloa Village, HI, USA), January 2017.
- [36] O. S. Oubbati, M. Atiquzzaman, P. Lorenz, M. H. Tareque, and M. S. Hossain, “Routing in flying ad hoc networks: Survey, constraints, and future challenge perspectives,” *IEEE Access*, vol. 7, pp. 81057–81105, 2019.

- [37] K. K. Kashyap, A. Agrawal, *et al.*, “FANET: Survey on design challenges, application scenario and communication protocols,” *IJRAR-International Journal of Research and Analytical Reviews (IJRAR)*, vol. 5, no. 4, pp. 1024–1032, 2018.
- [38] Z. Shen, X. Zhang, M. Zhang, W. Li, and D. Yang, “Self-sorting-based MAC protocol for high-density vehicular ad hoc networks,” *IEEE Access*, vol. 5, pp. 7350–7361, 2017.
- [39] G. V. Rossi, K. K. Leung, and A. Gkelias, “Density-based optimal transmission for throughput enhancement in vehicular ad-hoc networks,” in *2015 IEEE International Conference on Communications (ICC)*, (London, UK), pp. 6571–6576, June 2015.
- [40] S. Handouf, E. Sabir, and M. Sadik, “Energy-throughput tradeoffs in ubiquitous flying radio access network for IoT,” in *2018 IEEE 4th World Forum on Internet of Things (WF-IoT)*, (Singapore), pp. 320–325, May 2018.
- [41] S. Kang, M. Aldwairi, and K.-I. Kim, “A survey on network simulators in three-dimensional wireless ad hoc and sensor networks,” *International Journal of Distributed Sensor Networks*, vol. 12, no. 9, p. 1550147716664740, 2016.
- [42] A. Eroğlu, O. Yaman, and E. Onur, “Density-aware cellular coverage control: Interference-based density estimation,” *Computer Networks*, vol. 165, p. 106922, 2019.
- [43] M. A. Khan, I. M. Qureshi, and F. Khanzada, “A hybrid communication scheme for efficient and low-cost deployment of future flying ad-hoc network (FANET),” *Drones*, vol. 3, no. 1, 2019.
- [44] Z. Zheng, A. K. Sangaiah, and T. Wang, “Adaptive communication protocols in flying ad hoc network,” *IEEE Communications Magazine*, vol. 56, pp. 136–142, Jan 2018.
- [45] A. Hernandez, F. Vazquez-Gallego, L. Alonso, and J. Alonso-Zarate, “Performance evaluation of frame slotted-ALOHA with intra-frame and inter-frame successive interference cancellation,” in *2015 IEEE Global Communications Conference (GLOBECOM)*, (San Diego, CA, USA), pp. 1–6, February 2015.

- [46] J. Sun, R. Liu, and E. Paolini, "A dynamic access probability adjustment strategy for coded random access schemes," *Sensors*, vol. 19, no. 19, 2019.
- [47] A. Laya, C. Kalalas, F. Vazquez-Gallego, L. Alonso, and J. Alonso-Zarate, "Goodbye, ALOHA!," *IEEE Access*, vol. 4, pp. 2029–2044, 2016.
- [48] E. Paolini, G. Liva, and M. Chiani, "Coded slotted ALOHA: A graph-based method for uncoordinated multiple access," *IEEE Transactions on Information Theory*, vol. 61, no. 12, pp. 6815–6832, 2015.
- [49] Zhongbang Yao, V. O. K. Li, and Zhigang Cao, "Maximum throughput analysis and enhancement of slotted ALOHA for multihop ad hoc networks," in *2004 IEEE International Conference on Communications (IEEE Cat. No.04CH37577)*, vol. 7, (Paris, France), pp. 4162–4166 Vol.7, June 2004.
- [50] Y. Li and L. Dai, "Maximum sum rate of slotted aloha with successive interference cancellation," *IEEE Transactions on Communications*, vol. 66, no. 11, pp. 5385–5400, 2018.
- [51] P. Park, S. Coleri Ergen, C. Fischione, C. Lu, and K. H. Johansson, "Wireless network design for control systems: A survey," *IEEE Communications Surveys Tutorials*, vol. 20, pp. 978–1013, Secondquarter 2018.
- [52] F. Alassery, W. K. M. Ahmed, and V. Lawrence, "MDSA: Multi-dimensional slotted ALOHA MAC protocol for low-collision high-throughput wireless communication systems," in *2015 36th IEEE Sarnoff Symposium*, (NJIT, New Jersey), pp. 179–184, Sep. 2015.
- [53] W. Guo, S. Wang, X. Chu, J. Zhang, J. Chen, and H. Song, "Automated small-cell deployment for heterogeneous cellular networks," *IEEE Communications Magazine*, vol. 51, no. 5, 2013.
- [54] A. Eroglu, E. Onur, and H. Oguztuzun, "Estimating density of wireless networks in practice," in *Proc. of the PIMRC*, (Hong Kong, China), pp. 1476–1480, 2015.
- [55] E. Onur, Y. Durmus, and I. Niemegeers, "Cooperative density estimation in random wireless ad hoc networks," *IEEE Communications Letters*, vol. 16, pp. 331–333, Mar 2012.

- [56] S. Chatterjee, M. J. Abdel-Rahman, and A. B. MacKenzie, "Optimal base station deployment with downlink rate coverage probability constraint," *IEEE Wireless Communications Letters*, vol. 7, pp. 340–343, June 2018.
- [57] T. Zhang, J. Zhao, L. An, and D. Liu, "Energy efficiency of base station deployment in ultra dense hetnets: A stochastic geometry analysis," *IEEE Wireless Communications Letters*, vol. 5, pp. 184–187, April 2016.
- [58] L. Chiaraviglio, F. Cuomo, M. Maisto, A. Gigli, J. Lorincz, Y. Zhou, Z. Zhao, C. Qi, and H. Zhang, "What is the best spatial distribution to model base station density? a deep dive into two european mobile networks," *IEEE Access*, vol. 4, pp. 1434–1443, 2016.
- [59] M. Di Renzo, T. T. Lam, A. Zappone, and M. Debbah, "A tractable closed-form expression of the coverage probability in poisson cellular networks," *IEEE Wireless Communications Letters*, vol. 8, pp. 249–252, Feb 2019.
- [60] G. George, A. Lozano, and M. Haenggi, "Distribution of the number of users per base station in cellular networks," *IEEE Wireless Communications Letters*, pp. 1–1, 2018.
- [61] S. A. Hadiwardoyo, E. Hernández-Orallo, C. T. Calafate, J. C. Cano, and P. Manzoni, "Experimental characterization of UAV-to-car communications," *Computer Networks*, vol. 136, pp. 105 – 118, 2018.
- [62] H. Sallouha, M. M. Azari, A. Chiumento, and S. Pollin, "Aerial anchors positioning for reliable RSS-based outdoor localization in urban environments," *IEEE Wireless Communications Letters*, vol. 7, pp. 376–379, June 2018.
- [63] L. Wang, B. Hu, and S. Chen, "Energy efficient placement of a drone base station for minimum required transmit power," *IEEE Wireless Communications Letters*, pp. 1–1, 2018.
- [64] S. Sarkar, R. K. Ganti, and M. Haenggi, "Optimal base station density for power efficiency in cellular networks," in *2014 IEEE International Conference on Communications (ICC)*, pp. 4054–4059, June 2014.
- [65] M. H. Raza, L. Hughes, and I. Raza, "Density: A context parameter of ad hoc networks," in *Trends in Intelligent Systems and Computer Engineering*

- (O. Castillo, L. Xu, and S.-I. Ao, eds.), vol. 6 of *Lecture Notes in Electrical Engineering*, pp. 525–540, Springer US, 2008.
- [66] V. Iyer, A. Loukas, and S. Dulman, “NEST : A practical algorithm for neighborhood discovery in dynamic wireless networks using adaptive beaconing,” tech. rep., Delft University of Technology, 2012.
 - [67] D. López-Pérez, M. Ding, H. Claussen, and A. H. Jafari, “Towards 1 Gbps/UE in cellular systems: Understanding ultra-dense small cell deployments,” *IEEE Communications Surveys and Tutorials*, vol. 17, pp. 2078–2101, Fourthquarter 2015.
 - [68] S. Lee and K. Huang, “Coverage and economy of cellular networks with many base stations,” *IEEE Communications Letters*, pp. 1038–1040, 2012.
 - [69] V. Mordachev and S. Loyka, “On node density - outage probability tradeoff in wireless networks,” in *Proc. of the IEEE International Symposium on Information Theory*, (Toronto, ON, Canada), pp. 191–195, July 2008.
 - [70] D. Miorandi and E. Altman, “Coverage and connectivity of ad hoc networks presence of channel randomness,” in *Proc. of the IEEE Annual Joint Conf. of the IEEE Computer and Communications Societies.*, (Miami, FL, USA), pp. 491–502 vol. 1, March 2005.
 - [71] N. Panwar, S. Sharma, and A. K. Singh, “A survey on 5G: The next generation of mobile communication,” *Physical Communication*, vol. 18, pp. 64–84, 2016.
 - [72] A. Madhja, S. Nikolettseas, and A. A. Voudouris, “Adaptive wireless power transfer in mobile ad hoc networks,” *Computer Networks*, vol. 152, pp. 87 – 97, 2019.
 - [73] M. I. Khan, “Network parameters impact on dynamic transmission power control in vehicular ad hoc networks,” *CoRR*, vol. abs/1310.4475, 2013.
 - [74] J. Yao, W. Lou, C. Yang, and K. Wu, “Efficient interference-aware power control for wireless networks,” *Computer Networks*, vol. 136, pp. 68 – 79, 2018.

- [75] T. Zhang, L. An, Y. Chen, and K. K. Chai, "Aggregate interference statistical modeling and user outage analysis of heterogeneous cellular networks," in *2014 IEEE International Conference on Communications (ICC)*, (Sydney, NSW, Australia), pp. 1260–1265, June 2014.
- [76] S. Samarakoon, M. Bennis, W. Saad, M. Debbah, and M. Latva-aho, "Ultra dense small cell networks: Turning density into energy efficiency," *IEEE Journal on Selected Areas in Communications*, vol. 34, pp. 1267–1280, May 2016.
- [77] D. Cao, S. Zhou, and Z. Niu, "Optimal base station density for energy-efficient heterogeneous cellular networks," in *Proc. of the IEEE ICC*, (Sydney, NSW, Australia), pp. 4379–4383, June 2012.
- [78] X. Ge, X. Tian, Y. Qiu, G. Mao, and T. Han, "Small-cell networks with fractal coverage characteristics," *IEEE Transactions on Communications*, vol. 66, pp. 5457–5469, Nov 2018.
- [79] J. Chen, X. Ge, and Q. Ni, "Coverage and handoff analysis of 5G fractal small cell networks," *IEEE Transactions on Wireless Communications*, vol. 18, pp. 1263–1276, 2019.
- [80] X. Ge, Y. Qiu, J. Chen, M. Huang, H. Xu, J. Xu, W. Zhang, Y. Yang, C. Wang, and J. Thompson, "Wireless fractal cellular networks," *IEEE Wireless Communications*, vol. 23, pp. 110–119, October 2016.
- [81] P. Kyösti, J. Meinilä, L. Hentila, X. Zhao, T. Jämsä, C. Schneider, M. Narandzić, M. Milojević, A. Hong, J. Ylitalo, V.-M. Holappa, M. Alatossava, R. Bultitude, Y. Jong, and T. Rautiainen, "Ist-4-027756 WINNER II d1.1.2 v1.2 WINNER II channel models," *Inf. Soc. Technol*, vol. 11, 02 2008.
- [82] E. Paolini, C. Stefanovic, G. Liva, and P. Popovski, "Coded random access: applying codes on graphs to design random access protocols," *IEEE Communications Magazine*, vol. 53, pp. 144–150, 2015.
- [83] Y. Richter and I. Bergel, "Optimal and suboptimal routing based on partial CSI in random ad-hoc networks," *IEEE Transactions on Wireless Communications*, vol. 17, pp. 2815–2826, April 2018.

- [84] J. Sun, R. Liu, and E. Paolini, “Detecting the number of active users in IRSA access protocols,” in *2018 IEEE 29th Annual International Symposium on Personal, Indoor and Mobile Radio Communications (PIMRC)*, (Bologna, Italy), pp. 1972–1976, Sep. 2018.
- [85] J. Sun, R. Liu, and E. Paolini, “Detecting the number of active users in coded random access systems,” in *2018 IEEE 29th Annual International Symposium on Personal, Indoor and Mobile Radio Communications (PIMRC)*, (Bologna, Italy), pp. 1–7, Sep. 2018.
- [86] Z. Shafiq, R. Abbas, M. H. Zafar, and M. Basher, “Analysis and evaluation of random access transmission for UAV-Assisted vehicular-to-infrastructure communications,” *IEEE Access*, vol. 7, pp. 12427–12440, January 2019.
- [87] K. A. Yau, J. Qadir, C. Wu, M. A. Imran, and M. H. Ling, “Cognition-inspired 5G cellular networks: A review and the road ahead,” *IEEE Access*, vol. 6, pp. 35072–35090, 2018.
- [88] J. Zhu, M. Zhao, and S. Zhou, “An optimization design of ultra dense networks balancing mobility and densification,” *IEEE Access*, vol. 6, pp. 32339–32348, 2018.
- [89] W. Araujo, R. Fogarolli, M. Seruffo, and D. Cardoso, “Deployment of small cells and a transport infrastructure concurrently for next-generation mobile access networks,” *PLOS ONE*, vol. 13, pp. 1–17, 11 2018.
- [90] P. Madadi, F. Baccelli, and G. de Veciana, “On spatial and temporal variations in ultra dense wireless networks,” in *IEEE INFOCOM 2018-IEEE Conference on Computer Communications*, (Honolulu, HI, USA), pp. 2663–2671, IEEE, October 2018.
- [91] S. Zhou, D. Lee, B. Leng, X. Zhou, H. Zhang, and Z. Niu, “On the spatial distribution of base stations and its relation to the traffic density in cellular networks,” *IEEE Access*, vol. 3, pp. 998–1010, 2015.
- [92] C. Bockelmann, N. K. Pratas, G. Wunder, S. Saur, M. Navarro, D. Gregoratti, G. Vivier, E. De Carvalho, Y. Ji, Ā. Stefanović, P. Popovski, Q. Wang, M. Schellmann, E. Kosmatos, P. Demestichas, M. Raceala-Motoc, P. Jung,

- S. Stanczak, and A. Dekorsy, "Towards massive connectivity support for scalable mMTC communications in 5G networks," *IEEE Access*, vol. 6, pp. 28969–28992, 2018.
- [93] C. Shen, M. Yun, A. Arora, and H.-A. Choi, "Efficient mobile base station placement for first responders in public safety networks," in *Advances in Information and Communication* (K. Arai and R. Bhatia, eds.), (Cham), pp. 634–644, Springer International Publishing, 2019.
- [94] L. Wang, B. Hu, and S. Chen, "Energy efficient placement of a drone base station for minimum required transmit power," *IEEE Wireless Communications Letters*, pp. 1–1, 2018.
- [95] N. Zhao, W. Lu, M. Sheng, Y. Chen, J. Tang, F. R. Yu, and K. Wong, "UAV-Assisted emergency networks in disasters," *IEEE Wireless Communications*, vol. 26, pp. 45–51, February 2019.
- [96] S. H. Alsamhi, O. Ma, M. S. Ansari, and S. K. Gupta, "Collaboration of drone and internet of public safety things in smart cities: An overview of QoS and network performance optimization," *Drones*, vol. 3, no. 1, p. 3, 2019.
- [97] H. Zhang, C. Jiang, M. Bennis, M. Debbah, Z. Han, and V. C. M. Leung, "Heterogeneous ultra dense networks: Part 2," *IEEE Communications Magazine*, vol. 56, pp. 12–13, June 2018.
- [98] M. Habash, H. A. H. Hassan, and R. Achkar, "Analysis of using drone-base stations on the performance of heterogeneous cellular networks," in *2018 IEEE International Multidisciplinary Conference on Engineering Technology (IM-CET)*, (Beirut, Lebanon), pp. 1–5, Nov 2018.
- [99] I. Bor-Yaliniz and H. Yanikomeroglu, "The new frontier in RAN heterogeneity: Multi-tier drone-cells," *IEEE Communications Magazine*, vol. 54, pp. 48–55, November 2016.
- [100] L. Xie, Y. Shi, Y. T. Hou, W. Lou, H. D. Sherali, and S. F. Midkiff, "Bundling mobile base station and wireless energy transfer: Modeling and optimization," in *Proc. of the IEEE INFOCOM*, (Turin, Italy), pp. 1636–1644, April 2013.

- [101] J. Wu, Y. Zhang, M. Zukerman, and E. K. Yung, "Energy-efficient base-stations sleep-mode techniques in green cellular networks: A survey," *IEEE Communications Surveys Tutorials*, vol. 17, pp. 803–826, Secondquarter 2015.
- [102] X. Huang, S. Cheng, K. Cao, P. Cong, T. Wei, and S. Hu, "A survey of deployment solutions and optimization strategies for hybrid SDN networks," *IEEE Communications Surveys Tutorials*, vol. 21, pp. 1483–1507, Secondquarter 2019.
- [103] F. Yu, H. Chen, and J. Xu, "DMPO: Dynamic mobility-aware partial offloading in mobile edge computing," *Future Generation Computer Systems*, vol. 89, pp. 722 – 735, 2018.
- [104] S. Andreev, V. Petrov, M. Dohler, and H. Yanikomeroglu, "Future of ultra-dense networks beyond 5G: Harnessing heterogeneous moving cells," *IEEE Communications Magazine*, vol. 57, pp. 86–92, June 2019.
- [105] S. Zhang, Y. Zeng, and R. Zhang, "Cellular-enabled UAV communication: A connectivity-constrained trajectory optimization perspective," *IEEE Transactions on Communications*, vol. 67, pp. 2580–2604, March 2019.
- [106] A. Fotouhi, M. Ding, and M. Hassan, "Dynamic base station repositioning to improve performance of drone small cells," in *2016 IEEE Globecom Workshops (GC Wkshps)*, (Washington, DC, USA), pp. 1–6, Dec 2016.
- [107] Z. Ning, X. Wang, J. J. P. C. Rodrigues, and F. Xia, "Joint computation of offloading, power allocation, and channel assignment for 5G-Enabled traffic management systems," *IEEE Transactions on Industrial Informatics*, vol. 15, pp. 3058–3067, May 2019.
- [108] M. Liyanage, A. Gurtov, and M. Ylianttila, *Software Defined Mobile Networks (SDMN): Beyond LTE Network Architecture*. John Wiley & Sons, 2015.
- [109] Y. Zhang, L. Cui, W. Wang, and Y. Zhang, "A survey on software defined networking with multiple controllers," *Journal of Network and Computer Applications*, vol. 103, pp. , 101 – 118, 2018.
- [110] N. Panwar, S. Sharma, and A. K. Singh, "A survey on 5G: The next generation of mobile communication," *Physical Communication*, vol. 18, pp. 64 – 84,

2016. Special Issue on Radio Access Network Architectures and Resource Management for 5G.

- [111] S. M. Yu and S. Kim, “Downlink capacity and base station density in cellular networks,” in *2013 11th International Symposium and Workshops on Modeling and Optimization in Mobile, Ad Hoc and Wireless Networks (WiOpt)*, (Tsukuba Science City, Japan), pp. 119–124, May 2013.
- [112] A. Valkanis, A. Iossifides, P. Chatzimisios, M. Angelopoulos, and V. Katos, “IEEE 802.11ax spatial reuse improvement: An interference-based channel-access algorithm,” *IEEE Vehicular Technology Magazine*, vol. 14, pp. 78–84, June 2019.
- [113] M. Ding, D. Lopez-Perez, H. Claussen, and M. A. Kaafar, “On the fundamental characteristics of ultra-dense small cell networks,” *IEEE Network*, vol. 32, pp. 92–100, May 2018.
- [114] F. Gómez-Cuba, E. Erkip, S. Rangan, and F. J. González-Castaño, “Capacity scaling of cellular networks: Impact of bandwidth, infrastructure density and number of antennas,” *IEEE Transactions on Wireless Communications*, vol. 17, pp. 652–666, Jan 2018.
- [115] L. Xiao, H. Zhang, Y. Xiao, X. Wan, S. Liu, L. Wang, and H. V. Poor, “Reinforcement learning based downlink interference control for ultra-dense small cells,” *IEEE Transactions on Wireless Communications*, vol. 19, pp. 423 – 434, 2019.
- [116] B. Romanous, N. Bitar, A. Imran, and H. Refai, “Network densification: Challenges and opportunities in enabling 5G,” in *2015 IEEE 20th International Workshop on Computer Aided Modelling and Design of Communication Links and Networks (CAMAD)*, (Guildford, UK), pp. 129–134, Sep. 2015.
- [117] W. Huang and H. Zhang, “Coverage and throughput analysis for dual connectivity in ultra-dense heterogeneous networks,” in *ICC 2019 - 2019 IEEE International Conference on Communications (ICC)*, (Shanghai, China), pp. 1–6, May 2019.

- [118] C. Zhang, Z. Wei, Z. Feng, and W. Zhang, *Spectrum Sharing of Drone Networks*, pp. 1279–1304. Singapore: Springer Singapore, 2019.
- [119] X. Chai, T. Liu, C. Xing, H. Xiao, and Z. Zhang, “Throughput improvement in cellular networks via full-duplex based device-to-device communications,” *IEEE Access*, vol. 4, pp. 7645–7657, 2016.
- [120] A. J. Mahbas, H. Zhu, and J. Wang, “Impact of small cells overlapping on mobility management,” *IEEE Transactions on Wireless Communications*, vol. 18, pp. 1054–1068, Feb 2019.
- [121] C. Choi and F. Baccelli, “Coverage analysis in cellular networks with planar and vehicular base stations,” in *2018 IEEE International Symposium on Information Theory (ISIT)*, (Vail, CO, USA), pp. 46–50, June 2018.
- [122] A. Walid, E. Sabir, A. Kobbane, T. Taleb, and M. E. Koutbi, “Exploiting multi-homing in hyper dense LTE small-cells deployments,” in *2016 IEEE Wireless Communications and Networking Conference*, pp. 1–6, April 2016.
- [123] H. Zhang, S. Liu, L. Yang, and H. Zhu, “Energy efficient resource matching algorithm for multi-homing services in dynamic wireless environment,” *Wireless Networks*, vol. 26, pp. 1177–1192, Oct 2018.
- [124] S. Kassir, G. d. Veciana, N. Wang, X. Wang, and P. Palacharla, “Enhancing cellular performance via vehicular-based opportunistic relaying and load balancing,” in *IEEE INFOCOM 2019 - IEEE Conference on Computer Communications*, (Paris, France), pp. 91–99, April 2019.
- [125] S. Lou, G. Srivastava, and S. Liu, “A node density control learning method for the Internet of Things,” *Sensors*, vol. 19, no. 15, 2019.
- [126] A. Lavric, A. I. Petrariu, and V. Popa, “Long range sigfox communication protocol scalability analysis under large-scale, high-density conditions,” *IEEE Access*, vol. 7, pp. 35816–35825, 2019.
- [127] B. Gangopadhyay, J. Pedro, and S. Spaelter, “5G-ready multi-failure resilient and cost-effective transport networks,” *Journal of Lightwave Technology*, vol. 37, pp. 4062–4072, Aug 2019.

- [128] A. M. Hayajneh, S. A. R. Zaidi, D. C. McLernon, and M. Ghogho, "Drone empowered small cellular disaster recovery networks for resilient smart cities," in *2016 IEEE International Conference on Sensing, Communication and Networking (SECON Workshops)*, (London, UK), pp. 1–6, June 2016.
- [129] G. A. Rizzo and M. A. Marsan, "The energy saving potential of static and adaptive resource provisioning in dense cellular networks," in *2018 10th International Conference on Communication Systems Networks (COMSNETS)*, (Bengaluru, India), pp. 297–304, Jan 2018.
- [130] S. Mollahasani and E. Onur, "Density-aware power allocation in mobile networks using edge computing," in *2018 26th Signal Processing and Communications Applications Conference (SIU)*, (Izmir, Turkey), pp. 1–4, May 2018.
- [131] J. Liu, M. Sheng, L. Liu, and J. Li, "Effect of densification on cellular network performance with bounded pathloss model," *IEEE Communications Letters*, vol. 21, pp. 346–349, Feb 2017.
- [132] Y. Luo, Z. Shi, F. Bu, and J. Xiong, "Joint optimization of area spectral efficiency and energy efficiency for two-tier heterogeneous ultra-dense networks," *IEEE Access*, vol. 7, pp. 12073–12086, 2019.
- [133] I. A. Alimi, A. L. Teixeira, and P. P. Monteiro, "Toward an efficient C-RAN optical fronthaul for the future networks: A tutorial on technologies, requirements, challenges, and solutions," *IEEE Communications Surveys Tutorials*, vol. 20, pp. 708–769, Firstquarter 2018.
- [134] A. Fotouhi, H. Qiang, M. Ding, M. Hassan, L. G. Giordano, A. Garcia-Rodriguez, and J. Yuan, "Survey on UAV cellular communications: Practical aspects, standardization advancements, regulation, and security challenges," *IEEE Communications Surveys Tutorials*, vol. 21, pp. 3417–3442, 2019.
- [135] A. H. Sodhro, S. Pirbhulal, A. K. Sangaiah, S. Lohano, G. H. Sodhro, and Z. Luo, "5G-based transmission power control mechanism in fog computing for internet of things devices," *Sustainability*, vol. 10, no. 4, p. 1258, 2018.
- [136] R. Li, C. Zhang, P. Patras, R. Stanica, and F. Valois, "Learning driven mobil-

- ity control of airborne base stations in emergency networks,” *SIGMETRICS Perform. Eval. Rev.*, vol. 46, pp. 163–166, Jan. 2019.
- [137] A. Kishida, Y. Morihiro, T. Asai, and Y. Okumura, “Cell selection scheme for handover reduction based on moving direction and velocity of UEs for 5G multi-layered radio access networks,” in *2018 International Conference on Information Networking (ICOIN)*, (Chiang Mai, Thailand), pp. 362–367, Jan 2018.
- [138] S.-F. Chou, T.-C. Chiu, Y.-J. Yu, and A.-C. Pang, “Mobile small cell deployment for next generation cellular networks,” in *Proc. of the IEEE Globecom*, (Mayor of the City, Austin), pp. 4852–4857, IEEE, December 2014.
- [139] H. Zhang, H. Liu, J. Cheng, and V. C. M. Leung, “Downlink energy efficiency of power allocation and wireless backhaul bandwidth allocation in heterogeneous small cell networks,” *IEEE Transactions on Communications*, vol. 66, pp. 1705–1716, April 2018.
- [140] K. N. Qureshi, A. H. Abdullah, O. Kaiwartya, S. Iqbal, R. A. Butt, and F. Bashir, “A dynamic congestion control scheme for safety applications in vehicular ad hoc networks,” *Computers & Electrical Engineering*, vol. 72, pp. 774 – 788, 2018.
- [141] P. Szczytowski, A. Khelil, A. Ali, and N. Suri, “Tom: Topology oriented maintenance in sparse wireless sensor networks,” in *2011 8th Annual IEEE Communications Society Conference on Sensor, Mesh and Ad Hoc Communications and Networks*, pp. 548–556, June 2011.
- [142] S. Mollahasani and E. Onur, “Density-aware, energy- and spectrum-efficient small cell scheduling,” *IEEE Access*, vol. 7, pp. 65852–65869, 2019.
- [143] H. Zhang, N. Liu, X. Chu, K. Long, A. Aghvami, and V. C. M. Leung, “Network slicing based 5G and future mobile networks: Mobility, resource management, and challenges,” *IEEE Communications Magazine*, vol. 55, pp. 138–145, Aug 2017.
- [144] A. Eroglu, E. Onur, and M. Turan, “Density-aware outage in clustered ad hoc

- networks,” in *2018 9th IFIP International Conference on New Technologies, Mobility and Security (NTMS)*, (Paris, France), pp. 1–5, Feb 2018.
- [145] Z. Li, Y. Zhao, Y. Cui, and D. Xiang, “A density adaptive routing protocol for large-scale ad hoc networks,” in *2008 IEEE Wireless Communications and Networking Conference*, pp. 2597–2602, March 2008.
- [146] Y. Xu, W.-C. Lee, J. Xu, and G. Mitchell, “PSGR: priority-based stateless geo-routing in wireless sensor networks,” in *Proc. of the IEEE MASS*, pp. 680–688, Nov. 2005.
- [147] N. Akhtar, S. C. Ergen, and O. Ozkasap, “Analysis of distributed algorithms for density estimation in VANETs (poster),” in *2012 IEEE Vehicular Networking Conference (VNC)*, (Seoul, South Korea), pp. 157–164, Nov 2012.
- [148] J. Feng and Z. Feng, “Optimal Base Station Density of Dense Network: From the Viewpoint of Interference and Load,” *Sensors*, vol. 17, pp. 2077–2095, Sep 2017.
- [149] C. Fan, T. Zhang, Z. Zeng, and Y. Chen, “Optimal base station density in cellular networks with self-similar traffic characteristics,” in *2017 IEEE Wireless Communications and Networking Conference (WCNC)*, (San Francisco, CA, USA), pp. 1–6, March 2017.
- [150] J. Wang, Y. Huang, Z. Feng, C. Jiang, H. Zhang, and V. C. M. Leung, “Reliable traffic density estimation in vehicular network,” *IEEE Transactions on Vehicular Technology*, vol. 67, pp. 6424–6437, July 2018.
- [151] D. Lee, S. Zhou, X. Zhong, Z. Niu, X. Zhou, and H. Zhang, “Spatial modeling of the traffic density in cellular networks,” *IEEE Wireless Communications*, vol. 21, pp. 80–88, February 2014.
- [152] A. Achtzehn, J. Riihijarvi, and P. Mahonen, “Large-scale cellular network modeling from population data: An empirical analysis,” *IEEE Communications Letters*, vol. 20, pp. 2292–2295, Nov 2016.
- [153] N. Salman, M. Ghogho, and A. H. Kemp, “On the joint estimation of the RSS-based location and path-loss exponent,” *IEEE Wireless Communications Letters*, vol. 1, pp. 34–37, February 2012.

- [154] L. Zhang, W. Zhou, W. Tang, G. Wu, and Z. Chen, “Estimating the distance between macro base station and users in heterogeneous networks,” in *2017 14th IEEE Annual Consumer Communications Networking Conference (CCNC)*, (Las Vegas, NV, USA), pp. 928–932, Jan 2017.
- [155] N. Al-Falahy and O. Y. Alani, “Technologies for 5G networks: Challenges and opportunities,” *IT Professional*, vol. 19, pp. 12–20, Jan 2017.
- [156] S. S. Jaffry, S. F. Hasan, and X. Gui, “Mobile cells assisting future cellular communication,” *IEEE Potentials*, vol. 37, pp. 16–20, Sep. 2018.
- [157] S. Chen, T. Zhao, H. Chen, and W. Meng, “Downlink coordinated multi-point transmission in ultra-dense networks with mobile edge computing,” *IEEE Network*, vol. 33, pp. 152–159, March 2019.
- [158] S. Han, S. Xu, W. Meng, and C. Li, “Dense-device-enabled cooperative networks for efficient and secure transmission,” *IEEE Network*, vol. 32, pp. 100–106, March 2018.
- [159] A. Argyriou, K. Poularakis, G. Iosifidis, and L. Tassiulas, “Video delivery in dense 5G cellular networks,” *IEEE Network*, vol. 31, pp. 28–34, July 2017.
- [160] F. Elsherif, E. K. P. Chong, and J. Kim, “Energy-efficient base station control framework for 5G cellular networks based on markov decision process,” *IEEE Transactions on Vehicular Technology*, vol. 68, pp. 9267–9279, Sep. 2019.
- [161] S. Hur, S. Baek, B. Kim, Y. Chang, A. F. Molisch, T. S. Rappaport, K. Haneda, and J. Park, “Proposal on millimeter-wave channel modeling for 5G cellular system,” *IEEE Journal of Selected Topics in Signal Processing*, vol. 10, pp. 454–469, April 2016.
- [162] N. Zarin and A. Agarwal, “QoS based joint radio resource allocation for multi-homing calls in heterogeneous wireless access network,” in *Proceedings of the 16th ACM International Symposium on Mobility Management and Wireless Access, MobiWac’18*, (New York, NY, USA), pp. 37–42, ACM, 2018.
- [163] A. E. García, H. E. González, L. R. Arjona, M. Kubisch, and D. Schupke, “Evaluation of a wireless physical security method for flying objects based

on the frequency selectivity of the propagation channel,” in *2019 15th International Conference on the Design of Reliable Communication Networks (DRCN)*, (Coimbra, Portugal), pp. 59–66, March 2019.

- [164] E. Dahlman, S. Parkvall, and J. Skold, *4G: LTE/LTE-Advanced for Mobile Broadband: LTE/LTE-Advanced for Mobile Broadband*. Academic Press, 2011.
- [165] P. Popovski, K. F. Trillingsgaard, O. Simeone, and G. Durisi, “5G Wireless Network Slicing for eMBB, URLLC, and mMTC: A Communication-Theoretic View,” *IEEE Access*, vol. 6, pp. 55765–55779, 2018.
- [166] G. Pocovi, K. I. Pedersen, and P. Mogensen, “Joint link adaptation and scheduling for 5G ultra-reliable low-latency communications,” *IEEE Access*, vol. 6, pp. 28912–28922, MAY 2018.
- [167] A. Thomas and G. Raja, “Finder: A D2D based critical communications framework for disaster management in 5G,” *Peer-to-Peer Networking and Applications*, vol. 12, pp. 912–923, Jul 2019.
- [168] M. F. Hashim and N. I. Abdul Razak, “Ultra-dense networks: Integration with device to device (D2D) communication,” *Wireless Personal Communications*, vol. 106, pp. 911–925, May 2019.
- [169] O. Hayat, R. Ngah, and Y. Zahedi, “Device discovery signal design for proximal devices in D2D communication,” *Wireless Personal Communications*, vol. 2, pp. 865–878, May 2019.
- [170] Y. Zhang, S. Bi, and Y. J. A. Zhang, “User-centric joint transmission in virtual-cell-based ultra-dense networks,” *IEEE Transactions on Vehicular Technology*, vol. 67, pp. 4640–4644, May 2018.
- [171] H.-S. Ahn and C.-H. Won, “DGPS/IMU integration-based geolocation system: Airborne experimental test results,” *Aerospace Science and Technology*, vol. 13, no. 6, pp. 316 – 324, 2009.
- [172] A. K. s. Wong, T. K. Woo, A. T. L. Lee, X. Xiao, V. W. H. Luk, and K. W. Cheng, “An AGPS-based elderly tracking system,” in *2009 First Interna-*

tional Conference on Ubiquitous and Future Networks, (Hong Kong, China), pp. 100–105, June 2009.

- [173] J. Huang, Z. Huang, and K. Chen, “Combining low-cost inertial measurement unit (IMU) and deep learning algorithm for predicting vehicle attitude,” in *2017 IEEE Conference on Dependable and Secure Computing*, (Taipei, Taiwan), pp. 237–239, Aug 2017.
- [174] X. Jia, Q. Fan, W. Xu, and L. Yang, “Cross-tier dual-connectivity designs of three-tier hetnets with decoupled uplink/downlink and global coverage performance evaluation,” *IEEE Access*, vol. 7, pp. 16816–16836, 2019.
- [175] Y. Shi, H. Qu, J. Zhao, and G. Ren, “Analysis of dual connectivity for downlink access in 5G heterogeneous network,” *Wireless Personal Communications*, vol. 102, pp. 309–323, Sep 2018.
- [176] P. Mitharwal, C. Lohr, and A. Gravey, *Survey on Network Interface Selection in Multihomed Mobile Networks*, pp. 134–146. Cham: Springer International Publishing, 2014.
- [177] X. Wang, M. Jia, Q. Guo, I. Ho, and J. Wu, “Joint power, original bandwidth and detected hole bandwidth allocation for multi-homing heterogeneous networks based on cognitive radio,” *IEEE Transactions on Vehicular Technology*, vol. 3, pp. 1–1, 2019.
- [178] L. Chen, J. Wu, H. Dai, and X. Huang, “BRAINS: Joint bandwidth-relay allocation in multihoming cooperative d2d networks,” *IEEE Transactions on Vehicular Technology*, vol. 67, pp. 5387–5398, June 2018.
- [179] M. Niraula and T. McParland, “Aviation safety service IPv6 based air-to-ground communication: Multi-homing challenges,” in *2019 Integrated Communications, Navigation and Surveillance Conference (ICNS)*, (Herndon, VA, USA), pp. 1–5, April 2019.
- [180] A. D. L. Oliva, X. C. Perez, A. Azcorra, A. D. Giglio, F. Cavaliere, D. Tiegelbeekers, J. Lessmann, T. Haustein, A. Mourad, and P. Iovanna, “Xhaul: toward an integrated fronthaul/backhaul architecture in 5g networks,” *IEEE Wireless Communications*, vol. 22, pp. 32–40, October 2015.

- [181] A. B. Kihero, M. S. J. Solaija, and H. Arslan, "Inter-Numerology Interference for Beyond 5G," *IEEE Access*, vol. 7, pp. 146512–146523, 2019.
- [182] X. Yang, Y. Liu, and S. Gong, "Design of a wideband omnidirectional antenna with characteristic mode analysis," *IEEE Antennas and Wireless Propagation Letters*, vol. 17, pp. 993–997, June 2018.
- [183] Z. Sun and H. Li, "Using directional antenna for continuous moving object tracking in WSN with uncovered holes," *2013 IEEE 33rd International Conference on Distributed Computing Systems Workshops*, pp. 274–279, December 2013.
- [184] S. Kusaladharma, W. Zhu, and W. Ajib, "Stochastic geometry-based modeling and analysis of massive MIMO-Enabled millimeter wave cellular networks," *IEEE Transactions on Communications*, vol. 67, pp. 288–301, Jan 2019.
- [185] A. Umer, S. A. Hassan, H. Pervaiz, Q. Ni, L. Musavian, and S. H. Ahmed, "Secrecy outage analysis for massive MIMO-Enabled multi-tier 5G hybrid Het-Nets," in *2018 IEEE International Conference on Communications Workshops (ICC Workshops)*, pp. 1–6, May 2018.
- [186] H. Chen, R. Abbas, P. Cheng, M. Shirvanimoghaddam, W. Hardjawana, W. Bao, Y. Li, and B. Vucetic, "Ultra-reliable low latency cellular networks: Use cases, challenges and approaches," *IEEE Communications Magazine*, vol. 56, pp. 119–125, December 2018.
- [187] L. Wang, K. Wong, S. Lambotharan, A. Nallanathan, and M. ElKashlan, "Edge caching in dense heterogeneous cellular networks with massive MIMO-Aided self-backhaul," *IEEE Transactions on Wireless Communications*, vol. 17, pp. 6360–6372, Sep. 2018.
- [188] J. Ahn, S. H. Jeon, and H. Park, "A novel proactive caching strategy with community-aware learning in CoMP-Enabled small-cell networks," *IEEE Communications Letters*, vol. 22, pp. 1918–1921, Sep. 2018.
- [189] G. S. Paschos, G. Iosifidis, M. Tao, D. Towsley, and G. Caire, "The role of caching in future communication systems and networks," *IEEE Journal on Selected Areas in Communications*, vol. 36, pp. 1111–1125, June 2018.

- [190] X. Wang, M. Chen, T. Taleb, A. Ksentini, and V. C. M. Leung, "Cache in the air: exploiting content caching and delivery techniques for 5G systems," *IEEE Communications Magazine*, vol. 52, pp. 131–139, February 2014.
- [191] J. Yang, B. Yang, S. Chen, Y. Zhang, Y. Zhang, and L. Hanzo, "Dynamic resource allocation for streaming scalable videos in SDN-Aided dense small-cell networks," *IEEE Transactions on Communications*, vol. 67, pp. 2114–2129, March 2019.
- [192] Q. Zhang, X. Qiu, and X. Zhu, "A novel resource optimization algorithm for dynamic networks combined with NFV and SDN," in *Wireless and Satellite Systems* (M. Jia, Q. Guo, and W. Meng, eds.), (Cham), pp. 283–296, Springer International Publishing, 2019.
- [193] E. J. Kitindi, S. Fu, Y. Jia, A. Kabir, and Y. Wang, "Wireless network virtualization with SDN and C-RAN for 5G networks: Requirements, opportunities, and challenges," *IEEE Access*, vol. 5, pp. 19099–19115, 2017.
- [194] F. Y. Lin, C. Hsiao, Y. Wen, and Y. Wu, "Optimization-based resource management strategies for 5G C-RAN slicing capabilities," in *2018 Tenth International Conference on Ubiquitous and Future Networks (ICUFN)*, (Prague, Czech Republic), pp. 346–351, July 2018.
- [195] E. Björnson, L. Sanguinetti, and M. Kountouris, "Deploying dense networks for maximal energy efficiency: Small cells meet massive MIMO," *IEEE Journal on Selected Areas in Communications*, vol. 34, pp. 832–847, April 2016.
- [196] O. Yaman, A. Eroglu, and E. Onur, "Density-aware cell zooming," in *2018 21st Conference on Innovation in Clouds, Internet and Networks and Workshops (ICIN)*, (Paris, France), pp. 1–8, Feb 2018.
- [197] R.-T. Juang, P. Ting, H.-P. Lin, and D.-B. Lin, "Interference management of femtocell in macro-cellular networks," in *2010 Wireless Telecommunications Symposium (WTS)*, (Tampa, FL, USA), pp. 1–4, April 2010.
- [198] M. Yassin, M. A. AboulHassan, S. Lahoud, M. Ibrahim, D. Mezher, B. Cousin, and E. A. Sourour, "Survey of ICIC techniques in LTE networks under various

- mobile environment parameters,” *Wireless Networks*, vol. 23, pp. 403–418, Feb 2017.
- [199] J. Wen, M. Sheng, K. Huang, and J. Li, “Effects of base-station spatial interdependence on interference correlation and network performance,” *IEEE Transactions on Communications*, vol. 66, pp. 3092–3107, July 2018.
- [200] S. Hong, J. Brand, J. I. Choi, M. Jain, J. Mehlman, S. Katti, and P. Levis, “Applications of self-interference cancellation in 5G and beyond,” *IEEE Communications Magazine*, vol. 52, pp. 114–121, February 2014.
- [201] Y. Yamada, C. Z. Jing, N. H. Abd Rahman, K. Kamardin, I. I. Idrus, M. Rehan, T. Abd Latef, T. Abd Rahman, and N. Q. Dinh, “Unequally element spacing array antenna with butler matrix feed for 5G mobile base station,” in *2018 2nd International Conference on Telematics and Future Generation Networks (TAFGEN)*, (Kuching, Malaysia), pp. 72–76, July 2018.
- [202] B. Soret, K. I. Pedersen, N. T. K. Jørgensen, and V. Fernández-López, “Interference coordination for dense wireless networks,” *IEEE Communications Magazine*, vol. 53, pp. 102–109, January 2015.
- [203] P. Deb, A. Mukherjee, and D. De, “A study of densification management using energy efficient femto-cloud based 5G mobile network,” *Wireless Personal Communications*, vol. 101, pp. 2173–2191, Aug 2018.
- [204] A. Ghosh, J. Zhang, J. G. Andrews, and R. Muhamed, *Fundamentals of LTE*. Upper Saddle River, NJ, USA: Prentice Hall Press, 1st ed., 2010.
- [205] W. Shi, H. Zhou, J. Li, W. Xu, N. Zhang, and X. Shen, “Drone assisted vehicular networks: Architecture, challenges and opportunities,” *IEEE Network*, vol. 32, pp. 130–137, May 2018.
- [206] A. A. Zaidi, R. Baldemair, V. Moles-Cases, N. He, K. Werner, and A. Cedergren, “OFDM Numerology Design for 5G New Radio to Support IoT, eMBB, and MBSFN,” *IEEE Communications Standards Magazine*, vol. 2, pp. 78–83, JUNE 2018.
- [207] W. Khawaja, I. Guvenc, D. W. Matolak, U. Fiebig, and N. Schneckenburger, “A survey of air-to-ground propagation channel modeling for unmanned aerial

- vehicles,” *IEEE Communications Surveys Tutorials*, vol. 21, pp. 2361–2391, thirdquarter 2019.
- [208] C. Yan, L. Fu, J. Zhang, and J. Wang, “A comprehensive survey on UAV communication channel modeling,” *IEEE Access*, vol. 7, pp. 107769–107792, 2019.
- [209] M. Mozaffari, A. T. Z. Kasgari, W. Saad, M. Bennis, and M. Debbah, “3D cellular network architecture with drones for beyond 5G,” in *2018 IEEE Global Communications Conference (GLOBECOM)*, (Abu Dhabi, United Arab Emirates), pp. 1–6, Dec 2018.
- [210] J. Gora and S. Redana, “In-band and out-band relaying configurations for dual-carrier LTE-advanced system,” in *2011 IEEE 22nd International Symposium on Personal, Indoor and Mobile Radio Communications*, (Toronto, Canada), pp. 1820–1824, Sep. 2011.
- [211] P. K. Chartsias, A. Amiras, I. Plevrakis, I. Samaras, K. Katsaros, D. Kritharidis, E. Trouva, I. Angelopoulos, A. Kourtis, M. S. Siddiqui, A. Vines, and E. Escalona, “SDN/NFV-based end to end network slicing for 5G multi-tenant networks,” in *2017 European Conference on Networks and Communications (EuCNC)*, (Oulu, Finland), pp. 1–5, June 2017.
- [212] D. Moltchanov, “Distance distributions in random networks,” *Ad Hoc Networks*, vol. 10, no. 6, pp. 1146 – 1166, 2012.
- [213] E. W. Weisstein, “Circle-circle intersection,” *Wolfram Research, Inc.*, 2003.
- [214] M. G. Kendall and P. A. P. Moran, *Geometrical probability*. No. 10, C. Griffin, 1963.
- [215] S. D. Chitte, S. Dasgupta, and Z. Ding, “Distance estimation from received signal strength under log-normal shadowing: Bias and variance,” *IEEE Signal Processing Letters*, vol. 16, no. 3, pp. 216–218, 2009.
- [216] Z. Yang, Z. Zhou, and Y. Liu, “From RSSI to CSI: Indoor localization via channel response,” *ACM Computing Surveys*, vol. 46, pp. 25:1–25:32, Dec. 2013.

- [217] I. Guvenc and C. C. Chong, “A survey on TOA based wireless localization and NLOS mitigation techniques,” *IEEE Communications Surveys and Tutorials*, vol. 11, pp. 107–124, rd 2009.
- [218] M. Haenggi, “Efficient routing in wireless networks with random node distribution,” in *International Symposium on Information Theory*, (Chicago, IL, USA), p. 17, June 2004.
- [219] D. Moltchanov, “Distance distributions in random networks,” *Ad Hoc Networks*, vol. 10, no. 6, pp. 1146 – 1166, 2012.
- [220] M. Haenggi, “On distances in uniformly random networks,” *IEEE Transactions on Information Theory*, vol. 51, pp. 3584–3586, Oct 2005.
- [221] W. J. Cody, “An overview of software development for special functions,” in *Numerical Analysis* (G. A. Watson, ed.), (Berlin, Heidelberg), pp. 38–48, Springer Berlin Heidelberg, 1976.
- [222] Z. Liu, F. Li, Y. Qi, and J. Chen, “An effective receiver sensitivity measurement,” in *2015 IEEE Symposium on Electromagnetic Compatibility and Signal Integrity*, (Santa Clara, CA, USA), pp. 310–313, March 2015.
- [223] E. Arribas, V. Mancuso, and V. Cholvi, “Coverage optimization with a dynamic network of drone relays,” *IEEE Transactions on Mobile Computing*, pp. 1–1, 2019.
- [224] Byung-Jae Kwak, Nah-Oak Song, and L. E. Miller, “Performance analysis of exponential backoff,” *IEEE/ACM Transactions on Networking*, vol. 13, no. 2, pp. 343–355, 2005.
- [225] Dongxu Shen and V. O. K. Li, “Performance analysis for a stabilized multi-channel slotted ALOHA algorithm,” in *14th IEEE Proceedings on Personal, Indoor and Mobile Radio Communications, 2003. PIMRC 2003.*, vol. 1, (Beijing, China), pp. 249–253 Vol.1, 2003.
- [226] S. Tyagi and P. Jain, “Optimization of slotted-ALOHA using Q-learning,” in *2019 International Conference on Optical Wireless Technologies (OWT 2019)*, (Rajasthan, INDIA), 01 2019.

- [227] T. Rappaport, *Wireless Communications: Principles and Practice*. Upper Saddle River, NJ, USA: Prentice Hall PTR, 2nd ed., 2001.
- [228] G. Mao, B. Fidan, and B. D. Anderson, “Wireless sensor network localization techniques,” *Computer Networks*, vol. 51, no. 10, pp. 2529 – 2553, 2007.
- [229] S. D. Chitte, S. Dasgupta, and Z. Ding, “Distance estimation from received signal strength under log-normal shadowing: Bias and variance,” *2008 9th International Conference on Signal Processing*, pp. 256–259, December 2008.
- [230] V. I. Ogurtsov and D. B. Papkovsky, “Modeling of luminescence-based oxygen sensors with non-uniform distribution of excitation and quenching characteristics inside active medium,” *Sensors and Actuators B: Chemical*, vol. 88, no. 1, pp. 89 – 100, 2003.
- [231] A. K. Gupta and S. Nadarajah, *Handbook of beta distribution and its applications*. CRC press, 2004.
- [232] C. S. Chen and F. Baccelli, “Self-optimization in mobile cellular networks: Power control and user association,” in *IEEE International Conference on Communications (ICC)*, (Cape Town, South Africa), pp. 1–6, May 2010.
- [233] W. Zafar and B. Muhammad Khan, “Flying ad-hoc networks: Technological and social implications,” *IEEE Technology and Society Magazine*, vol. 35, no. 2, pp. 67–74, 2016.
- [234] P. K. Sharma and D. I. Kim, “Random 3D mobile UAV networks: Mobility modeling and coverage probability,” *IEEE Transactions on Wireless Communications*, vol. 18, no. 5, pp. 2527–2538, 2019.

CURRICULUM VITAE

PERSONAL INFORMATION

Surname, Name: Eroğlu, Alperen

Nationality: Turkish

Date and Place of Birth: 10.11.1986, Elazığ

E-mail: eroglu.alperen@gmail.com

EDUCATION

Degree	Institution	Year
P.H.D	Middle East Technical University - Computer Engineering	2020
M.Sc.	Middle East Technical University - Computer Engineering	2015
B.S.	Firat University - Electronics and Computer Education	2009

RESEARCH INTERESTS

Computer Networks, 5G, IoT, Wireless Networks, Embedded Systems, Ad-hoc Networks, Flying Ad-hoc Networks, Network Coverage and Performance, Propagation and Channel Modeling.

PROFESSIONAL EXPERIENCE

2010 - Present:

Department of Computer Engineering, METU, Ankara, Turkey

Position: Teaching / Research Assistant

Assisted Courses:

- CENG435 - Data Communications and Computer Networking
- CENG513 - Wireless Communication and Networks
- CENG530 - Computer Networks and Communications
- CENG230 - Introduction to C Programming
- CENG232 - Logic Design
- CENG331 - Computer Organization
- CENG336 - Introduction to Embedded Systems Development
- CENG599 - Term Project
- SE546 - Software Architecture

2015-2020:

Department of Computer Engineering, METU, Ankara, Turkey

Position: Internet-based Distance Education - Asynchronous (IDEA) Teaching Assistant

Assisted Courses:

- JVYA - Data Structures and Algorithms with JAVA Programming
- WP - Web Programming

2012 - 2015:

Department of Computer Engineering, METU, Ankara, Turkey

Position: System Administrator

High Performance Computing System (HPC) - "NAR" <https://ceng.metu.edu.tr/hpc>

User and system management.

2018:

Department of Computer Engineering, METU, Ankara, Turkey

Position: Mentor

APSCO Student Small Satellite Project, Introduction to Embedded Systems Lectures and Labs, 30th July – 17th August 2018, METU, Ankara, Turkey.

Membership

(Researcher) - Wireless Systems, Networks and CyberSecurity Laboratory (WinsLab) – (5G Testbed), Middle East Technical University (METU), Computer Engineering, B-Z19. <https://wins.ceng.metu.edu.tr/>

Research Projects

(Researcher) - TUBITAK 1001 , 215E127, Density-adaptive Wireless Networks, 2016-2018.

PUBLICATIONS

International SCI Journals

- Alperen Eroğlu, Okan Yaman, Ertan Onur, "Density-aware Cellular Coverage Control: Interference-based Density Estimation", Computer Networks, Vol. 165, p. 106922, Elsevier, Dec 2019, doi:10.1016/j.comnet.2019.106922.
- Shahram Mollahasani, Alperen Eroğlu, Ilker Demirkol, Ertan Onur, "Density-aware mobile networks: Opportunities and challenges", Computer Networks, Vol. 175, p. 107271, Elsevier, July 2020, doi:10.1016/j.comnet.2020.107271.

International Book Chapters

- Shahram Mollahasani, Alperen Eroğlu, A.Ömer Yamaç, Ertan Onur, "Simulators, Test Beds and Prototypes of 5G mobile Networking Architectures", Network of Future, ch. 10, 2017.
- Muhammed Çağrı Kaya, Alperen Eroğlu, Alper Karamanlıoğlu, Ertan Onur, Bedir Tekinerdoğan, and Ali H. Doğru, "Runtime Adaptability of Ambient Intelligence Systems Based on Component-Oriented Approach", Computer Communications and Networks: Guide to Ambient Intelligence in the IoT Environment: Principles, Technologies and Applications, Springer, 2019.

International Conferences

- Okan Yaman, Alperen Eroğlu, Ertan Onur, "Density-aware Cell Zooming", 21st Conference on Innovation in Clouds, Internet and Networks (ICIN 2018), Paris, Fransa, February, 2018.
- Alperen Eroğlu, Ertan Onur, Mehmet Turan, "Density-aware Outage in Clustered Ad Hoc Networks", 9th IFIP International Conference on New Technologies, Mobility and Security 26 to 28 February 2018. Paris, France (NTMS2018), February, 2018.
- Alperen Eroğlu, Ertan Onur, Halit Oğuztüzün, "Estimating density of wireless networks in practice", IEEE 26th Annual International Symp.on Personal, Indoor, and Mobile Radio Communications (PIMRC), (2015), p.1476 - 1480.
- Muhammed Çağrı Kaya, Alperen Eroğlu, Selim Temizer, "Control and Motion Planning for Mobile Robots via a Secure Wireless Communication Protocol", 1st International Symposium on Digital Forensics and Security (ISDFS 2013), (2013), p.227-230.
- İbrahim İleri, Alperen Eroğlu, Ali Doğru, "Component-based Variability Modeling", The 18th International Conference on Transformative Science and Engineering, Business and Social Innovation, (2013), p.55-62.

National Conferences

- Alperen Eroğlu, Shahram Mollahasani, Farnaz Hassanzadeh, Ertan Onur. Yoğunluk uyarlı gelecek nesil ağlarda fırsatlar ve zorluklar”, Türkiye Bilişim Derneği 35. Ulusal Bilişim Kurultayı, Bilişim 2018, 21 Kasım, Ankara.
- Alperen Eroğlu, Selim Temizer, "Control and Motion Planning for Mobile Robots with Microsoft Kinect Based Real-Time Hand Gestures", 4th Computer Science Student Workshop (CSW 2013).
- Alperen Eroğlu, Selim Temizer, "Control and Motion Planning for Mobile Robots with Microsoft Kinect-Based Real-Time Hand Gestures", 5th National Defense Applications Modeling and Simulation Conference (USMOS 2013), (2013), s.455-464.

Conference Committee Member

- BAŞARIM 2012 - 3th National High Performance Computing Conference (Organizing Committee)
- BAŞARIM 2015 - 4th National High Performance Computing Conference (Local Executive Committee)

Seminar

- Alperen Eroğlu, "Density-aware Cellular Coverage: Interference-based density estimator", 5G ve Ötesi Ortak Lisansüstü Destekleme Programı, BTK, 8th Nov, 2019, BMB5, METU, Ankara, Turkey.

Reviewer

In Journals

TURKISH JOURNAL OF ELECTRICAL ENGINEERING and COMPUTER SCIENCES

In Conferences

CCNC 2015, NOMS 2016, IEEE PIMRC 2017, ICC2017-WS07, IEEE WCNC 2017, CCNC 2017, IEEE WCNC 2018, IEEE WCNC FLEXNETs 2018, GLOBECOM 2018, IEEE PIMRC 2019, IEEE BLACKSEACOM 2019, IEEE WCNC 2019, INFOCOM 2019.